Fall 2013

Observability-enhanced dual-filter design for attitude estimation with minimum observations

Jason D. Searcy

Department: Mechanical and Aerospace Engineering

OBSERVABILITY-ENHANCED DUAL-FILTER DESIGN FOR ATTITUDE ESTIMATION WITH MINIMUM OBSERVATIONS

by

JASON DAVID SEARCY

A DISSERTATION

Presented to the Faculty of the Graduate School of the

MISSOURI UNIVERSITY OF SCIENCE AND TECHNOLOGY

In Partial Fulfillment of the Requirements for the Degree

DOCTOR OF PHILOSOPHY

in

AEROSPACE ENGINEERING

2013

Approved
Henry J. Pernicka, Advisor
S. N. Balakrishnan
Robert G. Landers
Joshua L. Rovey
Jagannathan Sarangapani

ABSTRACT

Determining spacecraft attitude in real time using only magnetometer data presents a challenging filtering problem. A flexible and computationally efficient method for solving the spacecraft attitude using only an inexpensive and reliable magnetometer would be a useful option for satellite missions, particularly those with modest budgets. The primary challenge is that magnetometers only instantaneously resolve two axes of the spacecraft attitude. Typically, magnetometers are used in conjunction with other sensors to resolve all three axes. However, by using a filter over an adequately long orbit arc, the magnetometer data can yield full attitude, and in near real time. The method presented solves the problem using a two-nested extended Kalman filter as a means to improve convergence. In the first filter, the magnetic field data are filtered to obtain the magnetic field derivative vector, which is combined with the magnetic field vector in the second filter to fully resolve the attitude.

As revealed by a literature review and previous research by the author, this method fails to accurately estimate the attitude unless the spacecraft is spin-stabilized with a relatively high angular velocity. To address this limiting restriction, the observability of the problem is examined from an analytical perspective. This study separates the problem into two stages and considers different methods for solving each stage. The first estimates the magnetic field derivative and possibly the angular rates, and then uses this information to calculate the attitude in the second stage. A new dynamic model is developed to estimate angular rates without estimating the attitude quaternion. MATLAB numerical routines are used to solve the complex nonlinear system of equations to yield a deterministic method. Finally, a parametric study analyzes the accuracy and utility of this method for different orbit trajectories and angular rates.

1. ACKNOWLEDGMENTS

This one page cannot possibly do justice to the people who deserve my thanks during my studies at Missouri University of Science and Technology. I have to start with Dr. Pernicka, my advisor. Without a tremendous effort by Dr. Pernicka to convince me, I may not have attended graduate school at all. My passion for aerospace engineering did not fully ignite until I was a student in his orbital mechanics class. From that moment on, my desire to learn about spacecraft and spaceflight could not be satisfied. Working with Dr. Pernicka has been a rewarding experience and has provided me with an invaluable asset to begin my professional career. My experiences working with him on the M-SAT Satellite team have yielded some of my most rewarding accomplishments. It has been a great privilege to get to know him and his family over the past years.

I had the privilege of having a second advisor of sorts during my graduate studies. I have had the pleasure of working on many research projects with Dr. Balakrishnan. These projects ranged from missile guidance, to orbit determination, to image processing. The vast array of research experience I gained has helped to shape the engineer I have become as much as my work in graduate school. Beyond professional research projects, Dr. Balakrishnan has been a friend whose personal guidance and advice have proven to be some of the most useful knowledge gained during my college career.

I would like to thank my committee members Dr. Landers, Dr. Rovey, and Dr. Sarangapani for sitting through my riveting presentations. As professors, they taught me during some of my most valuable classes.

Lastly, I would like to thank my family and friends. My wife, Sara, has been with me through the entirety of graduate school and has stood by me through every all-nighter and the through the grueling dissertation writing process. We were married in 2006 and after 7 years of marriage, she is still the supportive rock that propels me to better myself and our lives. I would also like to thank my son, J.J., who was born on May 9, 2013, for being the motivation that I will use to help reach my potential.

TABLE OF CONTENTS

Page

LIST OF ILLUSTRATIONS

Page

LIST OF TABLES

Page

1. INTRODUCTION

Attitude determination is a problem that has been examined in-depth over the last hundred years. Determining the orientation of an object in three-dimensional space has been an interest in dynamics and control since long before Sputnik launched in 1957. The application to spacecraft, of course, began shortly after Sputnik launched. As with any estimation problem, the challenge is to use the available measurements to estimate the spacecraft attitude. The measurements that have historically been used or experimented with are numerous and can be combined in different ways to achieve the necessary attitude estimation accuracy. This section describes a few of the key advances in the field of spacecraft attitude determination.

1.1. ATTITUDE DETERMINATION

One of the classic early works on spacecraft attitude determination was written by James R. Wertz.[22] Wertz's book on spacecraft attitude determination is still a handbook used by many professionals in the field. Wertz covers many aspects of vector-based attitude determination as well as the basic attitude quaternion derivation that is shown in this dissertation to reduce the complexities of having a nine element attitude matrix to determine and avoid mathematical singularities.[22] Other early attitude determination studies have resulted in the TRIAD method, the QUEST method, and additional solutions to Wabha's problem that are discussed later.[9]

Early attitude determination algorithms used least squares methods to obtain estimates. Over the years, those methods have evolved to the more complex Kalman filtering algorithms, and now nonlinear estimation techniques are becoming more common. The evolution may be due to growing estimation accuracy demand, but it is also likely that the increase in available computing power has played a large role in the transition to more complex methods. However, there is also a shift from large, expensive spacecraft to smaller, less expensive models. The most common attitude determination techniques today use the Kalman filter or some variant to estimate the spacecraft attitude.[3] The typical sequential filter works well for attitude determination as well. The

sequential filter works by taking measurements, one at a time, and updating an estimate at some time-step interval. The difference among most attitude determination techniques involves the creative use of measurements from different sensor types that allow the attitude to be estimated.[6]

There are several deterministic methods for calculating a spacecraft attitude using two inertially defined, body-fixed independent pointing vectors. If two such vector measurements exist, the attitude can be calculated directly using a method referred to as the TRIAD method.[12] The QUEST and FOAM methods can utilize more than two sets of attitude vector measurements.[9] For example, if a rigid body rotates freely in space, knowing one pointing vector will allow for the calculation of the attitude, except that the angle about the measurement axis itself will be unknown. Regardless of the spacecraft motion (i.e., rotation) about the measurement, the sensor will always read the same value. A second measurement is needed to fully resolve the attitude. This can be seen through Wahba's problem of minimizing a quadratic loss function.[21] Wahba posed the attitude determination problem of minimizing a quadratic loss function where the measurement residual is minimized. Solving Wahba's problem has been a task of great interest over the past forty-five years. Shuster solved the problem using Davenport's q-method.[24] Markley showed that Wahba's problem could be solved using singular value decomposition.[9] Each method has a different level of accuracy and efficiency. It becomes important, even if there are numerous measurements available to resolve the attitude, to find the most efficient way to solve the problem without losing accuracy.

Recently, there has been a significant amount of work in the field of GPS attitude determination. The process requires the use of multiple antennas, which provide multiple position measurements. Filtering of the GPS data can then fix the spacecraft's attitude. A minimum of three antennas are required to fix the attitude, with more being strongly preferred so that there is a better likelihood of having each antenna in view of several GPS satellites.[1] This method requires a minimum baseline of nearly seventy centimeters between each antenna to provide reasonable accuracy. This works well for most spacecraft, but for nanosatellites and small satellites, unless deployable booms are used, the distances between the antennas would not be sufficient to meet the baseline requirements.[1]

Although it is not necessary, a sensor that provides the angular rates of the spacecraft such as a gyroscope can be beneficial to the filter because the filter no longer has to rely on a range of data to sense that the spacecraft is rotating. This can decrease the time that is needed for the filter to converge to the steady-state. There has been an abundance of work in the area of attitude determination without a rate sensor because the reliability of gyroscopes is sometimes questionable. This dissertation study falls in that subset—that of attitude determination without the benefit of rate sensor data.

Work on attitude determination without a rate sensor usually includes the analysis of filters using measurements from magnetometers, Sun sensors, star trackers, horizon sensors, and so forth. A new focus on gyro-less spacecraft attitude determination systems has emerged. These studies show that it is possible to estimate both the attitude and the angular rates from a variety of pointing vector measurements.[2,4,6]

1.2. MAGNETOMETER-ONLY ATTITUDE DETERMINATION

The idea that the attitude of a spacecraft can be fully determined as long as two independent vectors are known and each is expressed in terms of two different coordinate frames (typically an inertial frame and the spacecraft body frame) forms the basis of the TRIAD algorithm. [11,13] From this fact, the use of several combinations of two or more sensors has been attempted to determine spacecraft attitude. Most use a combination of a magnetometer with either a Sun sensor, star tracker, or horizon sensor. The need for low-cost sensors that can provide sufficiently accurate attitude determination led Gebre-Egziabber, et al. to use an accelerometer to provide a measurement of the gravitational field.[2] Santoni and Bolotti showed that attitude determination can be achieved without the second sensor measurement.[4] The study creatively used the data that were available to the spacecraft, instead of adding a second sensor to obtain the second required pointing vector. It was proposed that the solar panels could be used as Sun sensors, because the direction of the Sun can be found by analyzing the power generation by each panel. This is another example of using fewer, cheaper sensors to provide the same accuracy of attitude determination.

These methods are the basis for the research described in this dissertation. However, the second vector measurement used in this research is obtained by manipulating the first measurement. The magnetic field vector provides the first vector measurement and filtering that series of measurements provides the magnetic field vector derivative as the second vector measurement, or in this case a "pseudo-measurement." The derivative, however, cannot be expressed relative to an inertial frame without knowledge of the angular velocity of the body frame. Therefore, the typical TRIAD algorithm does not apply in this particular scenario, motivating the development of the attitude filter described in Section 4. Other methods have been developed that use magnetometer-only data for attitude determination, and are detailed in this section.

One of the first attitude determination studies that use magnetometer-only data was completed when a satellite mission, the Earth Radiation Budget Experiment, became the victim of an attitude anomaly and was lost. The data that were able to be downlinked were used to try to determine the causes of the mission failure through post-processing. Among the available telemetry were data from a magnetometer. The magnetometer data were used with a method that was developed by Natanson, called DADMOD (Deterministic Attitude Determination using Magnetometer-Only Data).[14] The method solved for the attitude and angular rates from the magnetometer data by finite differencing the measurements to find the magnetic field derivative. The measurements of the magnetic field and its derivative were then used, along with the fact that the spacecraft angular acceleration is known, to estimate the attitude and angular velocities. The equations became quadratic so that there were multiple solutions, and DADMOD selected which of the two solutions was most likely to be the correct attitude.[14] The method worked well for post-processing, but as this research discovered, using noisy, real-time measurements prevents an accurate solution.

Challa expanded the idea to real-time using the Real-Time Sequential Filter, RTSF.[15] The RTSF estimates the spacecraft attitude and rates using only a magnetometer. The RTSF estimates the angular velocity error in similar manner to gyro bias. The error is then used to correct the angular velocity. The method was shown to work well using data from the SAMPEX and Earth Radiation Budget spacecraft missions. The overall attitude accuracy was shown to be less than one degree when

initialized by the DADMOD algorithm. DADMOD was used to obtain coarse initial estimates of the state, and then the RTSF was used to calculate a more accurate solution.[15] The method presented in this research has been shown to produce accuracies similar to those reported by the RTSF, which are on the order of 0.5 degrees in attitude pointing error and 0.001 degrees per second in angular rate estimation error. These are realized after initilization using the DADMOD algorithm to achieve accuracies of four degrees attitude pointing error and 0.01 degrees per second angular rate error. The method presented here uses higher initial error values and is able to converge to comparable or better results. This dissertation study extends previous dual filter work from Reference 32 to include the common (and thus important) scenario in which the spacecraft is inertially fixed and is not rotating. No methods were located in the literature that present a method for estimating angular velocity in this scenario. The observabilty is questionable in such a scenario because the change in the magnetic field vector is very small. In a scenario where the spacecraft is fixed with respect to the magnetic field vector, i.e. the magnetic field vector measurement does not change, the problem is completely unobservable. This research has shown, even in the case of an equitoral orbit with a nonrotating spacecraft, that although convergence times are greater, the attitude and rates can be estimated.

Another magnetometer-only attitude determination solution was given by Psiaki. The error magnitudes achieved by Psiaki's Kalman filtering method showed errors of around two-three degrees after about 100 seconds with low initial filter offset.[20] By using two nested Kalman filters, the method presented in this dissertation is able to achieve better accuracy than previous Kalman filter based magnetometer-only methods.

There have been many attempts to avoid using high power consuming, expensive, and fragile gyroscopes. MEMS devices have been created that allowed for the creation of solid-state IMUs, but most consider them to be too inaccurate and with inadequate resolution to give the results desired. In 1995, Lizarralde and Wen developed a controller without the need for angular velocity feedback. The controller made use of the passivity of the system, eliminating the need for a filter to directly determine the angular velocities.[7] The advantage to such a system resides in the processing requirements from the Command and Data Handling system. The disadvantage of the method is that there is

no knowledge of the angular velocity of the spacecraft. The controller can stabilize the attitude, but the spacecraft does not know its angular velocity, which is typically unacceptable for autonomous systems. One of the most recent attempts at magnetometer-only attitude determination was completed by Ma and Jiang. The authors used an Unscented Kalman Filter (UKF) with magnetometer measurements to estimate the attitude of a spacecraft and to calibrate the magnetometers.[5] The importance of this method is that it included the ability to account for additional error beyond the specifications of the magnetometer. This calibration could be done on the ground, although the difficulty persists that some residual magnetic fields created by the spacecraft could corrupt the measurements creating more noise. Also, the UKF is much less computationally efficient than the EKF, which presents an important drawback.[19] The method presented in this dissertation study, using the two-step EKF, provides the same magnitude errors and is quite robust, without the need to propagate several state vectors, or sigma points. Electromagnetic interference and electromagnetic compatibility (EMI/EMC) analysis can provide calibration of the magnetometer on the ground before the spacecraft is launched. The use of a Kalman filter with a calibrated sensor can thus provide better computational efficiency compared to UKF methods.

At this time there have been several attempts at developing methods of magnetometer-only attitude determination. Such a capability is a valuable asset for a spacecraft in case of a sensor failure or anomaly, or to reduce and implementation complexity by using only magnetometers by design. The first methods, shown using the SAMPEX mission, were executed during post processing, and failed when they were applied in real time. Earth's magnetic field is nonlinear, changes with time and position in space, and has different characteristics depending on the spacecraft's orbit. The sensor that reads the field, however, is relatively inexpensive, easy to implement, accurate, and reliable. If the proper steps are taken to mitigate minor complications with the magnetic field model, the result is a low-cost and viable alternative to expensive and complex sensors.

Natanson and Challa originally proposed, during post-processing, that finite differencing could be used to find the derivative of the magnetic field vector to provide a second vector measurement. This is not feasible in real time because of the nonlinearity

of the magnetic field. Slight fluctuations with a sample time of one second cause drastic errors in the derivative calculation. This work proposes the use of a pre-filter to filter the magnetic field data and yield the magnetic field derivative vector in (near) real time. This process works well as shown in Section 5. At most orbital inclinations, the filter provides a derivative estimation that has better accuracy than a Sun sensor would provide. Once the two vectors are available, it is assumed that the DADMOD method can be used to combine them and achieve an estimate of the spacecraft's attitude, following the approach of Natanson and Challa's work closely.

When the noisy magnetic field vector and derivative vectors were used in the DADMOD algorithm, though, the attitude estimates were in error by sixty to seventy degrees in most cases. When the truth model magnetic field vector and derivative were used (i.e., the noise-free case), attitude was successfully determined. It was determined that the DADMOD algorithm was overly sensitive to noise and inaccurate for real-time implementation. The difficulty is caused by the fact that the derivative vector expressed in terms of the body coordinate frame is not referenced relative to an inertial frame. Without accounting for the angular velocity of the body frame, which is unknown, the TRIAD and QUEST methods cannot be used.

The first solution developed in this study was conceived while exploring an analytical solution to the problem shown in Section 2. When the work was being completed, an algorithm was developed that calculates the magnetic field vector and its derivative *relative to the (rotating) body (spacecraft) frame* and the magnetic field vector and its derivative *relative to the inertial frame*. By using a pre-filter to provide the magnetic field vector and its derivative (pseudo-measurements) and knowing the inertially-referenced vectors from the model, the only unknowns were the attitude and angular rates. Making the attitude and angular rates the state vector for a Kalman filter, the equations can be differentiated to find the measurement matrix. The Kalman filter, once tuned properly, yields results that match and even surpass the magnetometer-only algorithms that have been found during the literature review and summarized previously in this section. The primary purpose/contribution of this dissertation study is creating a global filter sufficiently robust to provide accurate attitude determination in any low Earth orbit scenario.

1.3. MOTIVATION FOR RESEARCH

The general motivation for this research is two-fold. The first aspect that makes magnetometer-only attitude determination important is that as a tool for small-budget, small-volume spacecraft such as cubesats. Small satellite developers need to keep the cost and volume as low as possible and the opportunity to use only one sensor and only need one integration plan is beneficial. The second aspect is to provide a contingency to rate sensors. The specific motivation for this research originally began as a cost and volume savings for the M-SAT mission, described next.

1.3.1. M-SAT Mission Overview. The attitude determination and control (ADAC) research that is detailed in this dissertation was developed for use on a student-built microsatellite at the Missouri University of Science and Technology. The design needed to be low in cost and complexity but sufficiently versatile to accomplish the mission tasks. This section highlights the mission objectives as well as the satellite design and specifications.

The M-SAT (Missouri University of Science and Technology Satellite) research team is developing a mission using two satellites named MR SAT (Missouri Rolla Satellite) and MRS SAT (Missouri Rolla Second Satellite) designed and integrated on the Missouri S&T campus. The two satellites will be launched in a docked configuration. Once the satellite pair has powered up, detumbled, and run system diagnostics, the satellites will separate and fly in formation until MR SAT, the chasing satellite, fully consumes its propellant.

MR SAT is the chase satellite, and is therefore equipped with a propulsion system that provides more accurate attitude control (than MRS SAT). The MR SAT propulsion system will be used for orbital corrections as well as attitude corrections. MRS SAT is regarded as the target satellite and, as such, needs no propulsion. Only attitude control is required on MRS SAT to ensure the solar panels receive sufficient exposure to sunlight and to prevent excessive angular velocities from interfering with inter-satellite communications.

The satellite pair was developed under the strict guidelines of the Nanosat 7 competition sponsored by the Air Force Research Laboratory (AFRL) and the Air Force Office of Scientific Research (AFOSR). The competition involved ten domestic

universities and promoted the goal to each participant of fully developing a functional satellite within a two-year timeframe. The satellite project must meet all AFRL requirements, as well as promote new technologies related to spaceflight and Department of Defense needs by performing a useful function or experiment requiring a space environment to fully test.

1.3.2. ADAC Requirements for M-SAT. The ADAC subsystem is constrained by the mission objectives of the M-SAT mission and must allow all of the mission objectives to be achieved. The requirements placed on the ADAC system are based around meeting the mission objectives and goals. The ADAC system must keep the satellite oriented so that the communications antenna points toward the Earth, most critically when the spacecraft passes over the ground station. This requires the satellite to slew 360 degrees per orbit to keep the antennas pointed in the nadir direction. In order for this base requirement to be met, the spacecraft must be able to determine its attitude to within three degrees, and control the attitude to within six degrees. If this requirement is met, the space-to-ground antenna will not move more than six degrees from nadir, which is within the specifications of the antenna and transceiver (with a conservative factor of safety included).

It is also important to keep the satellite solar panels exposed to as much sunlight as possible. This can be accomplished by keeping the two panels without solar cells oriented away from the Sun. This must be done, though, while maintaining the satellite-to-ground communication link. These requirements drive the desired attitude and the spacecraft must be able to determine its attitude to within three degrees for the mission to be successful. Therefore, the magnetometer-only attitude determination system can only be used if it can be demonstrated through simulation that the system will determine the attitude of the spacecraft to within the requirement of three degrees.

1.3.3. ADAC System Design. Magnetometers can determine the attitude measured relative to the Earth's local magnetic field. The uncertainties and variability in the Earth's magnetic field govern the accuracy of this method. In spite of these uncertainties, sensor filters can provide attitude accuracies of 0.5 to 3 degrees. These sensors need to be isolated from electromagnets, either physically or by duty-cycling the electromagnets. They are not as accurate as star or horizon sensors; however, these lower accuracies are offset by the simplicity, reliability, lightweight, and low-cost of this sensor. The Earth's magnetic field can be continuously monitored, allowing for partial corrections to be made for these variable effects through adjustments in the filters. These variations tend to follow a daily cycle which can be programmed as weights into the filters. Magnetometers are approximately 0.3 to 1.2 kg in mass and consume less than 1 Watt of power.

Magnetometers were selected as the sensors to provide the on-orbit data to the attitude determination method within the autonomous control system running onboard MR SAT. These devices can provide an accurate value for the magnetic field vector at the location of the satellite. Magnetometers have acceptable accuracy, mass, and power consumption given the MR SAT design constraints.

In addressing the attitude determination of the MR SAT spacecraft, a magnetometer was chosen because of the simplicity and reliability available from the sensor. The choice to use only the magnetometer was finalized when it was realized that the angular rate measurement from IMUs would not yield the resolution that was required. More sensors could be added, but the decision was made to determine if the accuracy could be achieved using only a magnetometer. After a literature review, a study by Natanson was identified demonstrating the feasibility of achieving the needed accuracy during post-processing of magnetometer data.[14] The challenge then became in adapting the post-processing technique for use in a real-time attitude determination application on board the MR SAT spacecraft. This forms the key contribution of this research study.

1.4. RESEARCH FLOW

There are two stages to the proposed method of attitude determination. A "pre-filter" (which may or may not actually include a filter, this aspect is elaborated on later) and the attitude filter (responsible for outputting the estimated attitude quaternion and angular rates). This two-step process was shown to add observability to the study in Reference 32 when the spacecraft angular rate is low. The first stage is to estimate the magnetic field derivative. This was accomplished in Reference 32 using a Kalman filter and the methodology is presented in this study. As part of the study, an IMU sensor is simulated to add a measurement of angular velocity. The results of that simulation showed that the method converged with the extra measurements. It is also shown in this study that adding angular rate measurements with reasonable accuracy mitigate the ambiguities seen when the spacecraft angular velocity is too low. It was observed that the changing magnetic field measurements over time could allow for the estimation of the angular velocity during the first stage. If sufficiently accurate, this would also resolve the ambiguity and yield a robust method that is accurate over the entire range of angular velocity.

This study is organized as follows. The next section describes the attitude dynamics that provides a foundation for this dissertation. Section 3 discusses the different techniques that have been used to estimate the preliminary values for the attitude solver/filter. Section 4 shows how the information gained as described in Section 3 was used to develop processes for estimating the attitude and angular rates from the results of Section 3. Then Section 5 provides a culmination of the results into one method that is proposed. Finally, Section 6 summarizes the study findings and applicability of the methods presented, as well as presenting an analysis of the potential for future study or experimentation. Figure 1.1 provides a flow chart visually showing the research paths used to arrive at the final result.

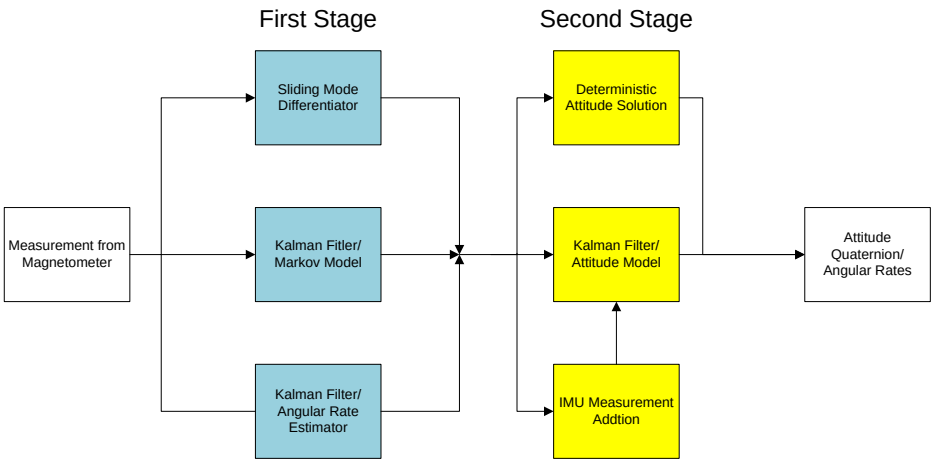

Figure 1.1. Research Flow Chart

1.5. BASELINE ORBIT SCENARIO

The baseline case was taken from Reference 32 with the purpose of creating and evaluating a magnetometer-only attitude algorithm for small spacecraft in low Earth orbit. The baseline scenario in which the simulations in this dissertation are based is described in this section.

The baseline case was defined as a circular, 400 km altitude orbit. The orbital inclination is set to forty degrees because that is the minimum inclination MR SAT can be placed in and still communicate with the Missouri S&T ground station, and it falls conveniently near the middle of the range between polar and equatorial. The right ascension is arbitrarily set to ten degrees. Because of the time dependence of the magnetic field, a simulation start date must be given. The simulations in this dissertation assume the epoch time is March 28, 2011. The initial conditions for the attitude quaternion and angular rates are arbitrarily selected as

$$q = \begin{bmatrix} 0.1031 \\ 0.5157 \\ 0.2063 \\ 0.8251 \end{bmatrix} \tag{1}$$

$$\omega = \begin{bmatrix} 2 \\ 3 \\ 5 \end{bmatrix} \text{deg/ sec} \tag{2}$$

The simulations are all run for 1000 seconds. The attitude rates change slowly over time due to the asymmetries in the spacecraft resulting in unequal principle moments of inertia. The principle moments of inertia used for the MR SAT spacecraft are

$$\begin{aligned} I_{xx} &= 0.8918222 \text{ kg} \cdot \text{m}^2 \\ I_{yy} &= 0.8753646 \text{ kg} \cdot \text{m}^2 \\ I_{zz} &= 0.6176641 \text{ kg} \cdot \text{m}^2 \end{aligned} \tag{3}$$

The measurements, which consist of the Earth's magnetic field vector components, are generated by adding Gaussian noise to the magnetic field truth model. The noise is assumed to be white noise with a norm of zero and a mean of 0.5 mG. Measurements are taken with a frequency of one per second.

The filter states are composed of the attitude quaternion and the angular rates. The initial estimates for the baseline scenario are

$$\hat{\mathbf{q}} = \begin{bmatrix} 0.28222 \\ 0.56443 \\ 0.18814 \\ 0.75258 \end{bmatrix} \tag{4}$$

$$\hat{\boldsymbol{\omega}} = \begin{bmatrix} 2.2 \\ 5.5 \\ 3.3 \end{bmatrix} \text{deg/ sec} \tag{5}$$

These initial estimates reflect an 11.48 degree attitude error and a 10% error in the initial angular velocity estimate. These estimates can be updated by using data available from the launch vehicle provider on expected tip off rates when the spacecraft is ejected onto orbit.

2. ATTITUDE DYNAMICS

2.1. RIGID BODY ATTITUDE DYNAMICS

This section provides an overview of the attitude dynamics used as a background of this dissertation. Because the attitude determination technique incorporates quaternions, the basic attitude quaternion is developed and the relationship to Euler's equations of motion is given. The section concludes with the presentation of a semi-analytic solution to the magnetometer-only attitude determination problem.

2.1.1. Euler's Equations of Motion. The basic rigid body attitude dynamics problem can be modeled using Euler's equations of motion. Euler's equations show that a rigid body's attitude dynamics are dependent on the object's moment of inertia, its angular velocity, and the applied torque. Euler's equations of motion that describe the angular acceleration of a rigid body (spacecraft) are

$$\begin{aligned}\dot{\omega}_x &= \frac{\tau_x - \left(I_{zz} - I_{yy}\right)\omega_y\omega_z}{I_{xx}} \\ \dot{\omega}_y &= \frac{\tau_y - \left(I_{xx} - I_{zz}\right)\omega_x\omega_z}{I_{yy}} \\ \dot{\omega}_z &= \frac{\tau_z - \left(I_{yy} - I_{xx}\right)\omega_x\omega_y}{I_{zz}}\end{aligned} \tag{6}$$

where I_{xx}, I_{yy}, and I_{zz} are the principal axes moments of inertia of the spacecraft and $\tau_{x\text{-}z}$ are the external torques applied to the satellite.[29]

2.1.2. Attitude Representation. The attitude of a spacecraft is often represented using a direction cosine matrix. This matrix represents a rotational transformation from one reference frame to another.

The spacecraft attitude matrix is used to relate the inertial frame to the body frame through

$$\mathbf{V}_I = A\mathbf{V}_b \tag{7}$$

where $\mathbf{V}_I$ is any vector expressed in terms of the inertial frame, while $\mathbf{V}_b$ is the same vector, expressed in terms of the body frame. The goal of attitude determination is to find this relationship (i.e., to determine the *A* matrix). The attitude matrix, *A*, has nine elements and is orthonormal. The problem cannot be solved by knowing one vector in terms of each frame, because, as can be seen from Equation (7), there are nine unknowns and only three scalar equations.

2.2. QUATERNIONS

Quaternions are four-dimensional vectors that can be used to express the attitude of an object. They are manipulated similarly to imaginary numbers. The benefit of using quaternions in this research is the ability to represent the spacecraft attitude using four elements instead of the nine elements of the typical attitude matrix associated with three Euler angle rotations. Quaternions also avoid the singularity issue that is commonly a difficulty when using Euler's rotations in a direction cosine matrix.[29]

2.2.1. Quaternion Overview/Basics. Quaternions can be used in many applications. As mentioned previously, a quaternion is a four-dimensional vector that is treated similarly to an imaginary number. In fact, Hamilton coined the term "quaternion" to refer to hyper-complex numbers of rank four.[27] The fundamental rule for quaternions is

$$i^2 = j^2 = k^2 = ijk = -1 \tag{8}$$

The above rule applies to the so-called "vector part" of the quaternion. The quaternion is typically broken up into a scalar and a vector part as

$$q = \left\langle q_o, \mathbf{v}_q \right\rangle \tag{9}$$

The components of $\mathbf{v}_q$ are usually denoted by q_1, q_2, and q_3. The next step is to define the operations necessary to utilize quaternions. Addition is performed by simply adding components, analogous to adding two four-dimensional vectors. Quaternions are multiplied using the relationship

$$pq = \left\langle p_0 q_0 - p \cdot q, p_0 \mathbf{v}_q + q_0 \mathbf{v}_p + \mathbf{v}_p \times \mathbf{v}_q \right\rangle \tag{10}$$

where p and q are quaternions whose scalar components are represented by p_0 and q_0 respectively, and vector components are $\mathbf{v}_p$ and $\mathbf{q}_p$ respectively. These relationships are important for using quaternions for attitude representation. Another useful property defines the complex conjugate of the quaternion as

$$q^c = \left\langle q_0, -\mathbf{v}_q \right\rangle \tag{11}$$

The conjugate provides similar functionality to the inverse in matrix multiplication. The next section shows how the quaternion and its properties can be used for representing attitude dynamics.

2.2.2. Attitude Representation with Quaternions. Quaternions can be used to describe a rotation in much the same way as an attitude matrix or a direction cosine matrix does. The attitude quaternion has unit magnitude so the rotation does not affect the magnitude of the vector being rotated. The inverse of the quaternion is the complex conjugate, similar to the inverse of the attitude matrix being equal to the transpose of the attitude matrix.

Let q be the attitude quaternion representing the attitude of a spacecraft, and let the spacecraft have angular velocity ω. The attitude matrix A in Equation (7) can be expressed in terms of the attitude quaternion q as

$$A = \begin{bmatrix} 1-2q_3^2-2q_4^2 & 2(q_2q_3-q_1q_4) & 2(q_2q_4-q_1q_3) \\ 2(q_2q_3-q_1q_4) & 1-2q_2^2-2q_4^2 & 2(q_3q_4-q_1q_2) \\ 2(q_2q_4-q_1q_3) & 2(q_3q_4-q_1q_2) & 1-2q_2^2-2q_3^2 \end{bmatrix} \tag{12}$$

where q_0, q_1, q_2, and q_3 are the elements of the attitude quaternion; the latter three make up the vector v_q. Note that by using quaternions, the attitude matrix in Equation (12) is a function of only four unknowns instead of nine as before with the rotation matrix.

The quaternion can be used to propagate the attitude over time through the dynamic equation

$$\dot{q} = \frac{1}{2} q\boldsymbol{\omega}^* \tag{13}$$

where $\boldsymbol{\omega}^*$ is the quaternion representation of the spacecraft angular velocity, $\langle 0, \boldsymbol{\omega} \rangle$.[27]

2.3. ATTITUDE CALCULATION FROM MAGNETIC FIELD DERIVATIVE

The attitude quaternion can be determined from a (somewhat complicated) quadratic equation shown in this section. Several attempts were made to find the solution to this equation before resorting to attempting the use of a Kalman filter to estimate the attitude quaternion. The system of equations was determined to be under-determined due to linearly dependent equations. Further details are shown in Section 4.2.

2.3.1. Attitude Derivation with Matrices. The basic attitude rotation matrix A relates the magnetic field vector when expressed using inertial and body frames through

$$\mathbf{B}_I = A\mathbf{B}_b \tag{14}$$

The attitude matrix A is a three-by-three matrix with nine separate elements. All elements must be determined to truly know the attitude of the spacecraft. The known quantities in Equation (9) are the magnetic field vector expressed in terms of both the inertial and body frames. The term $\mathbf{B}_\mathrm{I}$ is known from the magnetic field model after inputting the spacecraft position as provided from the orbit determination system. The $\mathbf{B}_\mathrm{b}$

term is the magnetic field measurement obtained directly from the magnetometer. The matrix equation can be broken down from one matrix equation to three scalar equations with nine unknowns. There are more equations relating the different elements of the attitude matrix to each other, which decrease the number of unknowns (these equations are accounted for later).

Differentiating Equation (24) with respect to time gives

$$\dot{\mathbf{B}}_I = \dot{A}\mathbf{B}_b + A\dot{\mathbf{B}}_b \tag{15}$$

It should be noted that by taking the derivative, more unknowns are introduced. However, by using the magnetometer measurement filter, the magnetic field derivative with respect to the body frame can be treated as known. Also, by finite differencing the magnetic field model, the magnetic field derivative with respect to the inertial frame can be considered known. With these two equations, there are now six scalar equations and eighteen unknowns. Although the difference between the number of equations and unknowns has grown, by differentiating one more time the second derivative of the attitude matrix appears. With an attitude model available to quantify the expected angular acceleration on the spacecraft due to perturbations, and knowing the control torques, the attitude second derivative can be considered to be known. Also, the second derivatives of the magnetic field vector expressed in terms of each frame would need to be calculated. If these are found, the system has nine equations and eighteen unknowns. Using the fact that the attitude matrix must not affect the magnitude of the vector it is transforming, nine more equations are gained, and the attitude can be determined.[29] However, the quaternion method, as described in the next section, shows that an analogous approach can be used with quaternion representation that does not require the second derivatives to determine the attitude.

2.3.2. Attitude Determination Using Quaternions. The quaternion approach uses the same basic steps detailed in the previous subsection, with quaternion transformations used instead of the direction cosine matrix. It is shown here that the

number of equations required to solve for the attitude, with the given position and magnetic field measurement, is significantly reduced.

First, start with a basic equation representing the magnetic field vector calculated from the measurement $\mathbf{B}_b$ as

$$\langle 0, \mathbf{B}_b \rangle = q^c \langle 0, \mathbf{B}_I \rangle q \tag{16}$$

where q is the spacecraft attitude quaternion, and q_c is the attitude quaternion conjugate, defined in Equation (11).

When expanded, Equation (16) yields three scalar equations and four unknowns (the elements of the attitude quaternion). Using the same approach as the previous section, the time derivative is taken of the magnetic field equation resulting in

$$\langle 0, \dot{\mathbf{B}}_b \rangle = \dot{q}^c \langle 0, \mathbf{B}_I \rangle q + q^c \langle 0, \dot{\mathbf{B}}_I \rangle q + q^c \langle 0, \mathbf{B}_I \rangle \dot{q} \tag{17}$$

Equations (16) and (17) represents six scalar equations and eight unknowns. By using the fact that the attitude quaternion has unit magnitude, the constraint equations[27]

$$q_0^2 + \mathbf{v}_q \cdot \mathbf{v}_q = 1 \tag{18}$$

$$2q_0\dot{q}_0 + 2q_1\dot{q}_1 + 2q_2\dot{q}_2 + 2q_3\dot{q}_3 = 0 \tag{19}$$

can be obtained.

These equations show that with the use of quaternions the attitude is fully determined without the need for finding the second derivative of the magnetic field vector. Due to the quaternion's lack of "gimbal lock" issues and the ability to resolve the attitude with fewer equations, the use of quaternions was selected over Euler angles with direction cosine matrices (and other options). Because both of these systems are

quadratic, however, multiple attitude and attitude rate combinations solve the given system, requiring a method by which to resolve the correct attitude solution.

The first attempt to address this issue was to solve the equations numerically with an optimization routine. When the initial guess is "close enough" the correct solution should be found. When implemented, however, the initial estimate was often not sufficiently close, causing the optimization routine to diverge. One solution to this problem, presented in the Section 5, is to use Equations (16, 17, 18, and 19) as the input measurement equations to a Kalman filter. The equations relate the measurements $\boldsymbol{B}_b$ and their derivatives to the system states, q, and its derivative. The filter uses the time history of the measurements to determine which attitude solution is the correct solution. An analytical solution would provide a faster solution to the problem and is examined in Section 5.2.

3. MAGNETIC FIELD MODELING

The attitude determination system using magnetometer-only data is dependent on an accurate magnetic field model for the filtering method to successfully converge to an accurate solution. This section describes the process of modeling the Earth's magnetic field and its implications on this research. The World Magnetic Model is used, and the derivative of the magnetic field with respect to time must be found in order to complete the attitude determination system.

3.1. WORLD MAGNETIC MODEL

The model used by the attitude determination system is the World Magnetic Model. [31] The World Magnetic Model uses spherical harmonics to quantify the Earth's magnetic field vector at any point in space over time. The model requires the current time and the position of the spacecraft be specified to return the corresponding magnetic field vector.

A magnetometer measures the direction and magnitude of the Earth's magnetic field in space. The magnetic field changes in direction and magnitude depending on the spatial position near Earth. Using the field as a measurement, and by knowing the spacecraft location, a filter can determine the satellite attitude. The measurements relate to the state-space through nonlinear spherical harmonics. The following sections describe the magnetic field model that relates the magnetic field to the Cartesian spacecraft position.

The Earth's magnetic field vector can be calculated at any point given the time and the position in spherical coordinates. The magnetic field model used in this work takes the form[31]

$$\mathbf{B}(\lambda,\varphi,r,t) = -\nabla V(\lambda,\varphi,r,t) \tag{20}$$

where

$$V(\lambda,\varphi,r,t) = a\left\{\sum_{n=1}^{N}\sum_{m=0}^{n}\left(g_n^m(t)\cos(m\lambda)+h_n^m(t)\sin(m\lambda)\right)\left(\frac{a}{r}\right)^{n+1}\breve{P}_n^m(\sin\varphi)\right\} \quad (21)$$

where spherical coordinates λ, φ, and r are the longitude, latitude, and radial distance to the center of the Earth respectively. The Schmidt semi-normalized associated Legendre polynomials are calculated using

$$\begin{aligned}\breve{P}_n^m(\nu) &= \sqrt{2\frac{(n-m)!}{(n+m)!}}P_{n,m}(\nu) \quad if \;\; m>0\\ \breve{P}_n^m(\nu) &= \qquad\qquad P_{n,m}(\nu) \;\; if \;\; m=0\end{aligned} \quad (22)$$

The parameters g and h in Equation (21) are determined empirically and are available in a tabular format in the World Magnetic Model. The parameter a is the geomagnetic reference radius. The longitude, latitude and radius for spherical coordinates can be easily found from Cartesian coordinates (with appropriate quadrant checks) using

$$r = \sqrt{x^2+y^2+z^2} \quad (23)$$

$$\lambda = \tan^{-1}\left(\frac{y}{x}\right) \quad (24)$$

$$\varphi = \tan^{-1}\left(\frac{z}{\sqrt{x^2+y^2}}\right) \quad (25)$$

The magnetic field vector, expressed in terms of Earth-fixed Cartesian coordinates, is then found by taking the gradient of the potential function, using the chain rule, and substituting in for latitude, longitude, and radius as

$$\mathbf{B}(x,y,z,t) = -J(x,y,z,t)^{\mathrm{T}} \nabla \mathbf{V}(\lambda,\varphi,r,t) \tag{26}$$

where

$$\nabla V(\lambda,\varphi,r,t) = \begin{bmatrix} \frac{\partial V}{\partial \lambda} \\ \frac{\partial V}{\partial \varphi} \\ \frac{\partial V}{\partial r} \end{bmatrix} = \begin{bmatrix} a\left\{\sum_{n=1}^{N}\sum_{m=0}^{n}\left(\frac{a}{r}\right)^{n+1} m\breve{P}_n^m[\sin\varphi]\left(h_n^m(t)\cos(m\lambda) - g_n^m(t)\sin(m\lambda)\right)\right\} \\ a\left\{\sum_{n=1}^{N}\sum_{m=0}^{n}\frac{d}{d\varphi}\left(\breve{P}_n^m[\sin\varphi]\right)\left(g_n^m(t)\cos(m\lambda) + h_n^m(t)\sin(m\lambda)\right)\right\} \\ -\left\{\sum_{n=1}^{N}\sum_{m=0}^{n}\left(h_n^m(t)\cos(m\lambda) - g_n^m(t)\sin(m\lambda)\right)(n+1)\left(\frac{a}{r}\right)^{n+2} m\breve{P}_n^m[\sin\varphi]\right\} \end{bmatrix} \tag{27}$$

$$\frac{d}{d\varphi}\breve{P}_n^m[\sin\varphi] = \sqrt{2\frac{(n-m)!}{(n+m)!}}\left(P_{n,m+1}\left[\sin(\varphi)\right] - m\tan(\varphi)P_{n,m}\left[\sin(\varphi)\right]\right) \tag{28}$$

and

$$J = \begin{bmatrix} \frac{-zx(x^2+y^2)^{-\frac{1}{2}}}{(x^2+y^2+z^2)} & \frac{-zy(x^2+y^2)^{-\frac{1}{2}}}{(x^2+y^2+z^2)} & \frac{\sqrt{x^2+y^2}}{(x^2+y^2+z^2)} \\ \frac{-y}{x^2+y^2} & \frac{1}{x+\frac{y^2}{x}} & 0 \\ \frac{x}{\sqrt{x^2+y^2+z^2}} & \frac{y}{\sqrt{x^2+y^2+z^2}} & \frac{z}{\sqrt{x^2+y^2+z^2}} \end{bmatrix} \tag{29}$$

The resulting vector is in the Earth-fixed frame and is then rotated to the Earth-centered inertial (ECI) frame. The above equations allow one to calculate the magnetic

field vector in units of nanoTesla, nT. The conversion to milliGauss, mG, is accomplished using the simple relationship

$$1\,mG = 100\,nT \tag{30}$$

The conversion is needed because the magnetometer used in this study measures in units of mG. The coefficients $g_n^m(t)$ and $h_n^m(t)$ are calculated as

$$\begin{aligned} g_n^m(t) &= g_n^m(t_0) + (t - t_0)\dot{g}_n^m(t_0) \\ h_n^m(t) &= h_n^m(t_0) + (t - t_0)\dot{h}_n^m(t_0) \end{aligned} \tag{31}$$

where t is in years and t_0 = 2010.0. The coefficients $g_n^m(t_0)$, $h_n^m(t_0)$ and their derivatives were taken from the World Magnetic Model database.

Using the equations above, the magnetic field vector can be calculated at any point in space and time. This model is used to simulate the magnetic field measurements, as well as provide the truth model for this research. The accuracy of this model does not reflect the overall accuracy of the final attitude filter because the truth model of the spacecraft attitude is what ultimately determines the accuracy achieved. However, because the method depends on the magnetic field derivative, that must also be modeled. Because an attempt to obtain the derivative analytically did not provide useful results, the magnetic field derivative model is found by finite differencing of the magnetic field model as detailed in the next section.

3.2. CALCULATING THE MAGNETIC FIELD DERIVATIVE

In order to use the magnetic field measurements to determine the satellite attitude, the actual magnetic field vector must be known. Additionally, the Earth's magnetic field is a highly complex, dynamic system, so the magnetic field varies with both location and time. Though highly nonlinear, the magnetic field can be modeled using spherical harmonics as shown in Section 3.1. Using the orbital position vector obtained from the

orbit determination process, the magnetic field vector is thereby known as a function of time and spacecraft position.

Time derivatives of the magnetic field must also be calculated for use later in the attitude determination algorithm. Finite differencing of the magnetic field model is used to calculate the needed magnetic field derivatives. The finite differencing technique used for this dissertation study was central differencing. The magnetic field derivative can be calculated from the chain rule as

$$\frac{d}{dt}B(x,y,z,t)=\begin{bmatrix}\frac{\partial B_x}{\partial x}\frac{dx}{dt}+\frac{\partial B_x}{\partial y}\frac{dy}{dt}+\frac{\partial B_x}{\partial z}\frac{dz}{dt}+\frac{\partial B_x}{\partial t}\\ \frac{\partial B_y}{\partial x}\frac{dx}{dt}+\frac{\partial B_y}{\partial y}\frac{dy}{dt}+\frac{\partial B_y}{\partial z}\frac{dz}{dt}+\frac{\partial B_y}{\partial t}\\ \frac{\partial B_z}{\partial x}\frac{dx}{dt}+\frac{\partial B_z}{\partial y}\frac{dy}{dt}+\frac{\partial B_z}{\partial z}\frac{dz}{dt}+\frac{\partial B_z}{\partial t}\end{bmatrix} \tag{32}$$

The equation can be rearranged such that

$$\frac{d}{dt}B(x,y,z,t)=\begin{bmatrix}\frac{\partial B_x}{\partial x} & \frac{\partial B_x}{\partial y} & \frac{\partial B_x}{\partial z}\\ \frac{\partial B_y}{\partial x} & \frac{\partial B_y}{\partial y} & \frac{\partial B_y}{\partial z}\\ \frac{\partial B_z}{\partial x} & \frac{\partial B_z}{\partial y} & \frac{\partial B_z}{\partial z}\end{bmatrix}\begin{bmatrix}\frac{dx}{dt}\\ \frac{dy}{dt}\\ \frac{dz}{dt}\end{bmatrix}+\begin{bmatrix}\frac{\partial B_x}{\partial t}\\ \frac{\partial B_y}{\partial t}\\ \frac{\partial B_z}{\partial t}\end{bmatrix} \tag{33}$$

The gradient of the magnetic field vector is given by

$$\nabla\mathbf{B}=\begin{bmatrix}\frac{\partial B_x}{\partial x} & \frac{\partial B_x}{\partial y} & \frac{\partial B_x}{\partial z}\\ \frac{\partial B_y}{\partial x} & \frac{\partial B_y}{\partial y} & \frac{\partial B_y}{\partial z}\\ \frac{\partial B_z}{\partial x} & \frac{\partial B_z}{\partial y} & \frac{\partial B_z}{\partial z}\end{bmatrix} \tag{34}$$

And the spacecraft velocity vector, **V**, is

$$\mathbf{V} = \begin{bmatrix} \frac{dx}{dt} \\ \frac{dy}{dt} \\ \frac{dz}{dt} \end{bmatrix} \tag{35}$$

The columns of the gradient matrix in Equation (82) are given by

$$\begin{aligned} \frac{\partial \mathbf{B}}{\partial x} &= \frac{\mathbf{B}(x+\Delta x, y, z, t) - \mathbf{B}(x-\Delta x, y, z, t)}{2\Delta x} \\ \frac{\partial \mathbf{B}}{\partial y} &= \frac{\mathbf{B}(x, y+\Delta y, z, t) - \mathbf{B}(x, y-\Delta y, z, t)}{2\Delta y} \\ \frac{\partial \mathbf{B}}{\partial z} &= \frac{\mathbf{B}(x, y, z+\Delta z, t) - \mathbf{B}(x, y, z-\Delta z, t)}{2\Delta z} \end{aligned} \tag{36}$$

Substituting the gradient of the magnetic field and the spacecraft velocity into Equation (33) yields

$$\dot{\mathbf{B}} = \nabla \mathbf{B}\mathbf{V} + \frac{\partial \mathbf{B}}{\partial t} \tag{37}$$

where

$$\frac{\partial \mathbf{B}}{\partial t} = \frac{\mathbf{B}(x, y, z, t+\Delta t) - \mathbf{B}(x, y, z, t-\Delta t)}{2\Delta t} \tag{38}$$

is also obtained through central finite differencing.

Equation (37) quantifies the magnetic field derivative, where **V** is the inertially referenced spacecraft velocity vector expressed using Cartesian coordinates.

4. FIRST STAGE FILTER DESIGN

The method described in this dissertation uses two steps or "stages." The first step is to determine more information from the magnetic field measurements and then use that information in the second step to estimate the spacecraft attitude. Finding the magnetic field derivative or the spacecraft's angular rate would be helpful in this case, as either one would provide the information necessary to determine the attitude. In a previous study, finding only the magnetic field derivative led to ambiguities if the spacecraft angular rate was not sufficiently high.[32] The purpose of this section is to examine and evaluate a few key methods for determining either the magnetic field derivative or the spacecraft angular rates for use in the second stage.

It is impossible to take a single magnetometer measurement and determine the spacecraft attitude at a single point in time. A measurement taken from one attitude (orientation) is the exact same as a measurement that would result after rotating the satellite (i.e., the magnetometer) about the local magnetic field vector. In typical spacecraft bus designs additional sensors provide sufficient information so that a particular set of measurements can only lead to one attitude without ambiguity. In order to perform magnetometer-only attitude determination, the time history of measurements must be used in some manner to allow the estimator to resolve the attitude about the local magnetic field vector. The approach used in this study involves the development of a dual stage filter. The problem is broken into two stages: first, find the magnetic field derivative, and second, use the derivative in conjunction with the measurement to estimate the spacecraft attitude. Three methods were tested in this study to perform this first stage operation and they are presented in subsequent sections.

4.1. EXTENDED KALMAN FILTER

The Extended Kalman Filter (EKF) can be used for both the pre-filter and the attitude filter. The Kalman filter provides a way to account for inaccuracies in the dynamic model of a system by combining sensor measurements with knowledge of the system dynamics. A dynamic model is used that describes the system, and measurements

are used that can be related to the states of the system, the quantities that are being estimated. With knowledge of how accurate the system model is, as well as knowledge of how accurate the sensor measurement is, an estimate of the system states is obtained. The Kalman filter propagates the state dynamics and error covariance forward in time.[26]

The Kalman filter is a linear filter so an adaptation must be made to expand to nonlinear systems. The EKF uses linearization on nonlinear systems. Although this is an approximation, it is usually a very good approximation. The EKF calculates the estimate covariance, propagates it, and then uses it to update the states. Consider the system

$$\dot{x} = f\left(x\right) + w \tag{39}$$

$$y = h(x) + v \tag{40}$$

where y is the measurement, w is the process noise and v is the measurement or sensor noise with a mean of zero, and a variance of Q and R, respectively. A set of partial derivative matrices is next defined as

$$\begin{aligned} F &= \frac{\partial}{\partial x} f(x) \\ H &= \frac{\partial}{\partial x} h(x) \end{aligned} \tag{41}$$

The F and H matrices in Equation (41) are the Jacobian matrices of the plant and measurement, respectively. The system is numerically integrated including the states and the estimate covariance.

The system dynamics in Equation (39) are used to propagate the states forward in time. The $f(x)$ function describes the system itself. The model can be very accurate or inaccurate, with the process noise, w, used to account for any inaccuracies. The covariance propagation equation for the EKF takes the form

$$\dot{P} = PF + F^T P + Q \tag{42}$$

where P is the estimate covariance, F is the Jacobian of the system dynamics, and Q is the process noise covariance. The results of the integration are known as the *a priori* state estimate and the covariance, and they are designated by a "bar" above the variable. *Posteriori* estimates are the state and covariance estimates after the filter update has been applied and are designated with a "caret" above them. The estimate and covariance are then updated using the equations

$$\begin{aligned} K_k &= \bar{P}_k H_k{}^T (H_k \bar{P}_k H_k{}^T + R_k)^{-1} \\ \hat{x}_k &= \bar{x}_k + K_k (y_k - h_k(\bar{x}_k, t_k)) \\ \hat{P}_k &= (I - K_k H_k)\bar{P}_k \end{aligned} \tag{43}$$

Results obtained from a Kalman filter are optimal for linear systems, and the Extended Kalman Filter is very accurate and robust in most cases. Another benefit to the Extended Kalman filter is that it is very computationally efficient. In this study, the EKF provided acceptable accuracy while minimizing the impact on the computational requirements.

4.2. MARKOV MODEL AND PRE-FILTER

This section describes how the magnetic field vector is used as a measurement to the pre-filter in order to estimate the magnetic field derivative. The Kalman filter uses a third-order Markov process to model the magnetic field, given by

$$\frac{\mathrm{d}^3}{\mathrm{d}t^3}\mathbf{B} = w \tag{44}$$

where $\mathbf{B}$ is the magnetic field vector and w is white Gaussian process noise. The filter is initialized by using finite differencing on the first three magnetometer measurements.

The use of a third-order Markov process allows the filter to estimate the first and second derivatives of the magnetic field vector as well as the field vector itself. The third-order Markov model used to estimate the magnetic field derivative is given by

$$\begin{aligned} \frac{\mathrm{d}}{\mathrm{d}t}\mathbf{B} &= \dot{\mathbf{B}} \\ \frac{\mathrm{d}}{\mathrm{d}t}\dot{\mathbf{B}} &= \ddot{\mathbf{B}} \\ \frac{\mathrm{d}}{\mathrm{d}t}\ddot{\mathbf{B}} &= \mathbf{0} \end{aligned} \tag{45}$$

The model in Equation (45) represents the dynamics of the pre-filter. The measurement is represented by

$$y = \begin{bmatrix} B_x \\ B_y \\ B_z \end{bmatrix} \tag{46}$$

The state dynamics can be represented as

$$\dot{\mathbf{x}} = \frac{d}{dt}\begin{bmatrix} B_x \\ B_y \\ B_z \\ \dot{B}_x \\ \dot{B}_y \\ \dot{B}_z \\ \ddot{B}_x \\ \ddot{B}_y \\ \ddot{B}_z \end{bmatrix} = \begin{bmatrix} \dot{B}_x \\ \dot{B}_y \\ \dot{B}_z \\ \ddot{B}_x \\ \ddot{B}_y \\ \ddot{B}_z \\ 0 \\ 0 \\ 0 \end{bmatrix} \tag{47}$$

The *F* matrix and measurement matrix, *H*, for the Kalman filter are given by

$$F = \begin{bmatrix} 0 & 0 & 0 & 1 & 0 & 0 & 0 & 0 & 0 \\ 0 & 0 & 0 & 0 & 1 & 0 & 0 & 0 & 0 \\ 0 & 0 & 0 & 0 & 0 & 1 & 0 & 0 & 0 \\ 0 & 0 & 0 & 0 & 0 & 0 & 1 & 0 & 0 \\ 0 & 0 & 0 & 0 & 0 & 0 & 0 & 1 & 0 \\ 0 & 0 & 0 & 0 & 0 & 0 & 0 & 0 & 1 \\ 0 & 0 & 0 & 0 & 0 & 0 & 0 & 0 & 0 \\ 0 & 0 & 0 & 0 & 0 & 0 & 0 & 0 & 0 \\ 0 & 0 & 0 & 0 & 0 & 0 & 0 & 0 & 0 \end{bmatrix} \tag{48}$$

$$H = \begin{bmatrix} 1 & 0 & 0 & 0 & 0 & 0 & 0 & 0 & 0 \\ 0 & 1 & 0 & 0 & 0 & 0 & 0 & 0 & 0 \\ 0 & 0 & 1 & 0 & 0 & 0 & 0 & 0 & 0 \end{bmatrix} \tag{49}$$

The Kalman Filter used for the first-stage filter calculates the *a priori* state estimate as

$$\bar{x}_k = f(\hat{x}_{k-1}, dt) \tag{50}$$

The *a priori* estimate is calculated using the dynamic model. The covariance is propagated using

$$\dot{P} = FP + PF^T + Q \tag{51}$$

The update stage of the Kalman filter proceeds as

$$\begin{aligned} K_k &= \bar{P}_k H_k{}^T (H_k \bar{P}_k H_k{}^T + R_k)^{-1} \\ \hat{x}_k &= \bar{x}_k + K_k (y_k - h_k(\bar{x}_k, t_k)) \\ \hat{P}_k &= (I - K_k H_k) \bar{P}_k \end{aligned} \tag{52}$$

where K is the filter gain, R is the measurement noise covariance, and the caret represents *a posteriori* information. The new estimate is represented by $\hat{x}$.

The first-stage filter results, given below in Figures 4.1 and 4.2, show the estimates of the magnetic field vector and derivative for a simulation running 1000 seconds. The first-stage filter is evaluated for the baseline case discussed in Section 1.5 (an orbit with a 400 km altitude, forty five degrees inclination, and an initial spacecraft angular velocity of [2, 3, 5] degrees per second). The simulation shows that the magnetic field derivative can be accurately estimated even without knowledge of the satellite rotation in the model. The estimates track very closely to the actual data. The error in the magnetic field vector and derivative estimates are shown in Figures 4.3 and 4.4.

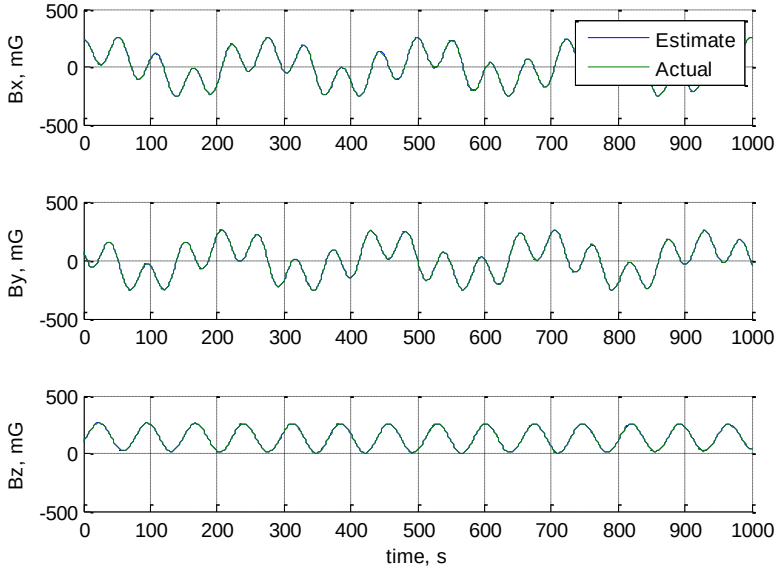

Figure 4.1. Estimated and Actual Magnetic Field Components

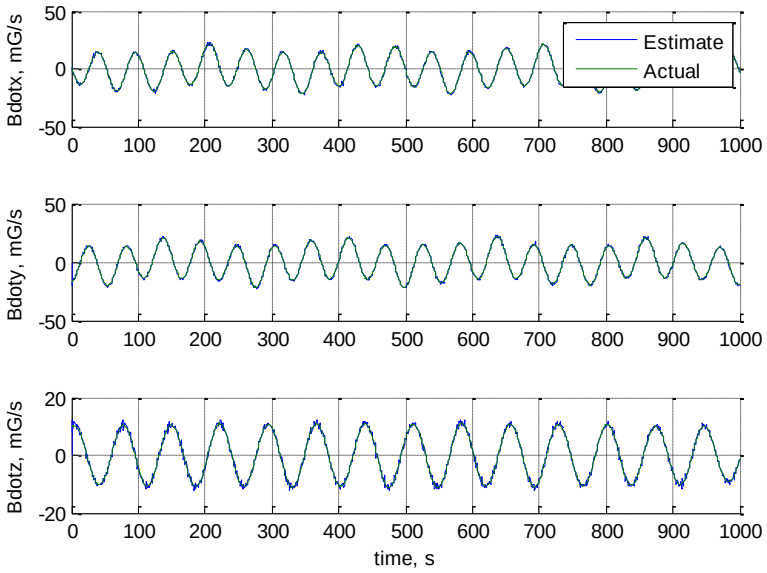

Figure 4.2. Estimated and Actual Magnetic Field Derivative Components

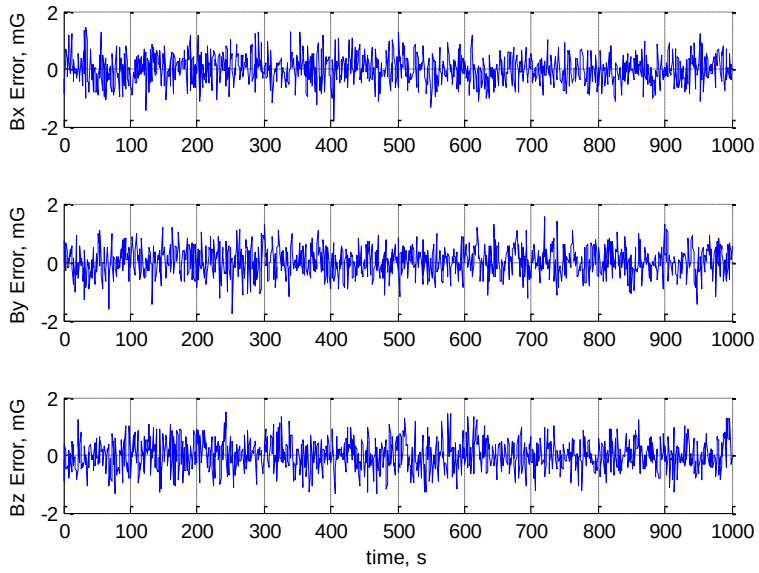

Figure 4.3. Magnetic Field Vector Component Estimation Error

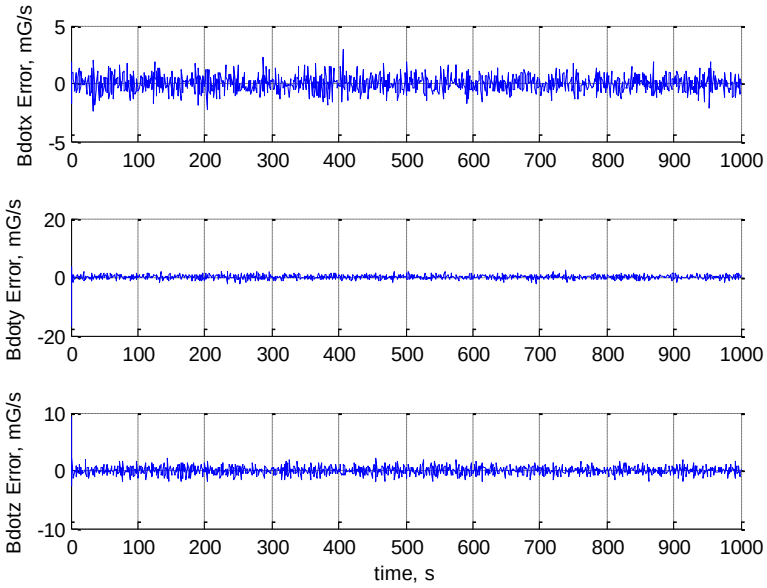

Figure 4.4. Magnetic Field Derivative Vector Component Estimation Error

The first stage filter estimates the magnetic field derivative with sufficient accuracy to calculate the spacecraft attitude. The filter can be tuned to obtain improved results depending on the orbit parameters, but the current initial error covariance and process noise covariance provide consistent results regardless of the simulation conditions considered. The filter parameters have been chosen to make the filter more robust, not specifically tailored to a particular orbit or initial condition.

4.3. CALCULATING OR ESTIMATING ANGULAR VELOCITY

The ability to calculate or estimate the angular velocity from magnetic field data is considered in this section. The link between the angular rate and magnetic field data can be found by using the basic kinematic equation to calculate the derivative of the magnetic field through

$$\dot{\mathbf{B}}_I = \dot{\mathbf{B}}_b + \boldsymbol{\omega} \times \mathbf{B}_b \tag{53}$$

where $\boldsymbol{\omega}$ is the spacecraft angular velocity. The subscripts represent the coordinate frames in which the vectors are referenced. The subscript *I* refers to the J2000 inertial frame, while the subscript *b* refers to the spacecraft body frame.

The complication with solving this equation is that there is no inverse for a cross product operation. Given values for $\dot{\mathbf{B}}_I$, $\dot{\mathbf{B}}_b$, and $\mathbf{B}_b$ there are an infinite number of angular velocity vectors that satisfy Equation (53). What is shown here is that while the equation provides three scalar equations, only two are linearly independent.

A cross product varies due to the length and direction of each vector. To identify a method to solve this equation, an approximation can be used estimate the magnitude of the unknown angular rate vector. The magnetic field with respect to the body frame changes for two reasons: one due to the magnetic field derivative in the inertial frame, and the other due to the rotation of the body frame. The change due to the rotation of the body frame is much more significant than the change in the field due to the temporal and spatial variations. The change due to rotation also does not change the magnitude of the magnetic field vector in either frame. It can be assumed then that the angle between the magnetic field vectors from consecutive measurements is primarily due to the rotation of the two frames. By calculating this angle and dividing by the time step, an angular rotation rate can be calculated that approximates the actual rotation rate magnitude of the body frame. The angle between two measurements can be calculated using

$$\theta = \cos^{-1}\left(\frac{\mathbf{B}_1 \cdot \mathbf{B}_2}{\|\mathbf{B}_1\|\|\mathbf{B}_2\|}\right) \tag{54}$$

Then the angular rate can be approximated as

$$\|\boldsymbol{\omega}\| \approx \frac{\theta}{\Delta t} \tag{55}$$

This is an approximation because the angular change is not solely due to the rotating frame - it also changes because of the spacecraft moving through the magnetic field and the slight variation of the magnetic field itself. This approach can also encounter difficulty if the rotation is about the magnetic field vector. For this reason, a time history should be examined. The following equation can be used as an additional equation to the system of equations and should provide more information to limit the number of solutions possible.

$$\|\boldsymbol{\omega}\|^2 = \omega_x^2 + \omega_y^2 + \omega_z^2 \tag{56}$$

This method shows promise, however there are some factors that could result in the approximation being inaccurate. The time step selected is important. If the time step is too small, the noise in the measurements will cause significant error in the estimate of the angular rate. However, if the time step is too large, the spacecraft could rotate in an "irregular" manner (for example, with a thruster or control mechanism activating) or it could rotate more than one revolution. The angle between the measurements is impossible to determine if the body frame rotates more than once per time step. These challenges are assessed when examining simulation results.

The first simulation is a test case that checks two important aspects: one if the angular velocity magnitude is calculated accurately and secondly to assess if adding this magnitude calculation to the system of equations generated by the cross product is sufficient to provide a unique solution, or at least one that can be solved using a numerical method.

The test scenario plots the angular velocity magnitude error for a case in which the angular velocity is zero. This case demonstrates the accuracy of the angular velocity magnitude estimator, and is the same as the baseline case.

Figure 4.5 shows that the error in the magnitude estimate is small, but could be improved. This simulation does include noisy measurements, so even in the presence of noise, the magnitude of the angular velocity can be calculated to within about 10% error.

The step size used to estimate the magnitude was 10 seconds to reduce the error due to noise.

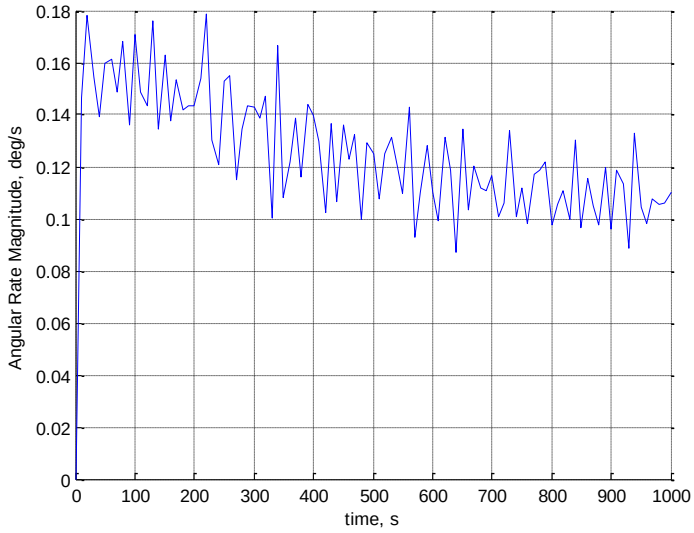

Figure 4.5. Angular Rate Magnitude Error

When trying to determine the "inverse" of a cross product, varying either the magnitude or direction of the vector can produce the same cross product, resulting in the existence of infinite solutions to the problem. The approach of this method is to fix the magnitude so that only the unit vector in the correct direction is required to be found, potentially making the problem solvable. Determining the magnitude of the angular rate vector accurately becomes the goal that is required to resolve the ambiguity. The angular velocity magnitude can be found using the method shown above, or it can be found using a filtering technique that allows for the consideration of a history of measurements (and not just be dependent on the last two measurements). The results of this analysis are used in Section 4.5 to enable successful development of the angular velocity estimator.

4.4. IMPROVED DYNAMIC MODEL

A Markov model was used in a previous section to represent the dynamics of the magnetic field. In this section, the model is updated to more accurately reflect the true dynamics. The basic kinematic equation is used to derive the state dynamics.

Using the basic kinematic equation to express the magnetic field vector derivative in terms of the spacecraft angular velocity results in the expression

$$\dot{\mathbf{B}}_I = \dot{\mathbf{B}}_b + \boldsymbol{\omega} \times \mathbf{B}_b \tag{57}$$

The equation is rearranged such that

$$\dot{\mathbf{B}}_b = \dot{\mathbf{B}}_I - \boldsymbol{\omega} \times \mathbf{B}_b \tag{58}$$

The term $\dot{\mathbf{B}}_I$ can be ignored because the change in the magnetic field vector due to the field changing at the spacecraft position as the spacecraft moves through the field on its orbit is very small compared to the term $\boldsymbol{\omega} \times \mathbf{B}_b$, and this inertial derivative is treated as process noise.

It is also desired to estimate the magnetic field derivative. The dynamic equation (58) can be differentiated to yield

$$\ddot{\mathbf{B}}_b = -\dot{\boldsymbol{\omega}} \times \mathbf{B}_b + \boldsymbol{\omega} \times \left(\boldsymbol{\omega} \times \mathbf{B}_b \right) \tag{59}$$

Because the angular velocity appears in the new dynamic equations, the angular velocity needs to be treated as a filter state. The angular velocity dynamic equations (i.e., Euler's equations of motion) depend on the moments of inertia of the spacecraft and the current angular velocity and are given by

$$\dot{\boldsymbol{\omega}} = \begin{bmatrix} \dfrac{M_x - (I_z - I_y)\omega_y\omega_z}{I_x} \\ \dfrac{M_y - (I_x - I_z)\omega_x\omega_z}{I_y} \\ \dfrac{M_z - (I_y - I_x)\omega_x\omega_y}{I_z} \end{bmatrix} \tag{60}$$

With the addition of the new state and the new dynamics, the Kalman filter matrices must change. The measurement input to this filter is still the same. The Kalman filter dynamics and measurements equations are presented below.

The measurements for the attitude filter are

$$y = \begin{bmatrix} B_{b_x} \\ B_{b_y} \\ B_{b_z} \end{bmatrix} \tag{61}$$

The system dynamics are represented using the magnetic field kinematic equations and Euler's equations of motion as

$$\frac{\mathrm{d}}{\mathrm{d}t}\begin{bmatrix} \mathbf{B}_b \\ \dot{\mathbf{B}}_b \\ \omega_x \\ \omega_y \\ \omega_z \end{bmatrix} = \begin{bmatrix} -\boldsymbol{\omega}\times\mathbf{B}_b \\ -\dot{\boldsymbol{\omega}}\times\mathbf{B}_b + \boldsymbol{\omega}\times\left(\boldsymbol{\omega}\times\mathbf{B}_b\right) \\ \dfrac{M_x - (I_z - I_y)\omega_y\omega_z}{I_x} \\ \dfrac{M_y - (I_x - I_z)\omega_x\omega_z}{I_y} \\ \dfrac{M_z - (I_y - I_x)\omega_x\omega_y}{I_z} \end{bmatrix} \tag{62}$$

The filter measurement matrix becomes

$$H = \begin{bmatrix} 1 & 0 & 0 & 0 & 0 & 0 & 0 & 0 & 0 \\ 0 & 1 & 0 & 0 & 0 & 0 & 0 & 0 & 0 \\ 0 & 0 & 1 & 0 & 0 & 0 & 0 & 0 & 0 \end{bmatrix} \tag{63}$$

The angular rate estimator uses a Kalman filter with the following initial covariance and noise covariance matrices.

$$P_0 = \begin{bmatrix} 10^3 I_{3\times3} & 0_{3\times3} & 0_{3\times3} \\ 0_{3\times3} & 10^5 I_{3\times3} & 0_{3\times3} \\ 0_{3\times3} & 0_{3\times3} & 10^{-2} I_{3\times3} \end{bmatrix} \tag{64}$$

$$Q = \begin{bmatrix} 10^{-3} I_{3\times3} & 0_{3\times3} & 0_{3\times3} \\ 0_{3\times3} & 10^{-1} I_{3\times3} & 0_{3\times3} \\ 0_{3\times3} & 0_{3\times3} & 10^{-9} I_{3\times3} \end{bmatrix} \tag{65}$$

$$R = 10^{-2} I_{3\times3} \tag{66}$$

The magnetic field model, known spacecraft velocity, and estimated initial angular rate can be used to provide an initial estimate for the magnetic field and its derivative. The magnetic field vector and its derivative were assumed to have a 3% error added to the true initial value to simulate this offset. The angular rates were initially assumed to be 0.1 degrees per second along each axis.

Figures 4.6-4.12 demonstrate the application of the new method to the baseline scenario.

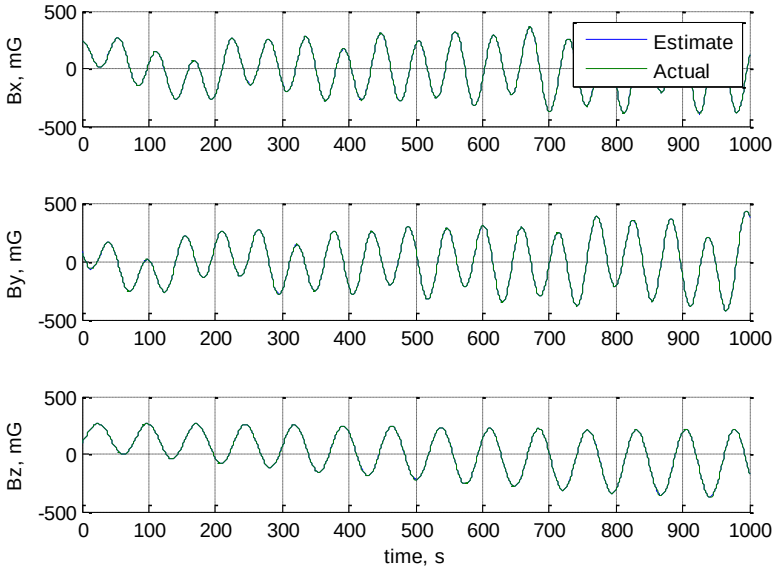

Figure 4.6. Magnetic Field Vector

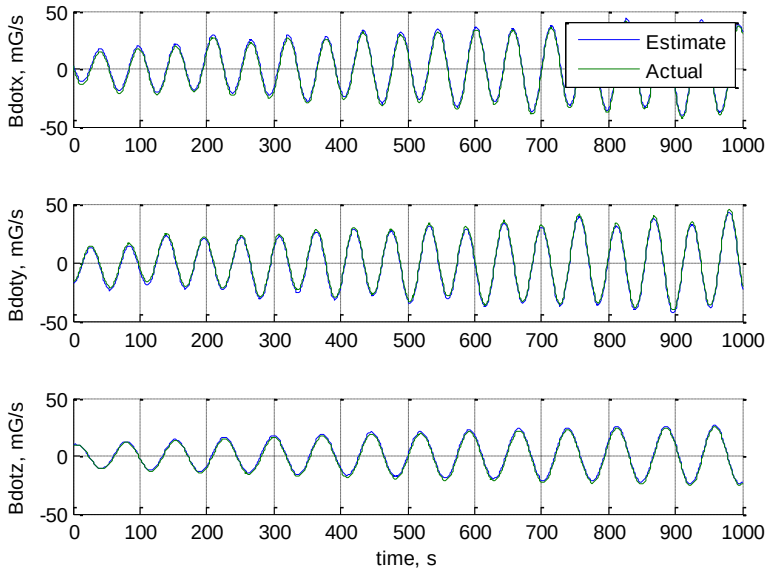

Figure 4.7. Magnetic Field Derivative Vector

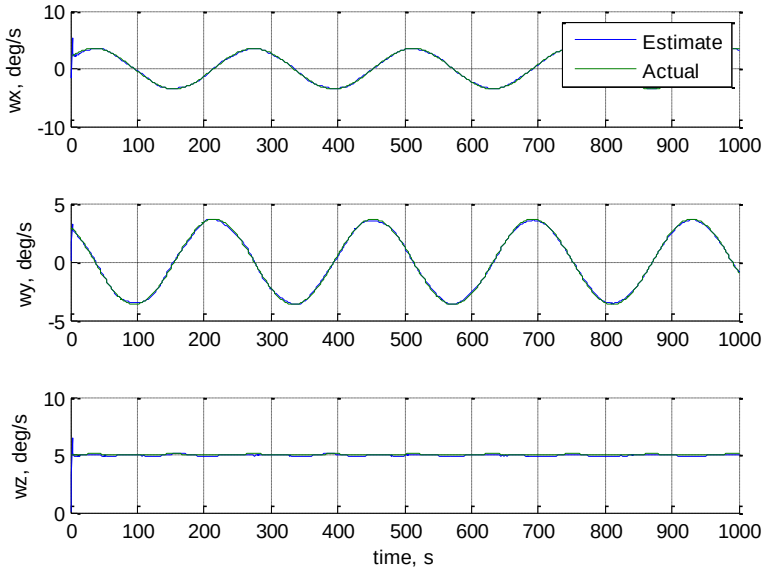

Figure 4.8. Spacecraft Angular Rate

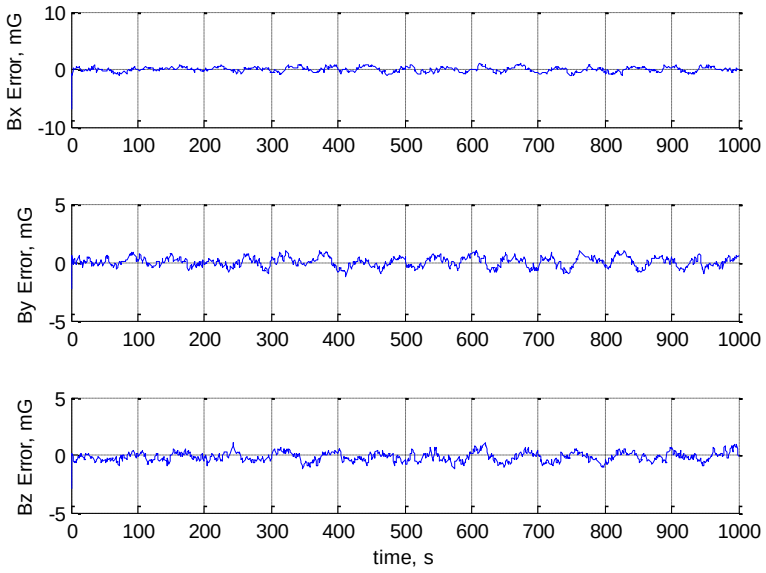

Figure 4.9. Magnetic Field Vector Error

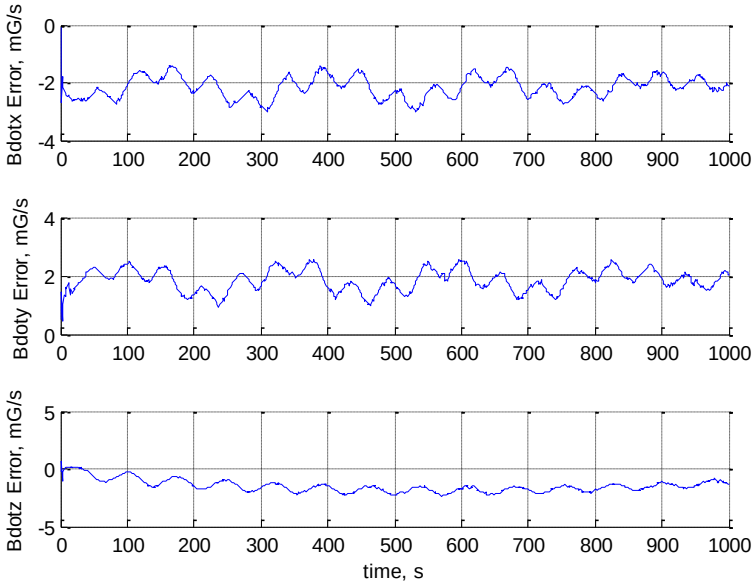

Figure 4.10. Magnetic Field Derivative Vector Error

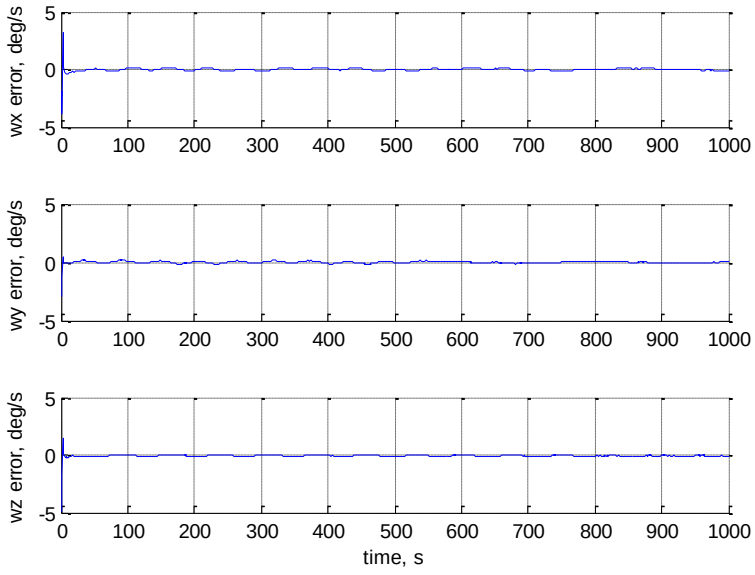

Figure 4.11. Spacecraft Angular Rate Error

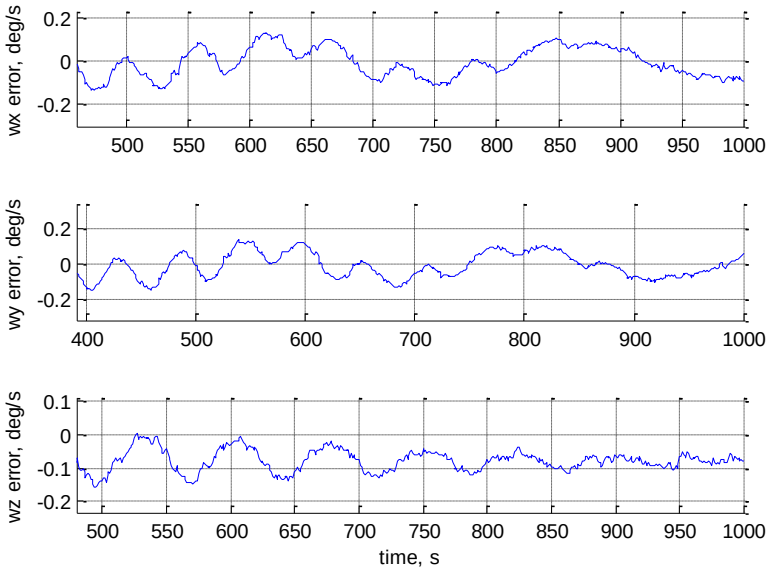

Figure 4.12. Spacecraft Angular Rate Error Zoomed

The estimator works very well for the baseline case. The case with no angular velocity presented convergence difficulties for the other filtering algorithms considered; therefore, it is important to test this case. The filter matrices are set to the same values as the previous simulation. Figures 4.13-4.19 show the estimates and errors from the three states in the state vector and a zoomed in view of the angular rate error. The error in this scenario is similar; however, there is more of a bias in the estimate.

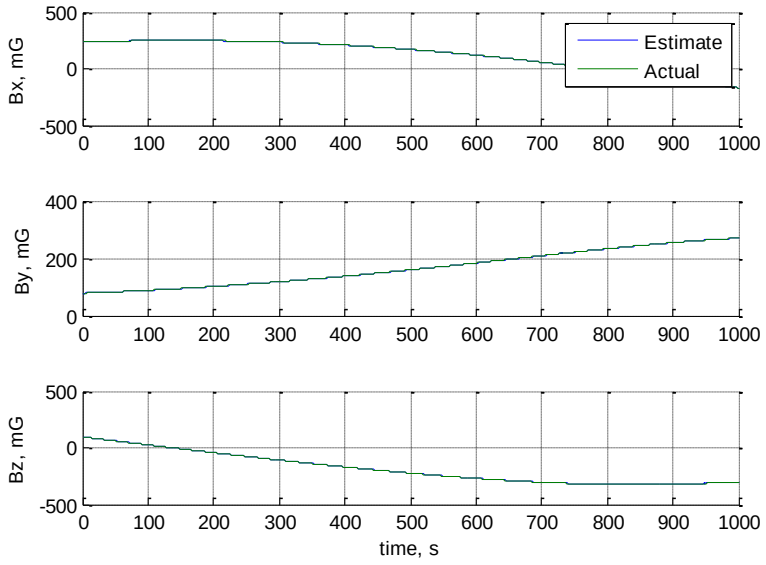

Figure 4.13. Magnetic Field Vector

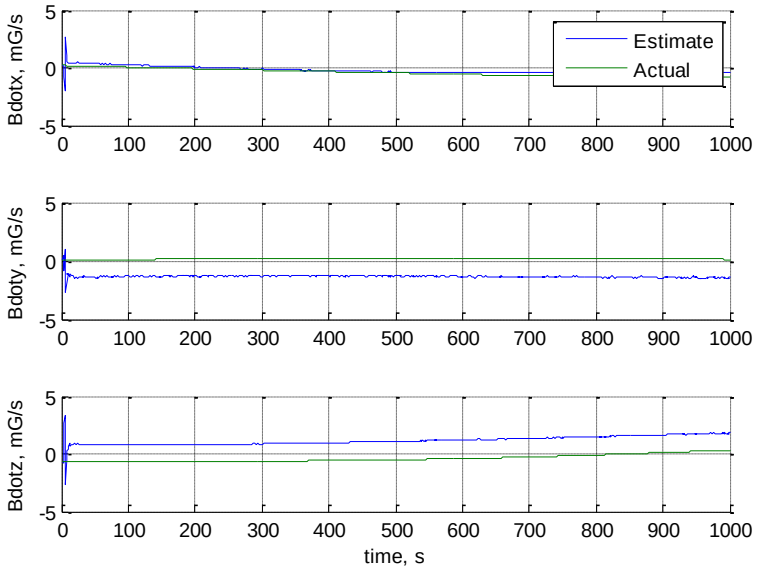

Figure 4.14. Magnetic Field Derivative Vector

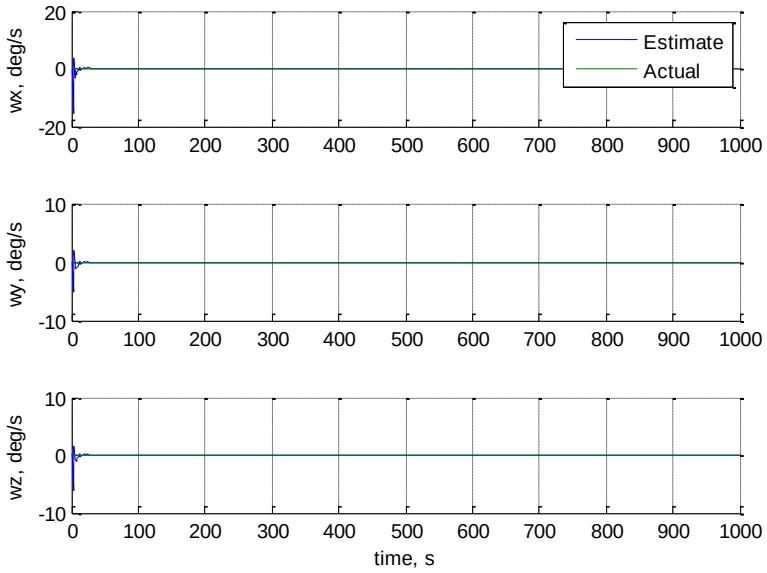

Figure 4.15. Spacecraft Angular Rate

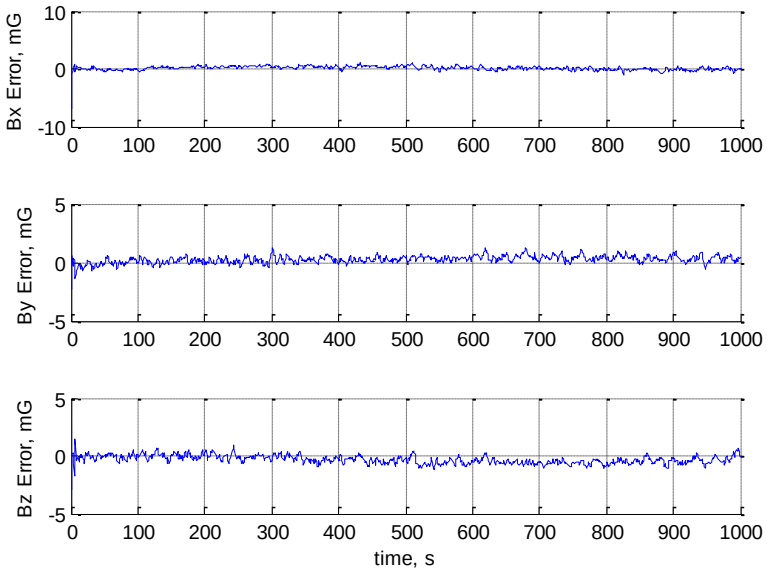

Figure 4.16. Magnetic Field Vector Error

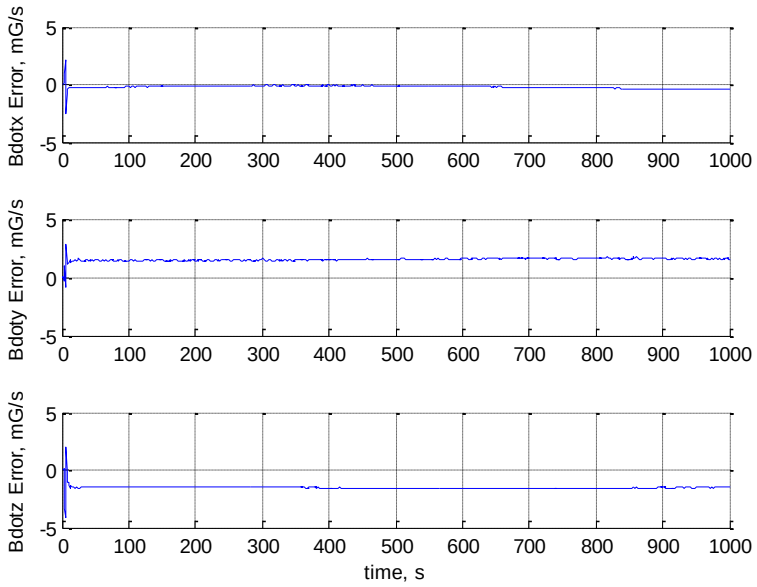

Figure 4.17. Magnetic Field Derivative Vector Error

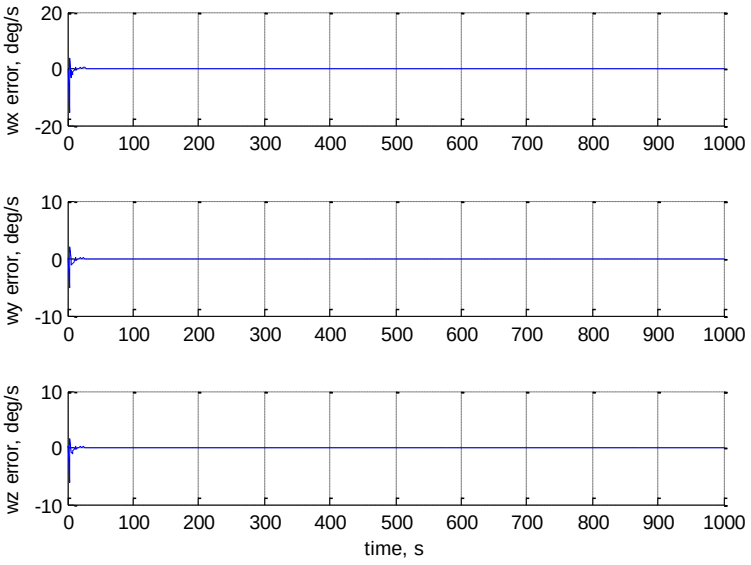

Figure 4.18. Spacecraft Angular Rate Error

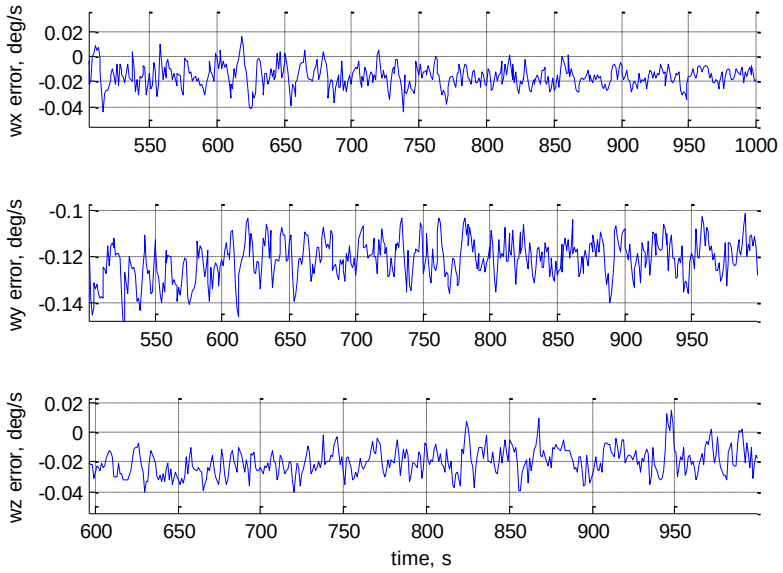

Figure 4.19. Spacecraft Angular Rate Error Zoomed

The estimate show that there is a bias in the estimate of ω_y. The next section addresses this limitation by attempting to remove the bias by adding the pseudomeasurement derived in Section 4.3.

4.5. ADDITION OF PSEUDOMEASUREMENT

The linear dependence observed in the equations of Section 4.3 may be the source of difficulties when the angular velocity is zero. There are an infinite number of solutions to the equations requiring the filter to use the time history of measurements to determine the correct state estimate. When the angular velocity is zero or low, there is very little change in the time history and observability could become marginal. As shown in Section 4.3, adding the magnitude of the angular velocity resolves the ambiguity with the underdetermined system. The magnitude of the angular velocity can be determined as shown in Section 4.3 by examining the magnetic field vector history.

The filter uses the square of the estimated angular velocity magnitude, simplifying the calculation of the Kalman filter measurement matrix. The system dynamics are

$$\frac{\mathrm{d}}{\mathrm{d}t}\begin{bmatrix}\mathbf{B}_b\\ \dot{\mathbf{B}}_b\\ \omega_x\\ \omega_y\\ \omega_z\end{bmatrix}=\begin{bmatrix}-\boldsymbol{\omega}\times\mathbf{B}_b\\ -\dot{\boldsymbol{\omega}}\times\mathbf{B}_b+\boldsymbol{\omega}\times\left(\boldsymbol{\omega}\times\mathbf{B}_b\right)\\ \dfrac{M_x-(I_z-I_y)\omega_y\omega_z}{I_x}\\ \dfrac{M_y-(I_x-I_z)\omega_x\omega_z}{I_y}\\ \dfrac{M_z-(I_y-I_x)\omega_x\omega_y}{I_z}\end{bmatrix} \tag{67}$$

The measurements for the filter are

$$y=\begin{bmatrix}B_{b_x}\\ B_{b_y}\\ B_{b_z}\\ \|\omega\|^2\end{bmatrix} \tag{68}$$

The filter measurement matrix becomes

$$H=\begin{bmatrix}1&0&0&0&0&0&0&0&0\\ 0&1&0&0&0&0&0&0&0\\ 0&0&1&0&0&0&0&0&0\\ 0&0&0&0&0&0&2\omega_x&2\omega_y&2\omega_z\end{bmatrix} \tag{69}$$

The baseline scenario used a Kalman filter with the following initial covariance and noise covariance matrices.

$$P_0 = \begin{bmatrix} 10^3 I_{3\times3} & 0_{3\times3} & 0_{3\times3} \\ 0_{3\times3} & 10^5 I_{3\times3} & 0_{3\times3} \\ 0_{3\times3} & 0_{3\times3} & 10^{-2} I_{3\times3} \end{bmatrix} \tag{70}$$

$$Q = \begin{bmatrix} 10^{-3} I_{3\times3} & 0_{3\times3} & 0_{3\times3} \\ 0_{3\times3} & 10^{-1} I_{3\times3} & 0_{3\times3} \\ 0_{3\times3} & 0_{3\times3} & 10^{-9} I_{3\times3} \end{bmatrix} \tag{71}$$

$$R = \begin{bmatrix} 10^{-2} I_{3\times3} & 0_{3\times1} \\ 0_{1\times3} & 10^{-4} \end{bmatrix} \tag{72}$$

The magnetic field vector and its derivative were assumed to have a 3% error added to the true initial value. The angular rates were initially assumed to be 0.1 degrees per second in each axis.

Figures 4.20-4.25 plot the results of the simulation using the baseline scenario and the new pseudomeasurement. The accuracy achieved in angular velocity estimation is around 0.1 degrees per second.

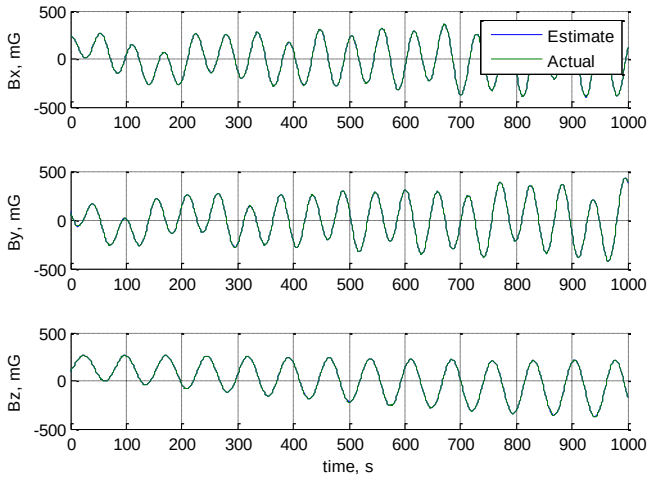

Figure 4.20. Magnetic Field Vector

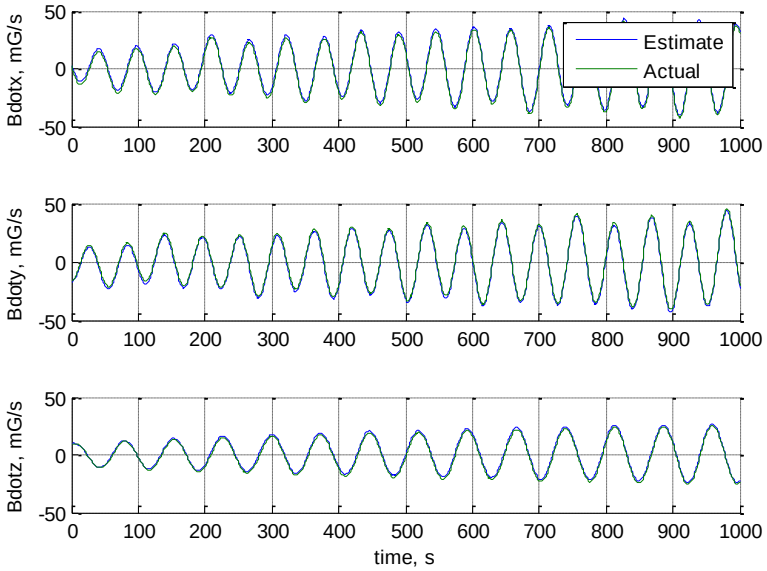

Figure 4.21. Magnetic Field Derivative Vector

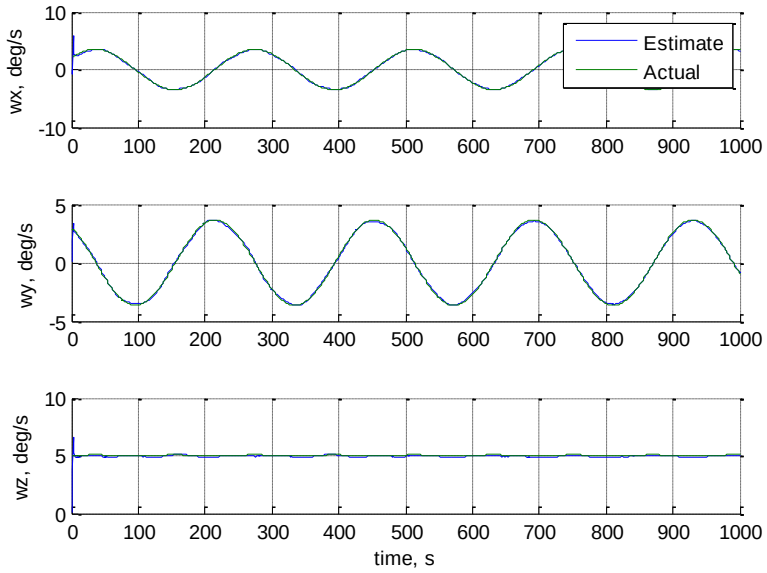

Figure 4.22. Spacecraft Angular Rate

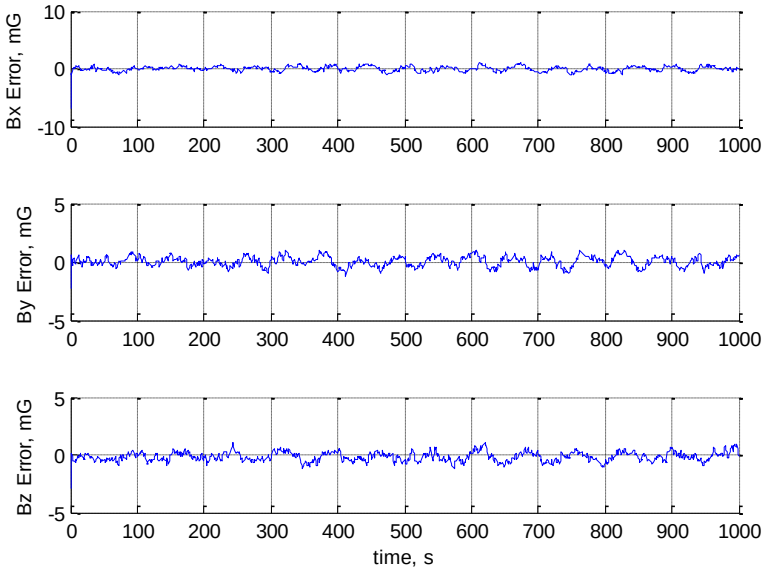

Figure 4.23. Magnetic Field Vector Error

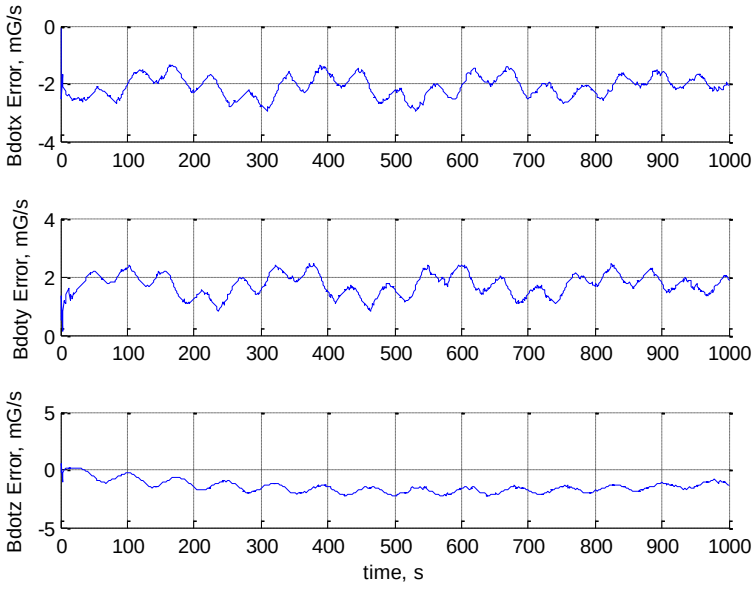

Figure 4.24. Magnetic Field Derivative Vector Error

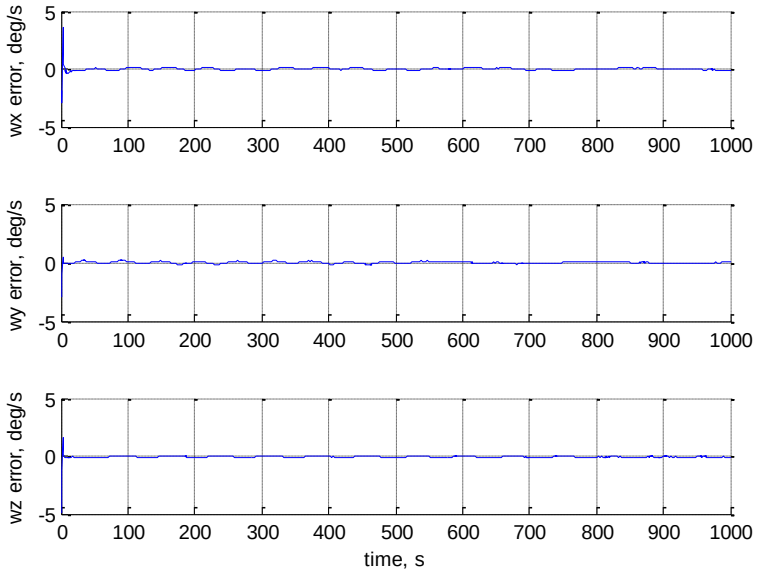

Figure 4.25. Spacecraft Angular Rate Error

As expected, the first stage filter is able to estimate the magnetic field derivative and the angular velocity very well. It is now important to investigate the scenario where the angular velocity is zero. The simulation results for the zero angular velocity case are displayed in Figures 4.26-4.32.

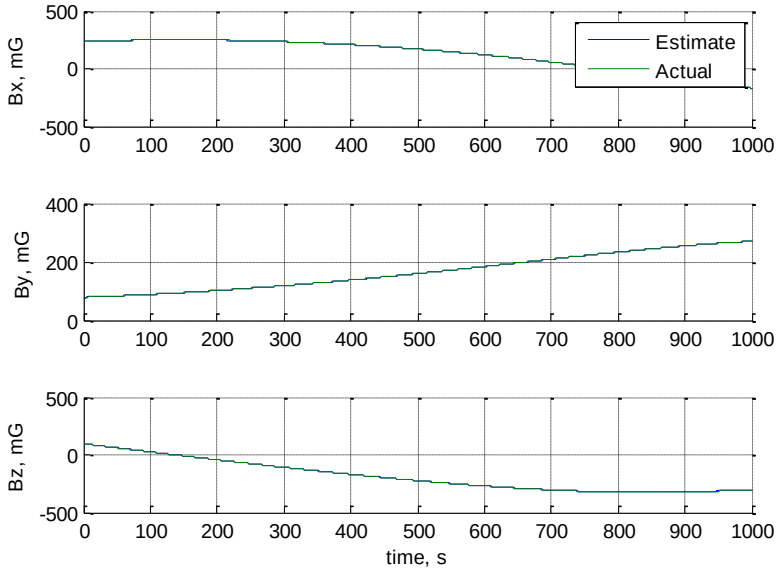

Figure 4.26. Magnetic Field Vector

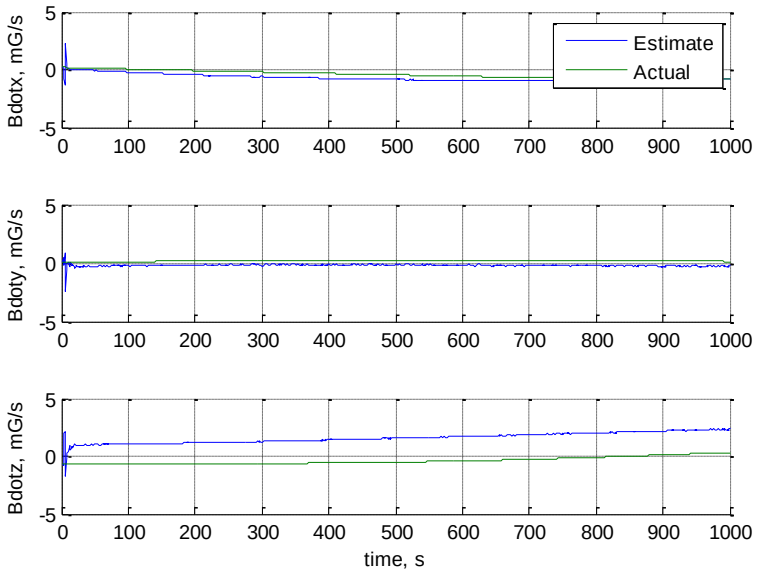

Figure 4.27. Magnetic Field Derivative Vector

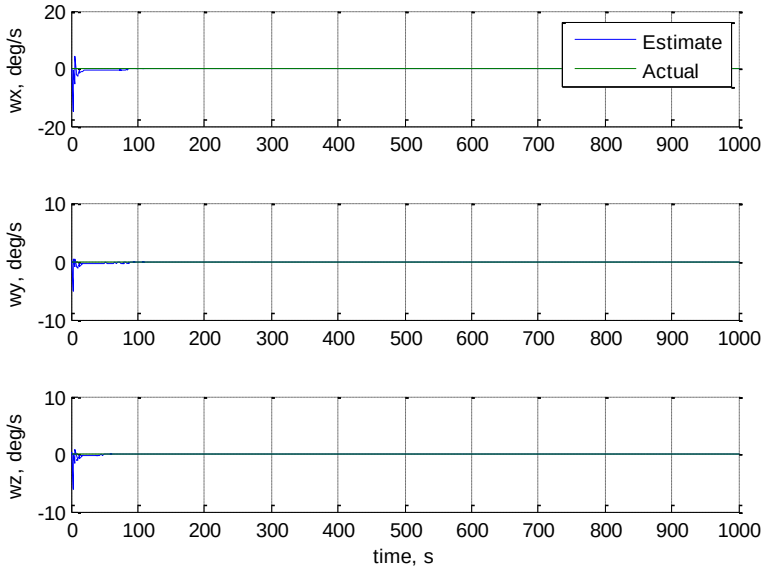

Figure 4.28. Spacecraft Angular Rate

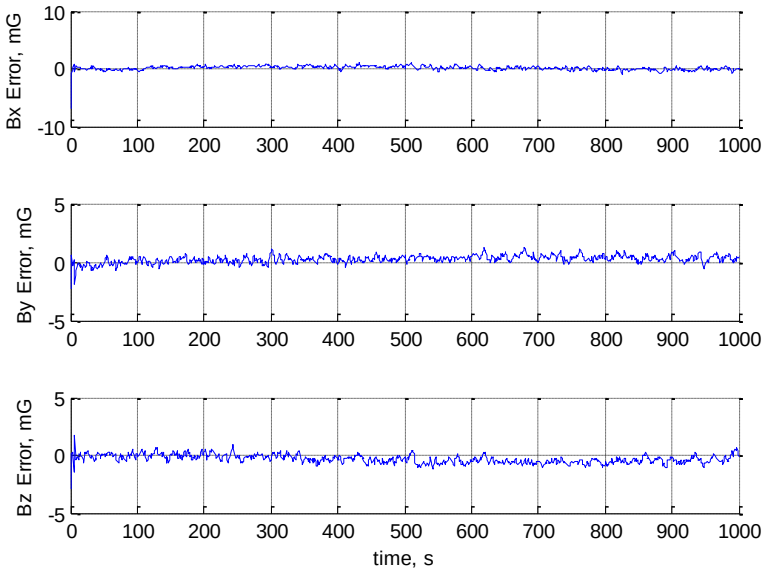

Figure 4.29. Magnetic Field Vector Error

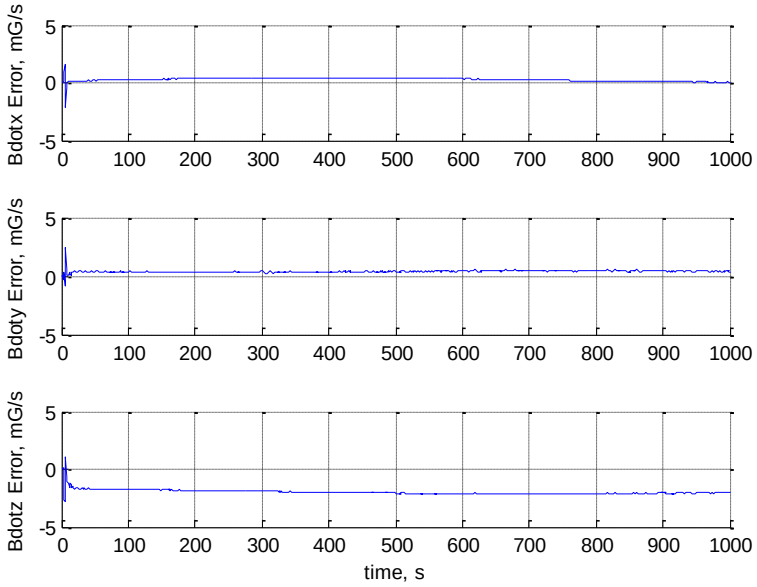

Figure 4.30. Magnetic Field Derivative Vector Error

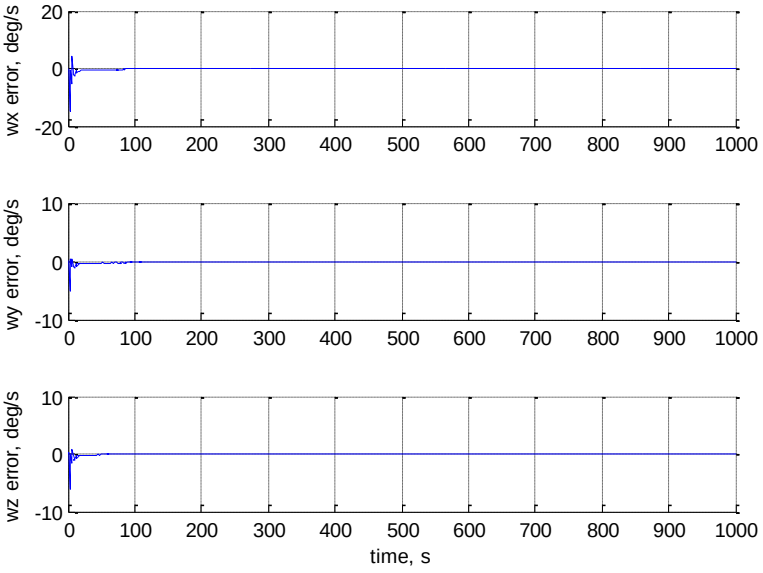

Figure 4.31. Spacecraft Angular Rate Error

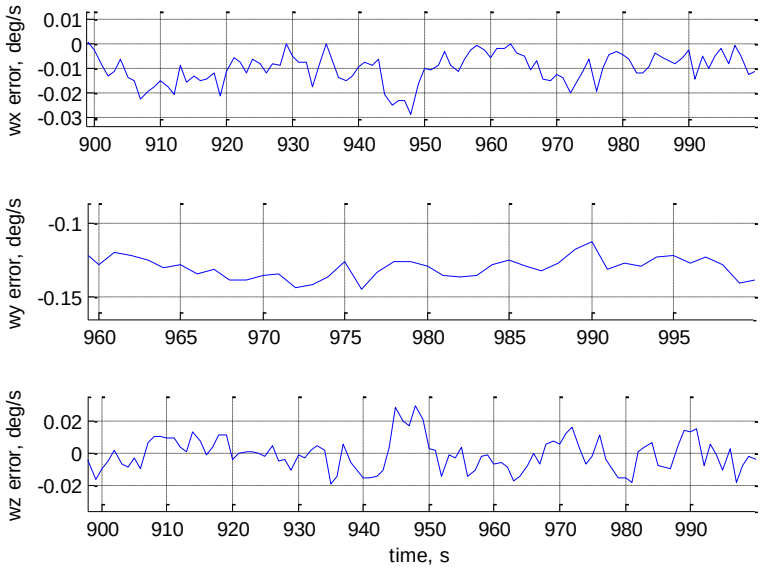

Figure 4.32. Spacecraft Angular Rate Error Zoomed

The simulation shows a slight improvement in the accuracy of the angular velocity estimate. Bias can still be observed in the estimation of ω_y and the elements of $\dot{\mathbf{B}}_b$. The bias in the angular rate could be due to limited observability caused by the lack of rotation or by ignoring the inertial magnetic field derivative. The bias in the magnetic field derivative vector is present because there is no filter update to $\dot{\mathbf{B}}_b$. The bias in angular rate directly causes the bias in $\dot{\mathbf{B}}_b$. This estimation process of the angular velocity is used in Section 5.5 to estimate the spacecraft attitude.

5. SECOND STAGE FILTER DESIGN

5.1. ATTITUDE DETERMINATION FILTER

Providing the first derivative of the magnetic field measurement to the attitude filter gives two vectors each expressed in terms of two different frames, which from past well-known attitude determination studies suggests that the TRIAD method may be a good choice to uniquely calculate the spacecraft attitude.[14] The TRIAD method is used to determine the attitude rotation that results from having two different vectors expressed in two different coordinate frames; however if one vector is a derivative, the rotation of the body frame must be accounted for in the applicable kinematic equations. Additionally, the magnetic field derivative depends not only on fluctuations in the Earth's magnetic field, but also on the satellite's angular velocity, due to the magnetic field derivative being expressed relative to the rotating body frame. The TRIAD algorithm requires all four vectors, two in each frame, to be inertially referenced. This leads to a complication in this study, because the attitude rate is needed and there are no onboard sensors to provide the attitude rate. This section shows the adjustment used to make the magnetometer-only system viable.

The governing equations for the spacecraft attitude quaternion with respect to the magnetic field vector and derivative are now used to define the filter. Equations (16, 17, 18, and 19) are used to relate the states, attitude quaternion and spacecraft angular rates to the pseudo-measurements, the magnetic field vector and its derivative. These attitude equations provide a system with eight equations and eight unknowns, and this system could theoretically be uniquely solved. However, as noted earlier in Section 2.3.2, the quadratic nature of the equations leads to multiple solutions, and the equations are difficult to solve. Another approach uses the system in a filter that processes a sequence of estimates and measurements to find the best estimate without needing to resolve between two solutions. Accordingly, the next step is to construct an Extended Kalman Filter using the magnetic field vector and its derivative as measurements and estimate the attitude quaternion and rates.

The attitude determination filter is configured to accept the magnetic field and its derivative as measurements with the states for the filter as the attitude quaternion and the

spacecraft angular rates. The states are related to the measurement through the *H* matrix that contains the derivatives of the quaternion equations derived in Section 3. Finite differencing is used to calculate the measurement matrix needed for the EKF filter used in the attitude determination code.

The measurements for the attitude filter are

$$y = \begin{bmatrix} B_{b_x} \\ B_{b_y} \\ B_{b_z} \\ \dot{B}_{b_x} \\ \dot{B}_{b_y} \\ \dot{B}_{b_z} \end{bmatrix} \tag{73}$$

By substituting Equations (13, 16, and 17) into Equation (73), the measurements can be related to the states as

$$y = \begin{bmatrix} q^c \langle 0, B_I \rangle q \\ \dot{q}^c \langle 0, B_I \rangle q + q^c \langle 0, \dot{B}_I \rangle q + q^c \langle 0, B_I \rangle \dot{q} \end{bmatrix} = \begin{bmatrix} q^c \langle 0, B_I \rangle q \\ \frac{1}{2} q^c \omega \langle 0, B_I \rangle q + q^c \langle 0, \dot{B}_I \rangle q + q^c \langle 0, B_I \rangle \frac{1}{2} q\omega \end{bmatrix} \tag{74}$$

Note that in the above equation, the multiplications are quaternion multiplications and the brackets around the magnetic field values indicate that a zero is added as the first element so that the vector becomes a four element vector that can be multiplied with quaternions. It is also assumed that the first element (which is always zero) of each resultant four-element vector is removed after the multiplications (in order to preserve the dimension of *y* having six elements instead of eight).

The system dynamics are represented using quaternion dynamics and Euler's equations of motion as

$$\frac{\mathrm{d}}{\mathrm{d}t}\begin{bmatrix} q_0 \\ q_1 \\ q_2 \\ q_3 \\ \omega_x \\ \omega_y \\ \omega_z \end{bmatrix} = \begin{bmatrix} \frac{1}{2} q\omega \\ \frac{M_x - (I_z - I_y)\omega_y\omega_z}{I_x} \\ \frac{M_y - (I_x - I_z)\omega_x\omega_z}{I_y} \\ \frac{M_z - (I_y - I_x)\omega_x\omega_y}{I_z} \end{bmatrix} \tag{75}$$

The filter dynamics matrix becomes

$$F = \begin{bmatrix} 0 & -\frac{1}{2}\omega_x & -\frac{1}{2}\omega_y & -\frac{1}{2}\omega_z & -\frac{1}{2}q_1 & -\frac{1}{2}q_2 & -\frac{1}{2}q_3 \\ \frac{1}{2}\omega_x & 0 & \frac{1}{2}\omega_z & -\frac{1}{2}\omega_y & \frac{1}{2}q_0 & -\frac{1}{2}q_3 & \frac{1}{2}q_2 \\ \frac{1}{2}\omega_y & -\frac{1}{2}\omega_z & 0 & \frac{1}{2}\omega_x & \frac{1}{2}q_3 & -\frac{1}{2}q_0 & -\frac{1}{2}q_1 \\ \frac{1}{2}\omega_z & \frac{1}{2}\omega_y & -\frac{1}{2}\omega_x & 0 & -\frac{1}{2}q_2 & \frac{1}{2}q_1 & \frac{1}{2}q_0 \\ 0 & 0 & 0 & 0 & 0 & \frac{-(I_z - I_y)\omega_z}{I_x} & \frac{-(I_z - I_y)\omega_y}{I_x} \\ 0 & 0 & 0 & 0 & \frac{-(I_x - I_z)\omega_z}{I_y} & 0 & \frac{-(I_x - I_z)\omega_x}{I_y} \\ 0 & 0 & 0 & 0 & \frac{-(I_y - I_x)\omega_y}{I_z} & \frac{-(I_y - I_x)\omega_x}{I_z} & 0 \end{bmatrix} \tag{76}$$

To assess the performance of the filter, a simulation was run using an orbit with 400 km altitude, zero eccentricity, and 40 degrees inclination. This baseline case is described in more detail in Section 6.1. Figure 5.1 shows the attitude angular estimation error for the simulation. The requirement used in the case of the MR SAT spacecraft is that the attitude be determined within three degrees with a goal of determination within one degree. Figure 5.1 shows that the requirement and goal for this case would be met. The error drops to about one degree within about 800 seconds, which corresponds to about one sixth of an orbit.

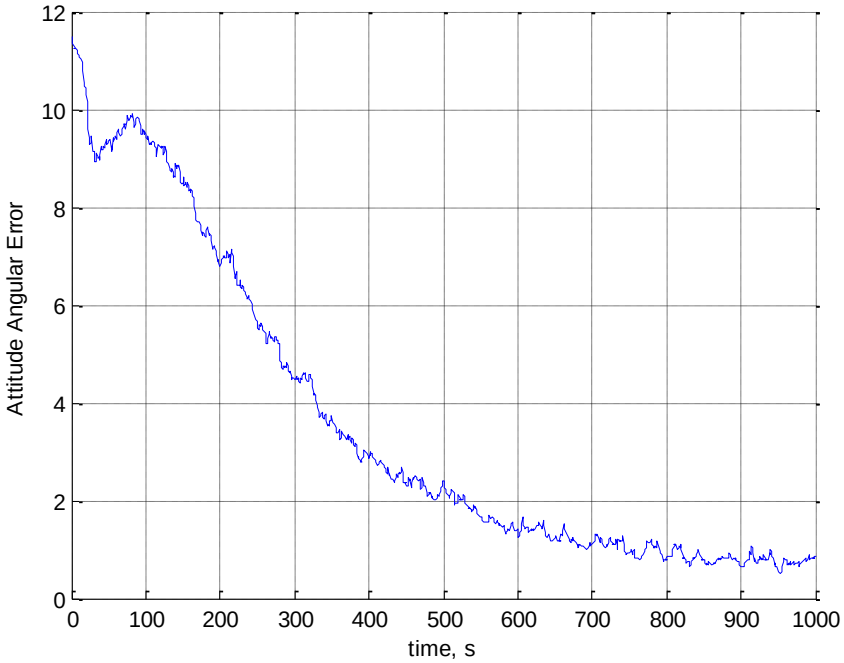

Figure 5.1. Attitude Angular Estimation Error, in Degrees

The error in the filter states, the attitude quaternion and the angular velocity are shown in Figures 5.2 and 5.3. The seven states composed of the four elements of the attitude quaternion and the three angular rates are all estimated accurately. The components of the attitude quaternion are estimated to within about 0.01, and the angular velocity components to within 0.03 degrees per second. This helps to understand why the error covariance matrix needs to be small. When simulating this scenario for the first time, the initial error covariance was set relatively high. An initial spike in the state error was exacerbated by a high initial error covariance matrix, and in response the matrix diagonals were reduced until the spike was diminished.

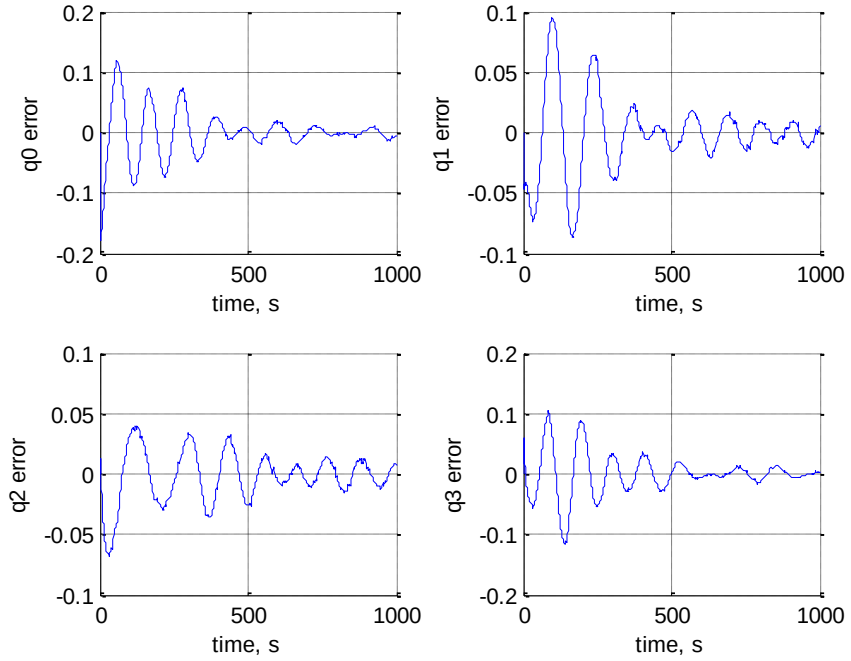

Figure 5.2. Attitude Quaternion Estimation Error

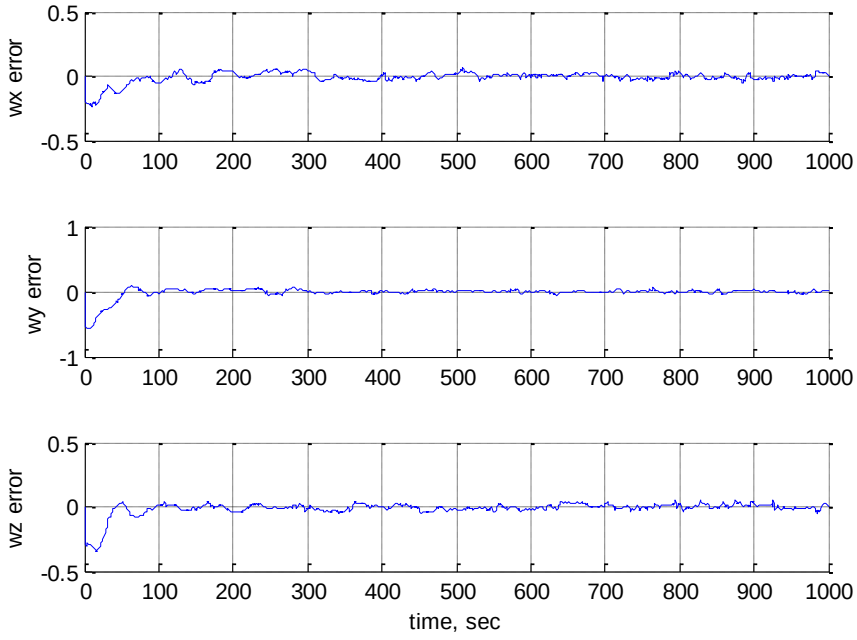

Figure 5.3. Angular Rate Estimation Error in Degrees/Second

The histories of the diagonal elements of the error covariance matrix are shown in Figure 5.4. The diagonals start small, and remain small. The elements corresponding to the quaternion show an oscillatory behavior similar to the magnetic field vector estimates. Typically, when using the EKF filter, the diagonal elements of the covariance matrix start high, then fall to a fairly constant steady state value. In this simulation, although the behavior is not typical, the matrix diagonal elements stay small and bounded, without any signs of divergence.

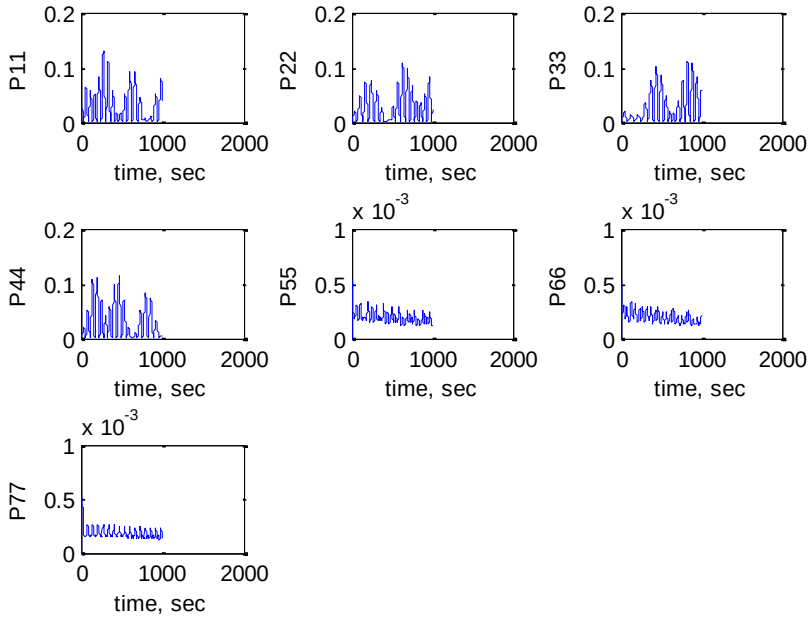

Figure 5.4. *A Posteriori* State Estimate Covariance Diagonals

The baseline simulation shows very promising results. These results are dependent on the spacecraft orbit parameters, the mass properties, the spacecraft angular

velocity, and the filter tuning parameters. With so many variables, a parametric study was used in Reference 32 to determine the accuracies of the method for different conditions. It was shown that only cases with no angular velocity, i.e., a three-axis inertially fixed attitude, presented convergence difficulties for the filter method. When the angular velocity is low, the magnetic field vector changes very slowly. This change allows the filter to determine how the spacecraft is oriented about the magnetic field vector. If the spacecraft were completely fixed on the magnetic field vector or only rotating about that particular axis, the attitude would not be observable. The rest of this section is devoted to improving the performance of the filter in these low angular rate cases.

5.2. SOLUTION OF ATTITUDE EQUATIONS

The quaternion attitude equations shown in Section 2.3.2 are difficult to solve, but an analytic solution promises a quick and accurate solution to magnetometer-only attitude determination. The difficulty is that an analytic solution will likely have multiple solutions because the equations are quadratic. This section steps through reducing the quaternion multiplications to scalar equations and details attempts at solving the equations.

Starting with the equation for the magnetic field vector in terms of the attitude quaternion given as

$$\mathbf{B}_b = q^c \left\langle 0, \mathbf{B}_I \right\rangle q \tag{77}$$

The time derivative is taken to yield

$$\dot{\mathbf{B}}_b = \dot{q}^c \left\langle 0, \mathbf{B}_I \right\rangle q + q^c \left\langle 0, \dot{\mathbf{B}}_I \right\rangle q + q^c \left\langle 0, \mathbf{B}_I \right\rangle \dot{q} \tag{78}$$

Then, knowing that $\dot{q}$ is a function of the quaternion and angular velocity,

$$\dot{q} = \frac{1}{2} q\omega \tag{79}$$

is substituted into Equation (78) giving

$$\dot{B}_b = \frac{1}{2} q^c \omega \langle 0, B_I \rangle q + q^c \langle 0, \dot{B}_I \rangle q + q^c \langle 0, B_I \rangle \frac{1}{2} q\omega \tag{80}$$

As mentioned in Section 2.3.2, Equations (77) and (80), when multiplied out, yield six equations while there are seven unknowns (all four elements of q and three elements of ω). The fact that the quaternion is of unit magnitude is used to provide the seventh equation.

These equations are then expanded to scalar form so that they can be more easily manipulated are produced. First multiplying out Equation (77) gives

$$\begin{aligned} B_{b_x} &= B_{I_x} q_0^2 - 2B_{I_z} q_0 q_2 + 2B_{I_y} q_0 q_3 + B_{I_x} q_1^2 + 2B_{I_y} q_1 q_2 \ldots \\ &\quad + 2B_{I_z} q_1 q_3 - B_{I_x} q_2^2 - B_{I_x} q_3^2 \end{aligned} \tag{81}$$

$$\begin{aligned} B_{b_y} &= B_{I_y} q_0^2 + 2B_{I_z} q_0 q_1 - 2B_{I_x} q_0 q_3 - B_{I_y} q_1^2 + 2B_{I_x} q_1 q_2 \ldots \\ &\quad + B_{I_y} q_2^2 + 2B_{I_z} q_2 q_3 - B_{I_y} q_3^2 \end{aligned} \tag{82}$$

$$\begin{aligned} B_{b_z} &= B_{I_z} q_0^2 - 2B_{I_y} q_0 q_1 + 2B_{I_x} q_0 q_2 - B_{I_z} q_1^2 + 2B_{I_x} q_1 q_3 \ldots \\ &\quad - B_{I_z} q_2^2 + 2B_{I_y} q_2 q_3 + B_{I_y} q_3^2 \end{aligned} \tag{83}$$

Now the equations for $\dot{\mathbf{B}}_b$ are broken into three parts, one for each term, as

$$\begin{bmatrix} \dot{B}_{b_x} \\ \dot{B}_{b_y} \\ \dot{B}_{b_z} \end{bmatrix} = \begin{bmatrix} T_{1_x} + T_{2_x} + T_{3_x} \\ T_{1_y} + T_{2_y} + T_{3_y} \\ T_{1_z} + T_{2_z} + T_{3_z} \end{bmatrix} \tag{84}$$

$$\begin{aligned} T_{1_x} = {} & B_{I_y} q_0^2 \omega_z - B_{I_z} q_0^2 \omega_y + B_{I_z} q_1^2 \omega_y - B_{I_y} q_1^2 \omega_z + B_{I_z} q_2^2 \omega_y + B_{I_y} q_2^2 \omega_z \ldots \\ & - B_{I_z} q_3^2 \omega_y - B_{I_y} q_3^2 \omega_z + 2B_{I_y} q_0 q_1 \omega_y - 2B_{I_x} q_0 q_2 \omega_y + 2B_{I_z} q_0 q_1 \omega_z - \ldots \\ & 2B_{I_x} q_0 q_3 \omega_z + 2B_{I_x} q_1 q_2 \omega_z - 2B_{I_x} q_1 q_3 \omega_y - 2B_{I_y} q_2 q_3 \omega_y + 2B_{I_z} q_2 q_3 \omega_z \end{aligned} \tag{85}$$

$$\begin{aligned} T_{1_y} = {} & B_{I_z} q_0^2 \omega_x - B_{I_z} q_1^2 \omega_x - B_{I_x} q_0^2 \omega_z - B_{I_z} q_2^2 \omega_x - B_{I_x} q_1^2 \omega_z + B_{I_z} q_3^2 \omega_x \ldots \\ & + B_{I_x} q_2^2 \omega_z + B_{I_x} q_3^2 \omega_z - 2B_{I_y} q_0 q_1 \omega_x + 2B_{I_x} q_0 q_2 \omega_x + 2B_{I_x} q_1 q_3 \omega_x - \ldots \\ & 2B_{I_z} q_0 q_2 \omega_z - 2B_{I_y} q_0 q_3 \omega_z - 2B_{I_y} q_1 q_2 \omega_z + 2B_{I_y} q_2 q_3 \omega_x - 2B_{I_z} q_1 q_3 \omega_z \end{aligned} \tag{86}$$

$$\begin{aligned} T_{1_z} = {} & B_{I_x} q_0^2 \omega_y - B_{I_y} q_0^2 \omega_x + B_{I_y} q_1^2 \omega_x + B_{I_x} q_1^2 \omega_y - B_{I_y} q_2^2 \omega_x - B_{I_x} q_2^2 \omega_y + \ldots \\ & B_{I_y} q_3^2 \omega_x - B_{I_x} q_3^2 \omega_y - 2B_{I_z} q_0 q_1 \omega_x + 2B_{I_x} q_0 q_3 \omega_x - 2B_{I_x} q_1 q_2 \omega_x - \ldots \\ & 2B_{I_z} q_0 q_2 \omega_y + 2B_{I_y} q_0 q_3 \omega_y + 2B_{I_y} q_1 q_2 \omega_y + 2B_{I_z} q_1 q_3 \omega_y + 2B_{I_z} q_2 q_3 \omega_x \end{aligned} \tag{87}$$

$$\begin{aligned} T_{2_x} = {} & \dot{B}_{I_x} q_0^2 - 2\dot{B}_{I_z} q_0 q_2 + 2\dot{B}_{I_y} q_0 q_3 + \dot{B}_{I_x} q_1^2 + 2\dot{B}_{I_y} q_1 q_2 + \ldots \\ & 2\dot{B}_{I_z} q_1 q_3 - \dot{B}_{I_x} q_2^2 - \dot{B}_{I_x} q_3^2 \end{aligned} \tag{88}$$

$$\begin{aligned} T_{2_y} = {} & \dot{B}_{I_y} q_0^2 + 2\dot{B}_{I_z} q_0 q_1 - 2\dot{B}_{I_x} q_0 q_3 - \dot{B}_{I_y} q_1^2 + 2\dot{B}_{I_x} q_1 q_2 + \ldots \\ & 2\dot{B}_{I_z} q_2 q_3 + \dot{B}_{I_y} q_2^2 - \dot{B}_{I_y} q_3^2 \end{aligned} \tag{89}$$

$$\begin{aligned} T_{2_z} = {} & \dot{B}_{I_z} q_0^2 - 2\dot{B}_{I_y} q_0 q_1 + 2\dot{B}_{I_x} q_0 q_2 - \dot{B}_{I_z} q_1^2 + 2\dot{B}_{I_x} q_1 q_3 + \ldots \\ & 2\dot{B}_{I_y} q_2 q_3 - \dot{B}_{I_z} q_2^2 + \dot{B}_{I_z} q_3^2 \end{aligned} \tag{90}$$

$$\begin{aligned} T_{3_x} = &\left(q_0\omega_z + q_1\omega_y - q_2\omega_x\right)\left(B_{I_y}q_0 + B_{I_z}q_1 - B_{I_x}q_3\right) - \ldots \\ &\left(q_0\omega_y - q_1\omega_z + q_3\omega_x\right)\left(B_{I_z}q_0 - B_{I_y}q_1 + B_{I_x}q_2\right) + \ldots \\ &\left(q_0\omega_x + q_2\omega_z - q_3\omega_y\right)\left(B_{I_x}q_1 + B_{I_y}q_2 + B_{I_z}q_3\right) - \ldots \\ &\left(q_1\omega_x + q_2\omega_y + q_3\omega_z\right)\left(B_{I_x}q_0 - B_{I_z}q_2 + B_{I_y}q_3\right) \end{aligned} \tag{91}$$

$$\begin{aligned} T_{3_y} = &\left(q_0\omega_x + q_2\omega_z - q_3\omega_y\right)\left(B_{I_z}q_0 - B_{I_y}q_1 + B_{I_x}q_2\right) - \ldots \\ &\left(q_0\omega_z - q_1\omega_y + q_2\omega_x\right)\left(B_{I_x}q_0 - B_{I_z}q_2 + B_{I_y}q_3\right) + \ldots \\ &\left(q_0\omega_y - q_1\omega_z + q_3\omega_x\right)\left(B_{I_x}q_1 + B_{I_y}q_2 + B_{I_z}q_3\right) - \ldots \\ &\left(q_1\omega_x + q_2\omega_y + q_3\omega_z\right)\left(B_{I_y}q_0 + B_{I_z}q_1 - B_{I_x}q_3\right) \end{aligned} \tag{92}$$

$$\begin{aligned} T_{3_z} = &\left(q_0\omega_z + q_1\omega_y - q_2\omega_x\right)\left(B_{I_x}q_1 + B_{I_y}q_2 + B_{I_z}q_3\right) - \ldots \\ &\left(q_1\omega_x + q_2\omega_y + q_3\omega_z\right)\left(B_{I_z}q_0 - B_{I_y}q_1 + B_{I_x}q_2\right) + \ldots \\ &\left(q_0\omega_y - q_1\omega_z + q_3\omega_x\right)\left(B_{I_x}q_0 - B_{I_z}q_2 + B_{I_y}q_3\right) - \ldots \\ &\left(q_0\omega_x + q_2\omega_z - q_3\omega_y\right)\left(B_{I_y}q_0 + B_{I_z}q_1 - B_{I_x}q_3\right) \end{aligned} \tag{93}$$

Using the six equations representing $\mathbf{B}_b$ and $\dot{\mathbf{B}}_b$, along with

$$q_0^2 + q_1^2 + q_2^2 + q_3^2 = 1 \tag{94}$$

forms a system of seven scalar equations and seven unknowns. The system of equations could not be solved using MATLAB or MAPLE software packages. The system of equations was then converted to an optimization problem. The first numerical solution approach was to use Newton-Rhapson method. This method requires the calculation of the Jacobian. The calculated Jacobian is not full rank, a requirement for the method to converge and leads to the conclusion that it contains at least one or more equation that is linearly dependent on another. This would mean that multiple solutions exist.

There is still the possibility that if an initial guess at the solution is sufficiently close, an optimization routine could converge. MATLAB's built-in function "fsolve" is used to solve a system of equations by converting the problem to an optimization problem. The system of equations is manipulated so that all terms are moved to one side. It is then attempted to drive each equation to zero. The "fsolve" routine minimizes the error in the root sum square of the residual of the equations. A test case was selected to determine if "fsolve" would converge to the correct solution.

The attitude truth model was used to generate a data point with the necessary known information and a true answer. This instance had the magnetic field and derivative values as

$$B_I = \begin{bmatrix} -17.0005 \\ 42.2604 \\ 261.717 \end{bmatrix} mG \tag{95}$$

$$\dot{B}_I = \begin{bmatrix} -0.712938 \\ -0.158539 \\ -0.060110 \end{bmatrix} mG/s \tag{96}$$

$$B_b = \begin{bmatrix} 235.381 \\ 78.4491 \\ 94.9307 \end{bmatrix} mG \tag{97}$$

$$\dot{B}_b = \begin{bmatrix} 0.209230 \\ 0.084478 \\ -0.697219 \end{bmatrix} mG/s \tag{98}$$

The condition described by this set of magnetic field data has the correct attitude quaternion and angular rates as

$$q = \begin{bmatrix} 0.103142 \\ 0.515711 \\ 0.206284 \\ 0.825137 \end{bmatrix} \tag{99}$$

$$\omega = \begin{bmatrix} 0 \\ 0 \\ 0 \end{bmatrix} rad/s \tag{100}$$

Entering the exact solution as the initial guess for the "fsolve" function yields

$$q = \begin{bmatrix} 0.103142 \\ 0.515711 \\ 0.206284 \\ 0.825137 \end{bmatrix} \tag{101}$$

$$\omega = \begin{bmatrix} 0.000001 \\ 0.000000 \\ 0.000000 \end{bmatrix} rad/s \tag{102}$$

As expected, with a perfect initial guess, the solution of the "fsolve" function is correct. Although, MATLAB generates an error that states the problem "appears to be locally singular." Testing using an arbitrary initial guess yields

$$q = \begin{bmatrix} 0.105449 \\ 0.515932 \\ 0.204645 \\ 0.825116 \end{bmatrix} \tag{103}$$

$$\omega = \begin{bmatrix} -0.494384 \\ -0.164771 \\ -0.199380 \end{bmatrix} rad/s \tag{104}$$

It can be seen that the attitude quaternion is calculated somewhat accurately, however, the angular velocity is quite inaccurate. The test case was successful only if the initial guess is very close to the actual solution. The only way to determine if the solution is sufficiently accurate is to implement it in the orbit and attitude simulation.

The baseline case is used as the test case for this optimization solver routine. The Kalman filter first estimates the magnetic field derivative and then the estimate is used with the magnetic field vector measurement as inputs into the equation solver. The attitude quaternion and angular rates are calculated using the "fsolve" function developed. The noise is at first removed from the simulation to reduce the number of factors that could pose challenges to the software.

The results show that when the measurements are exact, even in the presence of initial quaternion error, the optimization of the equations allow for the calculation of the quaternion and angular rates and produce quality results as shown in Figures 5.5-5.7.

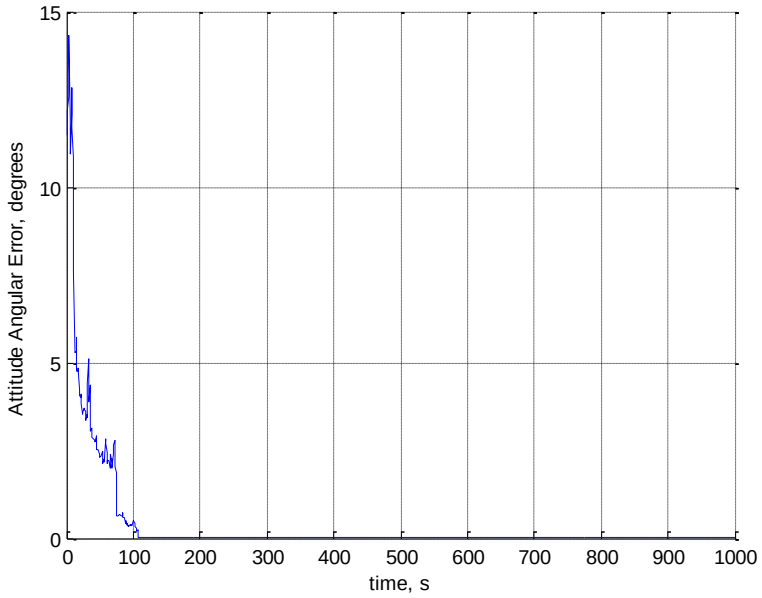

Figure 5.5. Attitude Angular Estimation Error

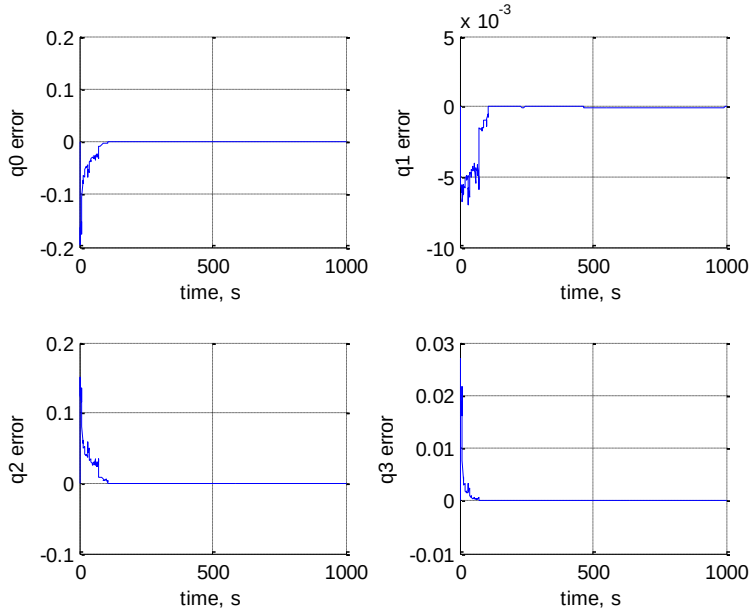

Figure 5.6. Attitude Quaternion Error

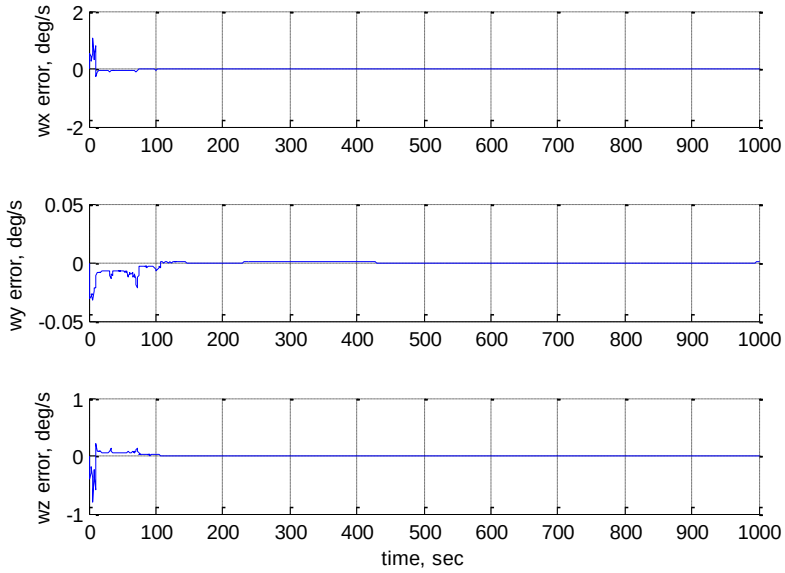

Figure 5.7. Attitude Angular Rate Error

Now to assess if the optimization routine is sufficiently accurate in the presence of measurement noise, noisy measurements are introduced into the solving routine. The results of the more realistic simulation indicate that the method is sensitive to noise. Adding noise to the measurements causes errors that tend to divert the solving routine toward other potential solutions. The solver finds an accurate solution; however, the solution is not the true solution that is being sought, as it is one of the many solutions available because of the linearly dependent equations resulting in an underdetermined system.

The noise causes a significant amount of error in the estimates of the attitude quaternion and the angular rates. Both the magnetic field and its derivative are estimated adequately by the first-stage filter. However, even the small error in the magnetic field vector and its derivative degrade the attitude estimates.

It is possible that a more accurate first-stage filter could allow the solver to perform with the desired accuracy; however, none of the pre-filter techniques were much more effective in the presence of noise. The next section expands this analytical solution search to include more information that can be gathered from the magnetometer measurement.

5.3. DETERMINISTIC SOLUTION

The addition of the angular velocity magnitude pseudomeasurement to the system in Section 4.3 helped to alleviate problems by narrowing the possible solutions. The same technique was applied to the equations derived in Section 5.2.

Adding

$$\|\omega\|^2 = \omega_x^2 + \omega_y^2 + \omega_z^2 \tag{105}$$

to the system of equations and using the same “fsolve” technique improves the results (with noise included). The simulation with the angular velocity set to zero and including measurement noise produces the following results, shown in Figures 5.8-5.9.

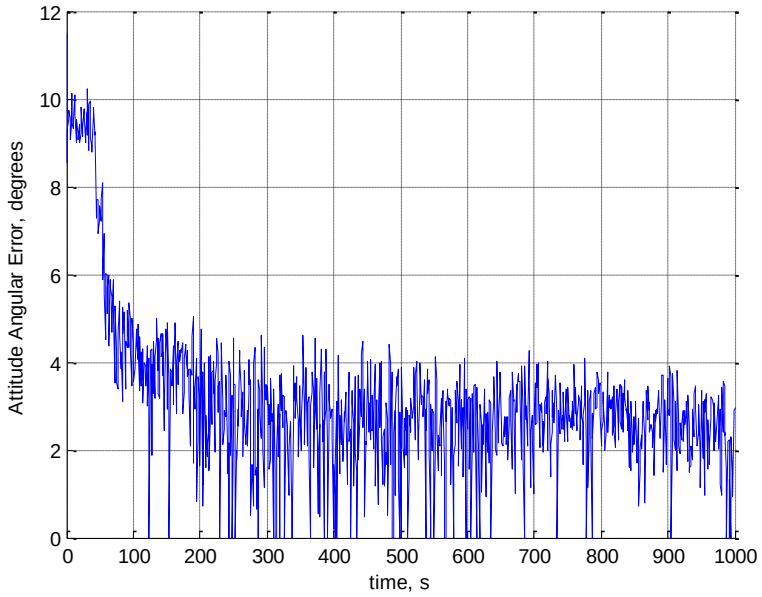

Figure 5.8. Attitude Angular Estimation Error

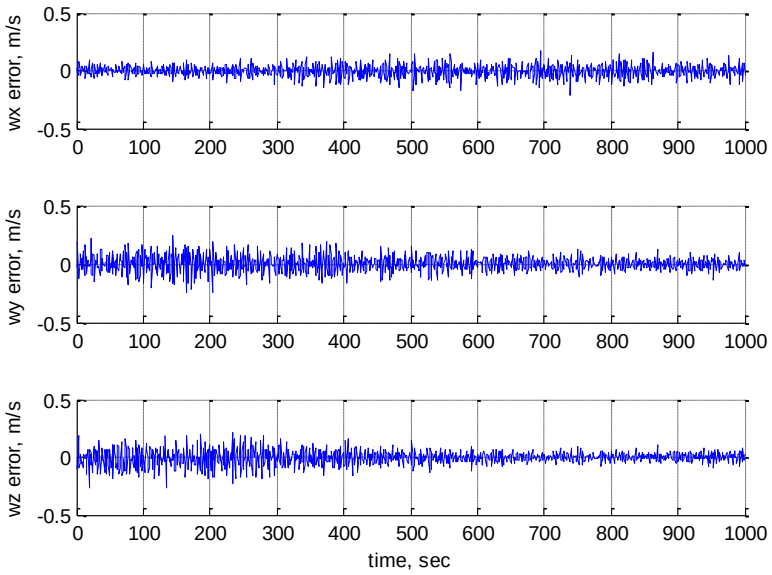

Figure 5.9. Angular Rate Error

The addition of the angular velocity magnitude equation to the system of equations adds enough information to constrain the possible solutions and converge to the correct attitude when noise is in the simulation, even when the spacecraft is inertially fixed.

5.4. ADDITION OF RATE SENSORS

This section is provided as a comparison of the magnetometer-only method to instances where angular rate sensors are used. The method presented here is novel in that it uses the same dual filter approach as the developed magnetometer-only method. The pre-filter is used to filter the magnetic field measurement and estimate the magnetic field derivative. To evaluate the performance of this method, the Kalman filter pre-filter technique is used. After the pre-filter is applied, the EKF is used to estimate the attitude quaternion and angular rates with the additional angular rate measurement provided by an IMU.

The measurements for the attitude filter in this case are

$$y = \begin{bmatrix} B_{b_x} \\ B_{b_y} \\ B_{b_z} \\ \dot{B}_{b_x} \\ \dot{B}_{b_y} \\ \dot{B}_{b_z} \\ \omega_x \\ \omega_y \\ \omega_z \end{bmatrix} \tag{106}$$

The measurements in terms of the states become

$$y = \begin{bmatrix} q^c \langle 0, B_I \rangle q \\ \frac{1}{2} q^c \omega \langle 0, B_I \rangle q + q^c \langle 0, \dot{B}_I \rangle q + q^c \langle 0, B_I \rangle \frac{1}{2} q\omega \\ \omega_x \\ \omega_y \\ \omega_z \end{bmatrix} \tag{107}$$

The quaternion version of the formulation was used for brevity. The system dynamics and *F* matrix are identical to those used in Section 5.1. The *H* matrix is augmented with the identity matrix as

$$H_{new} = \begin{bmatrix} H_{old} & 0_{4x3} \\ 0_{3x4} & I_{3x3} \end{bmatrix} \tag{108}$$

There are nine measurements in this simulation. The simulation was run with the same conditions as the baseline scenario except that the angular velocity was zero. The noise in the angular velocity measurement was modeled as zero-mean Gaussian noise with a variance of 0.1^2. The addition of the angular velocity measurements enable the filter to converge to an acceptable attitude error as shown in Figures 5.10-5.16.

With the augmentation of the angular rate data, the system performance is good even with zero angular velocity, which was a limitation when the angular rate data were not present. Now, the baseline case is examined to determine if the "spinning scenario" is affected by the addition of IMU measurements. Figures 5.17-5.23 show the results of this spinning scenario.

These plots show that the IMU measurement actually slows the convergence of the filter. The accuracy is still down to one degree; therefore, the added benefit of being robust to the zero angular velocity case would be worth sacrificing some convergence time. The remainder of this section is devoted to determining if the need for an IMU can be circumvented.

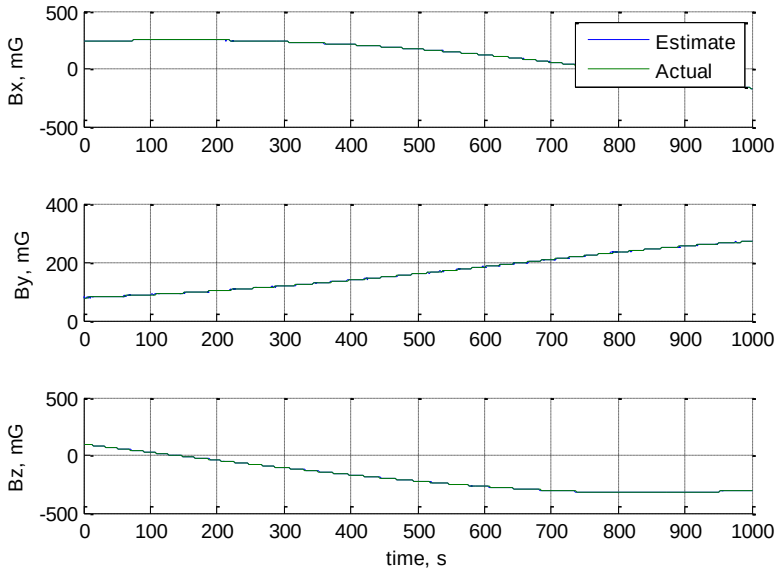

Figure 5.10. Magnetic Field Vector Estimate

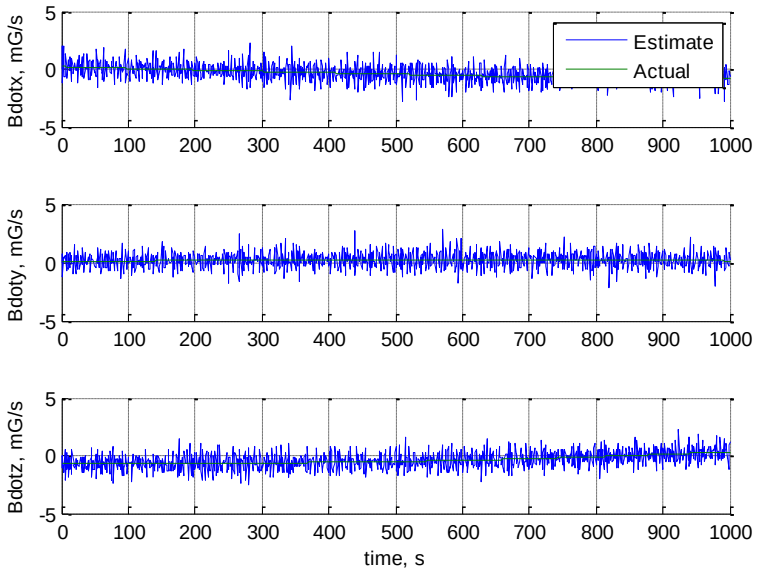

Figure 5.11. Magnetic Field Derivative Estimate

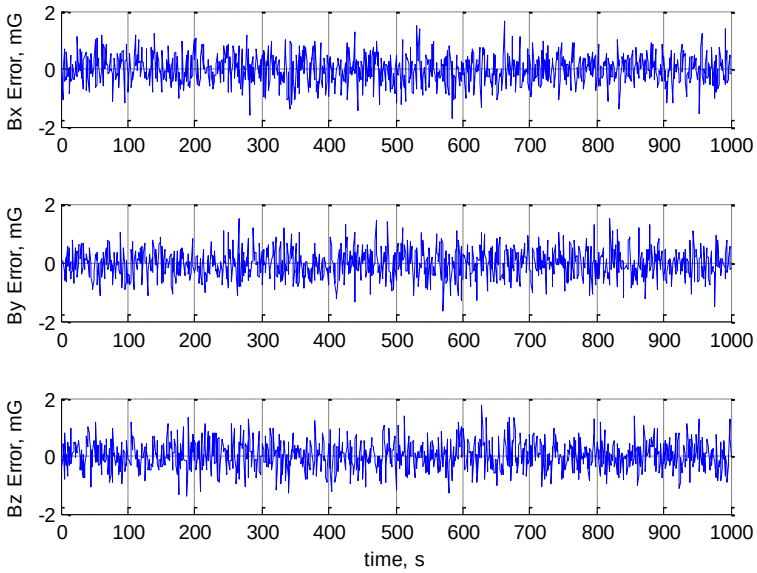

Figure 5.12. Magnetic Field Vector Estimation Error

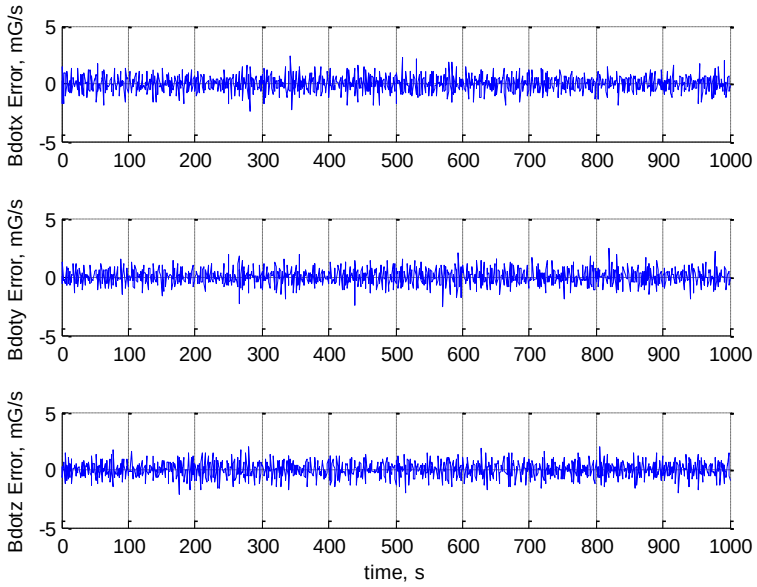

Figure 5.13. Magnetic Field Derivative Estimation Error

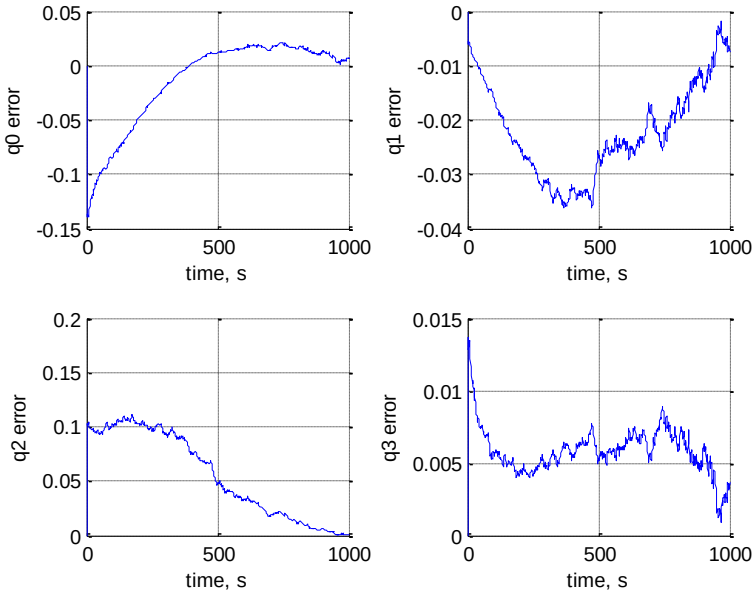

Figure 5.14. Attitude Quaternion Estimation Error

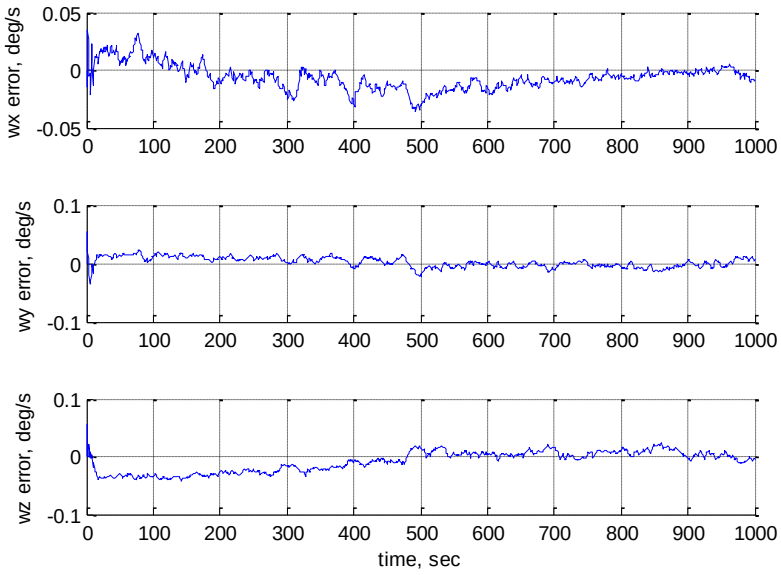

Figure 5.15. Angular Rate Estimate Error

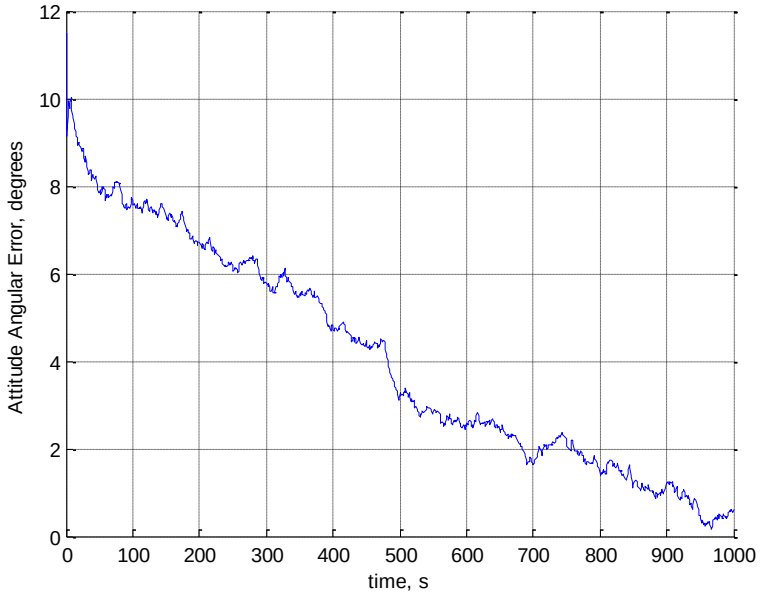

Figure 5.16. Attitude Angular Estimation Error

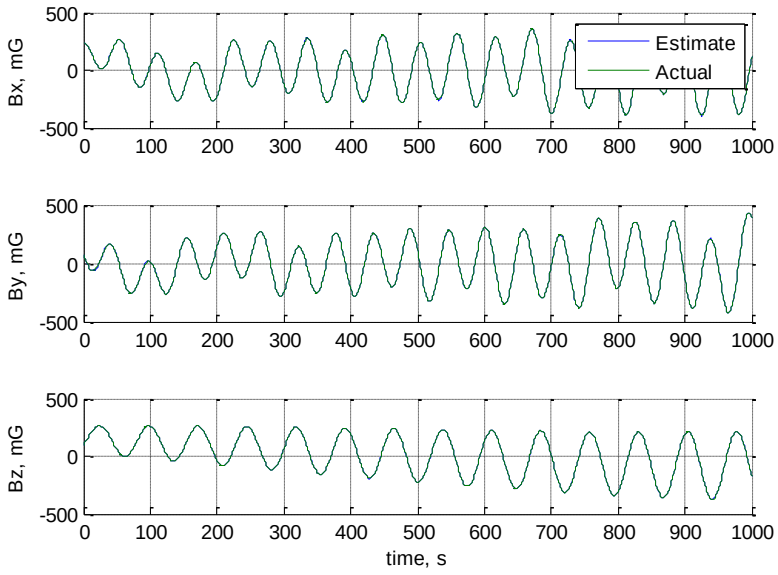

Figure 5.17. Magnetic Field Vector Estimate

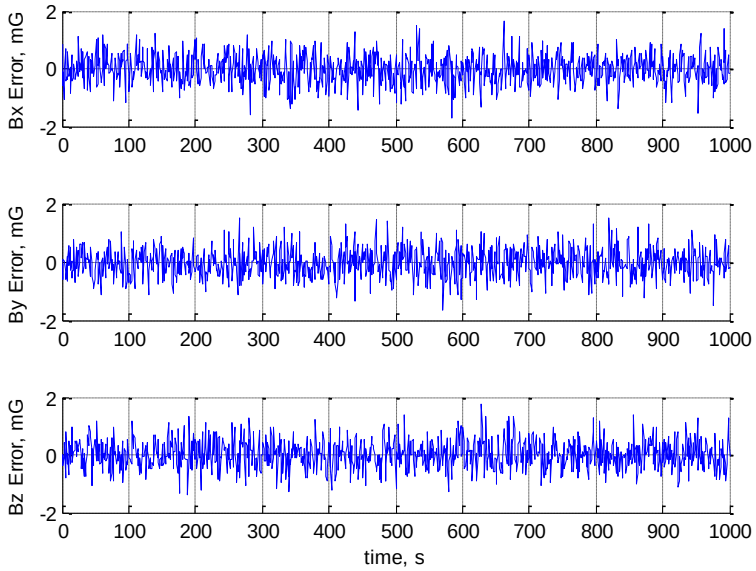

Figure 5.18. Magnetic Field Vector Estimation Error

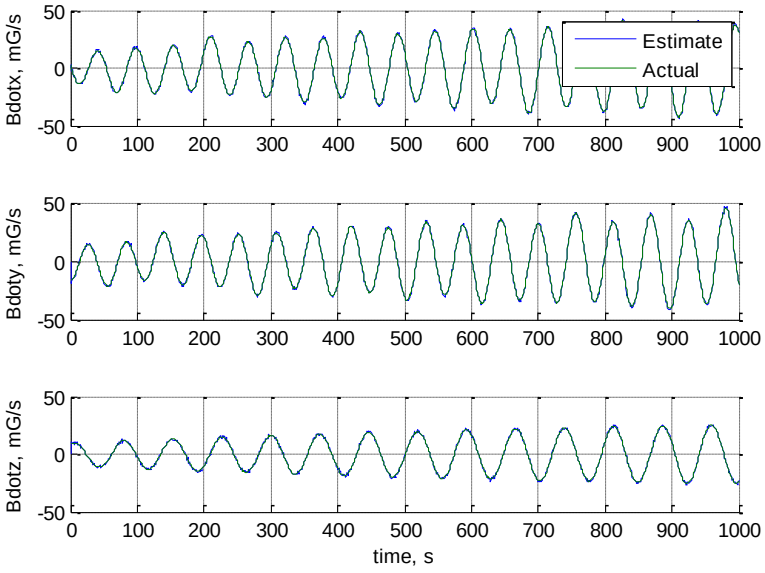

Figure 5.19. Magnetic Field Derivative Estimate

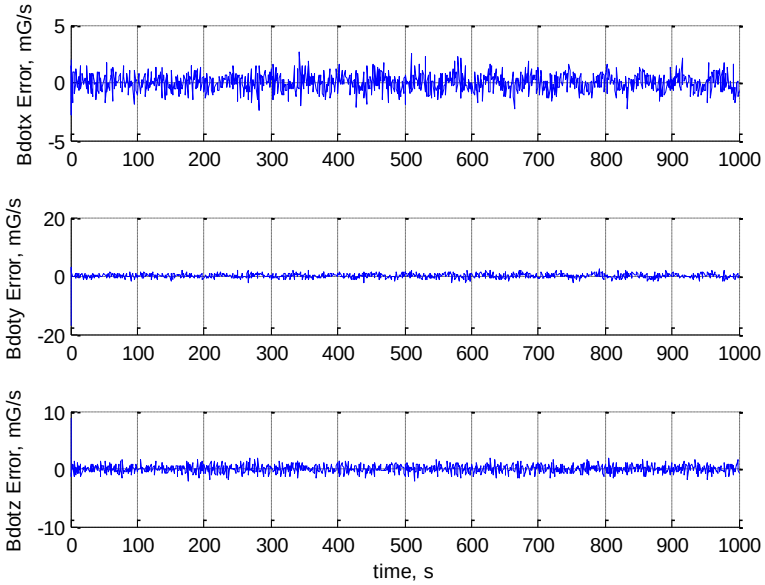

Figure 5.20. Magnetic Field Derivative Estimation Error

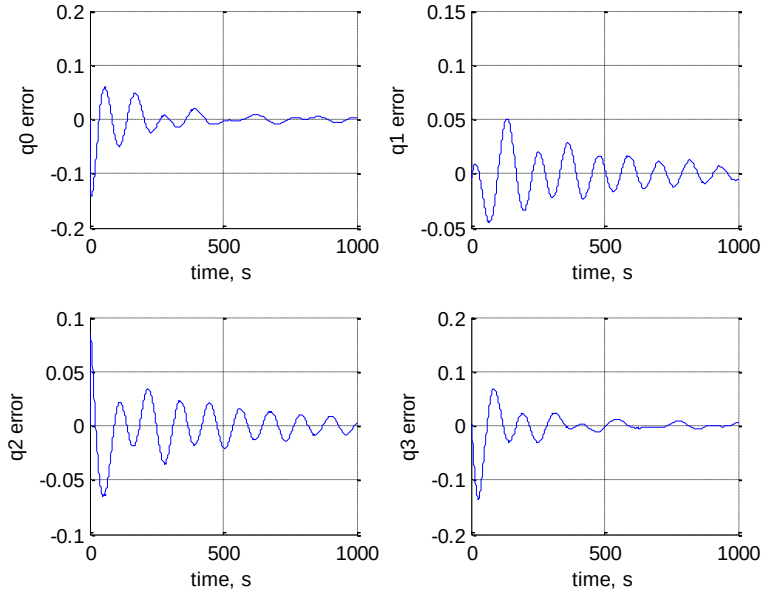

Figure 5.21. Attitude Quaternion Estimation Error

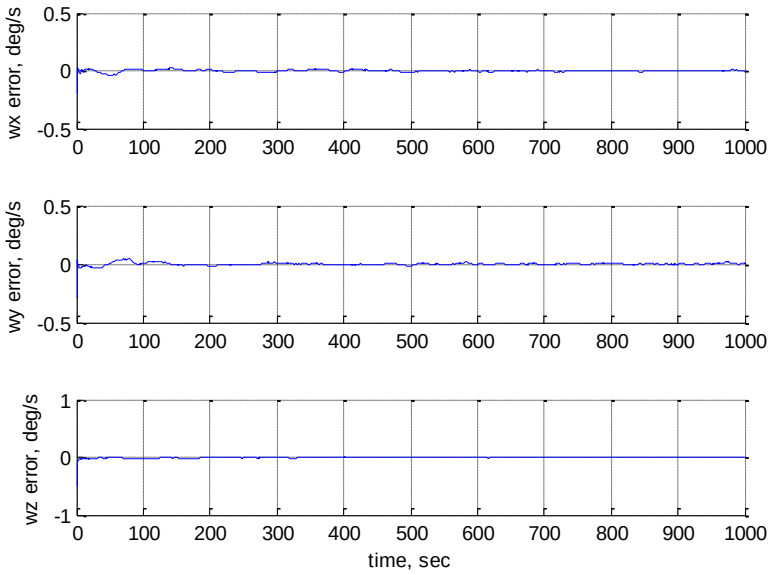

Figure 5.22. Angular Rate Estimate Error

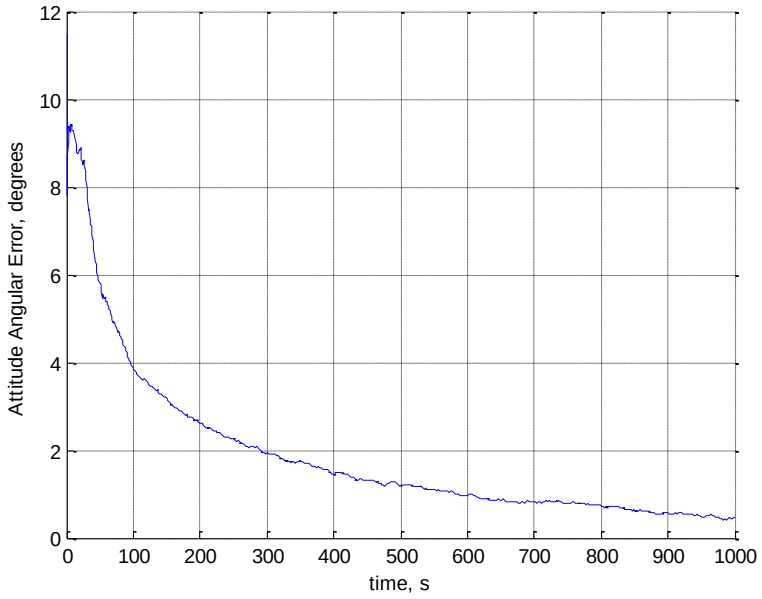

Figure 5.23. Attitude Angular Estimation Error

5.5. FILTERING WITH ANGULAR VELOCITY MAGNITUDE AS A PSUEDOMEASUREMENT

This section shows the performance of the attitude filter when using the pseudo measurement from Section 3.7. To take advantage of the new measurements, the filter needs to be augmented with the angular velocity as the measurements in an analogous method as shown in the previous section. This filter, however, will use angular velocity pseudomeasurements instead of measurements from an IMU.

The first simulation was performed using the baseline scenario. The first stage filter from Section 4.4 was used to generate the angular velocity pseudomeasurements. The accuracy of the angular velocity pseudomeasurements needs to be analyzed to so that the filter matrices can be conditioned appropriately. The measurements appear to be similar in accuracy to the measurements produced by the IMU, so the same filter matrices were used.

The results shown in Figures 5.24-5.33 indicate that the performance of the filter is degraded with the new measurements due to the slight bias in the filter measurements.

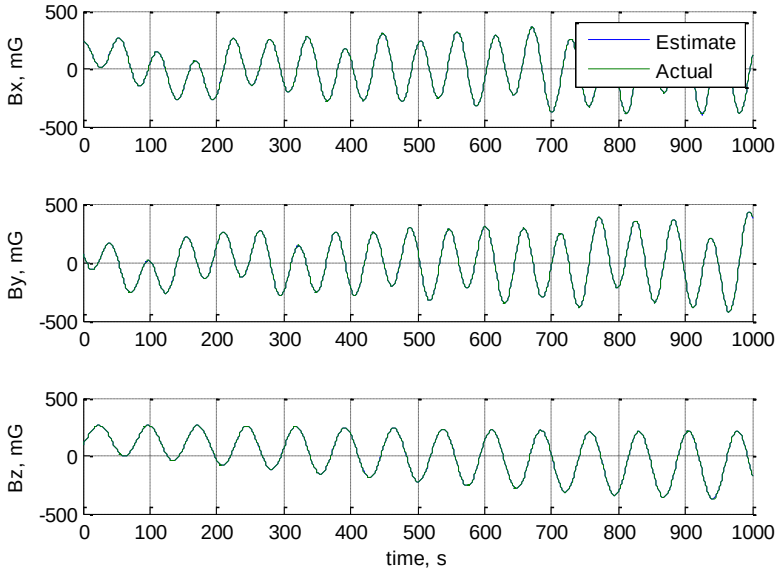

Figure 5.24. Magnetic Field Vector

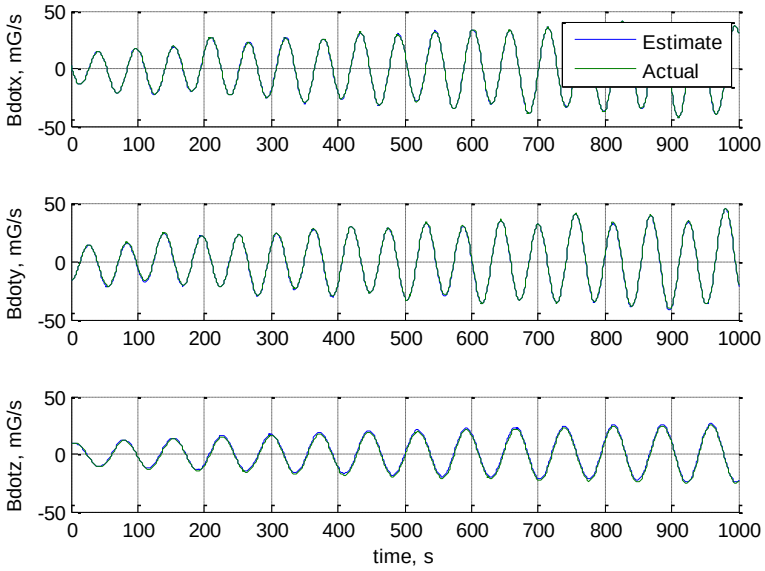

Figure 5.25. Magnetic Field Vector Derivative

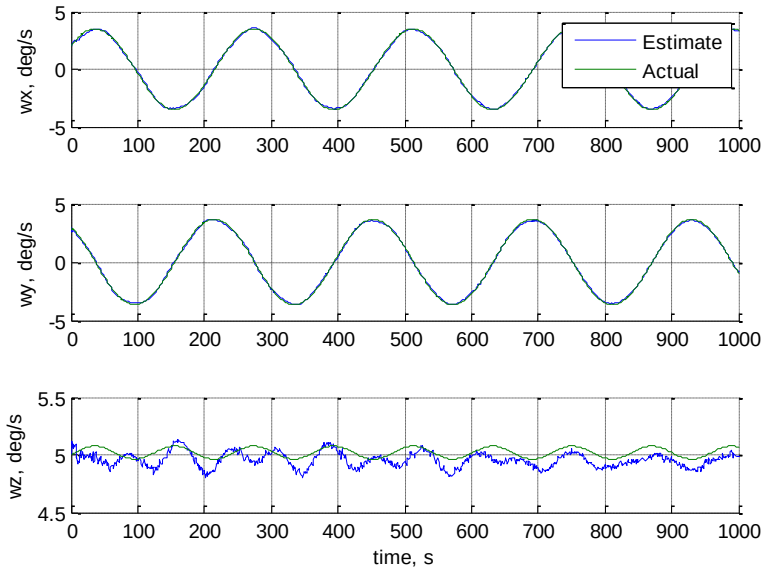

Figure 5.26. Angular Velocity From First Stage Filter

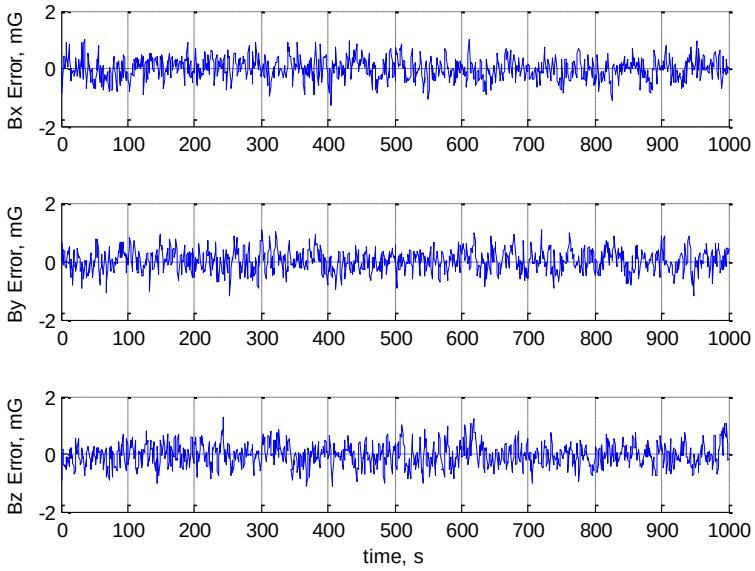

Figure 5.27. Magnetic Field Vector Error

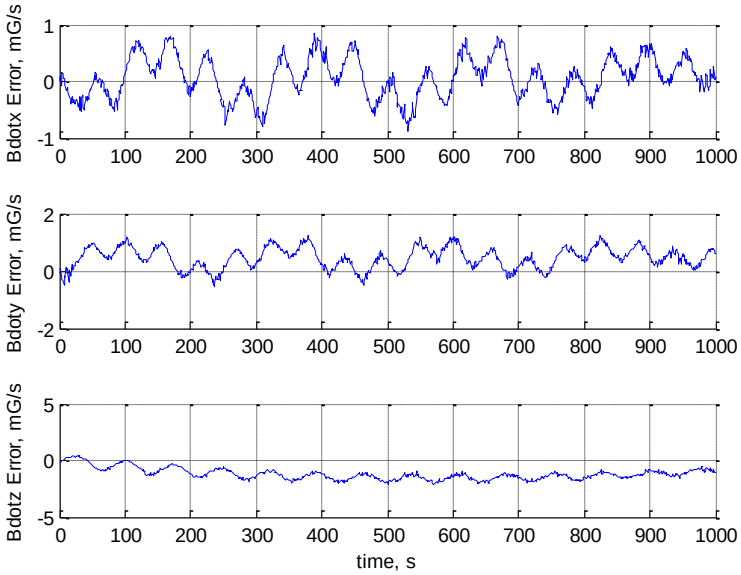

Figure 5.28. Magnetic Field Vector Derivative Error

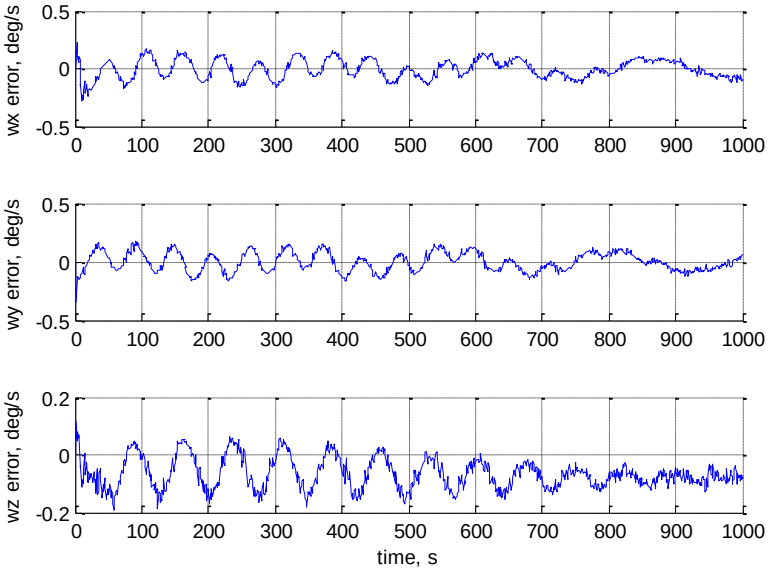

Figure 5.29. Angular Velocity Error From Stage-One Filter

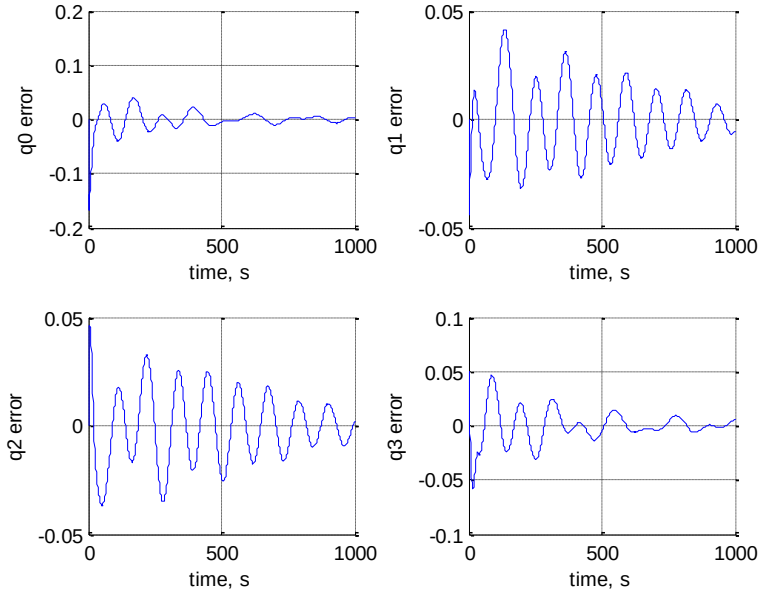

Figure 5.30. Attitude Quaternion Error

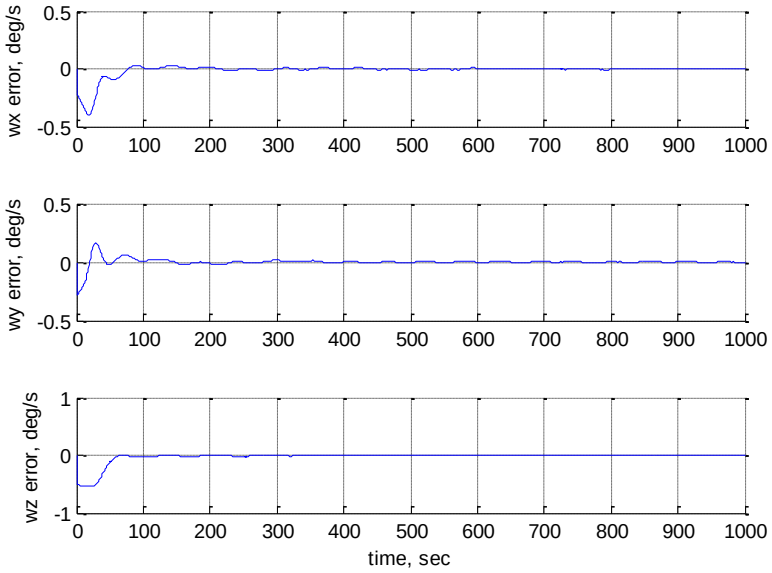

Figure 5.31. Angular Velocity Error From Stage-Two Filter

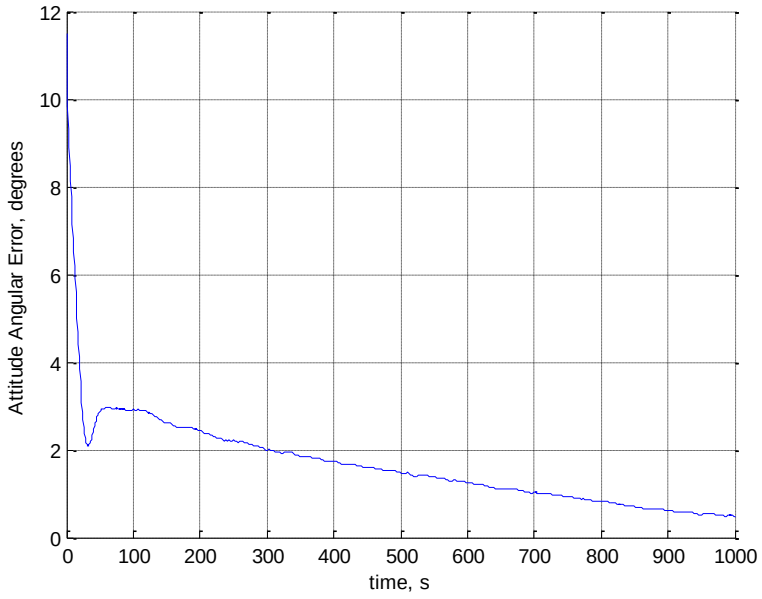

Figure 5.32. Attitude Angular Estimation Error

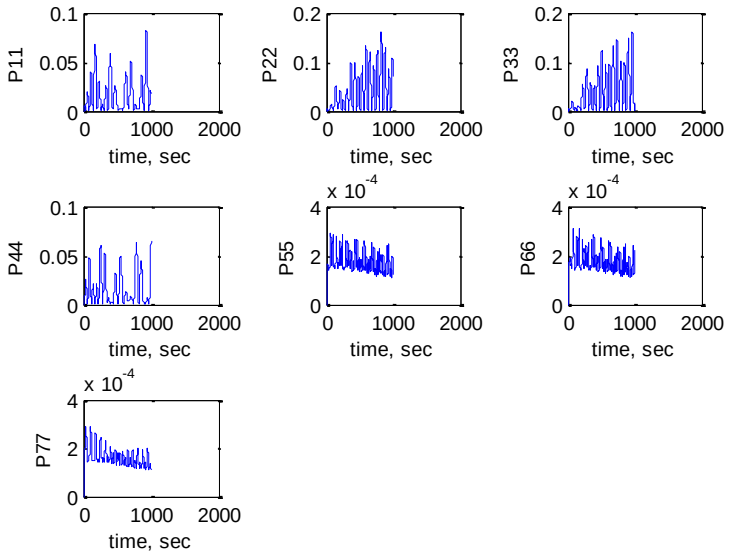

Figure 5.33. Stage-Two Filter Error Covariance Diagonals

Lowering the angular velocity to zero along each axis and repeating the simulation shows that the filter is still unable to perform adequately with the additional angular velocity pseudomeasurements. These Results are shown in Figures 5.34-5.42.

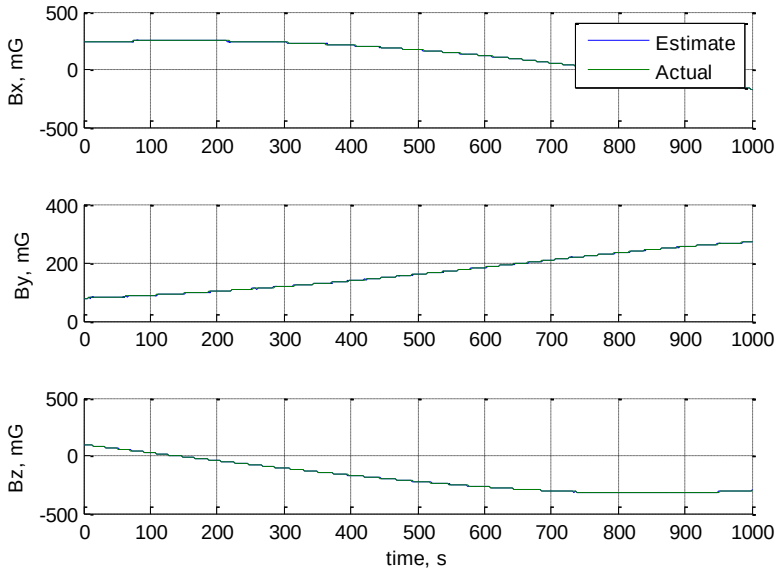

Figure 5.34. Magnetic Field Vector

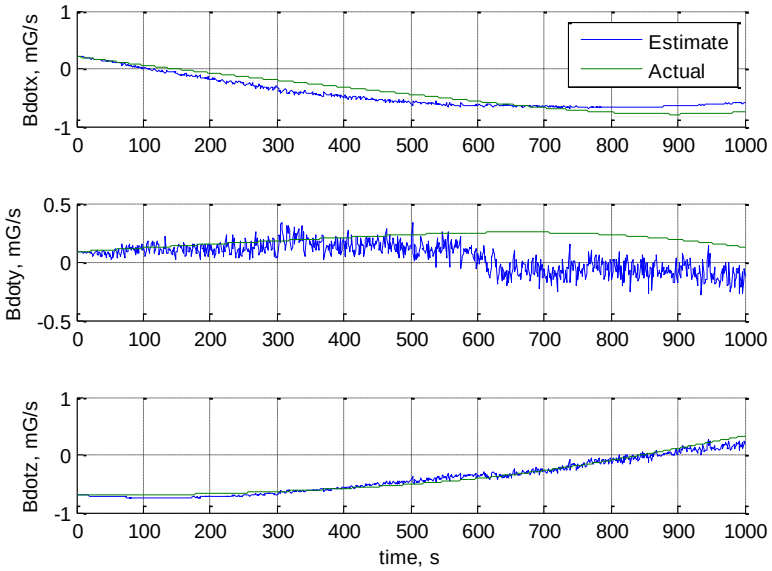

Figure 5.35. Magnetic Field Vector Derivative

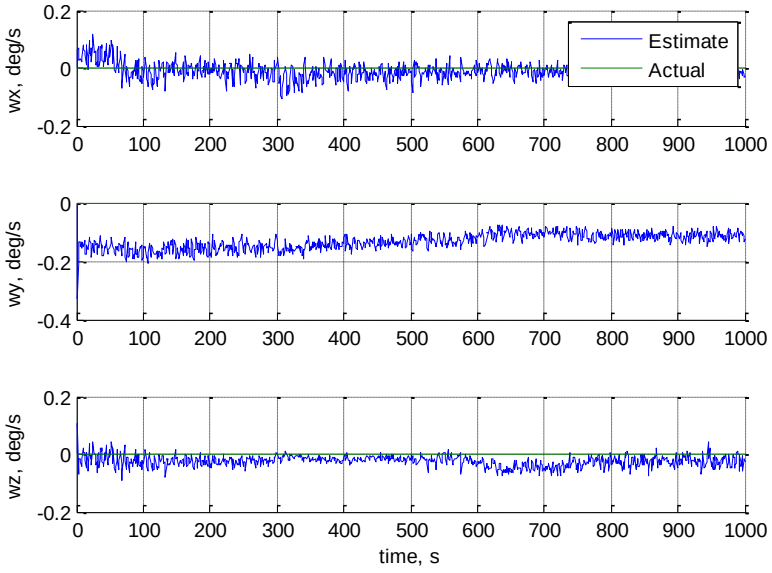

Figure 5.36. Angular Velocity Error From Stage-One Filter

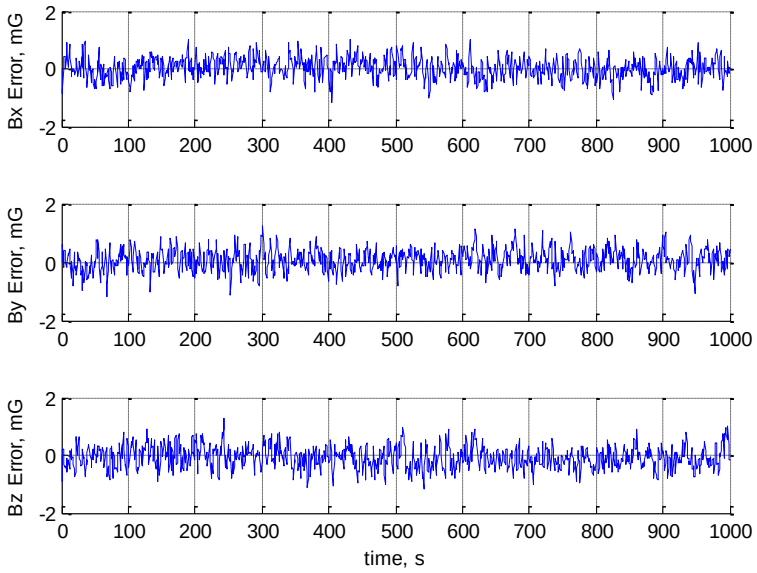

Figure 5.37. Magnetic Field Vector Error

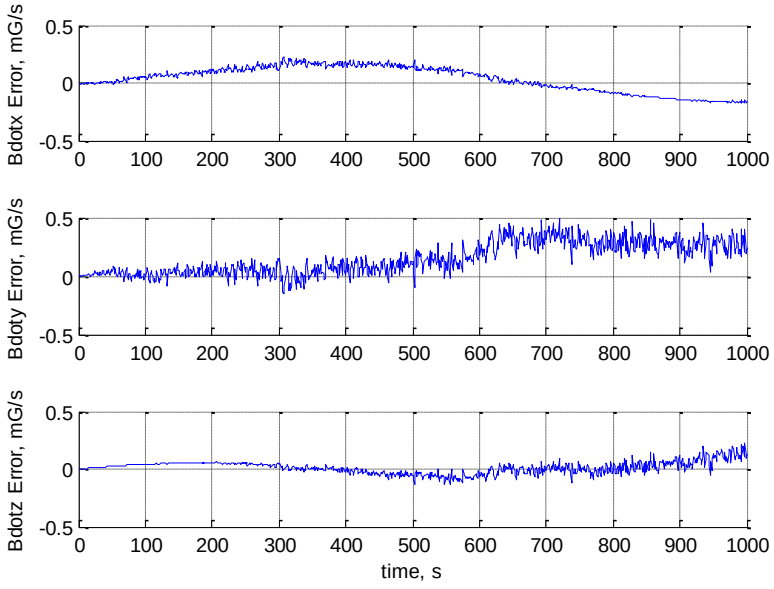

Figure 5.38. Magnetic Field Vector Derivative Error

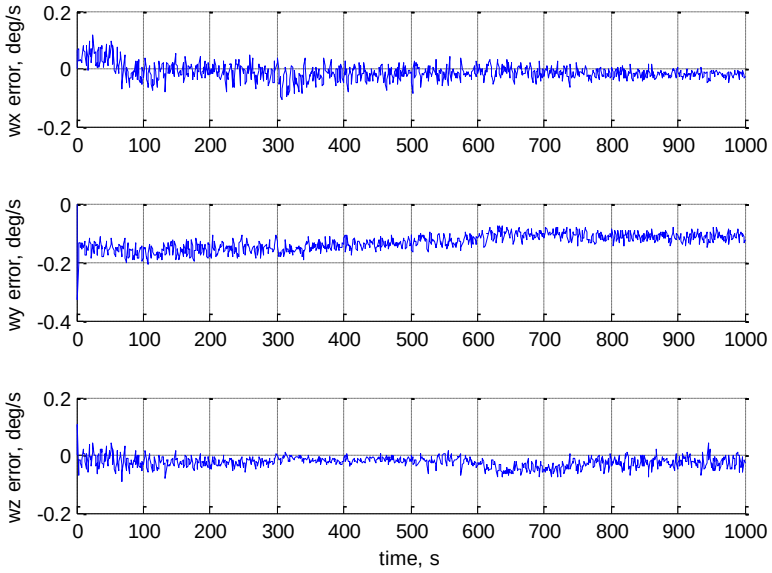

Figure 5.39. Angular Velocity Error From Stage-One Filter

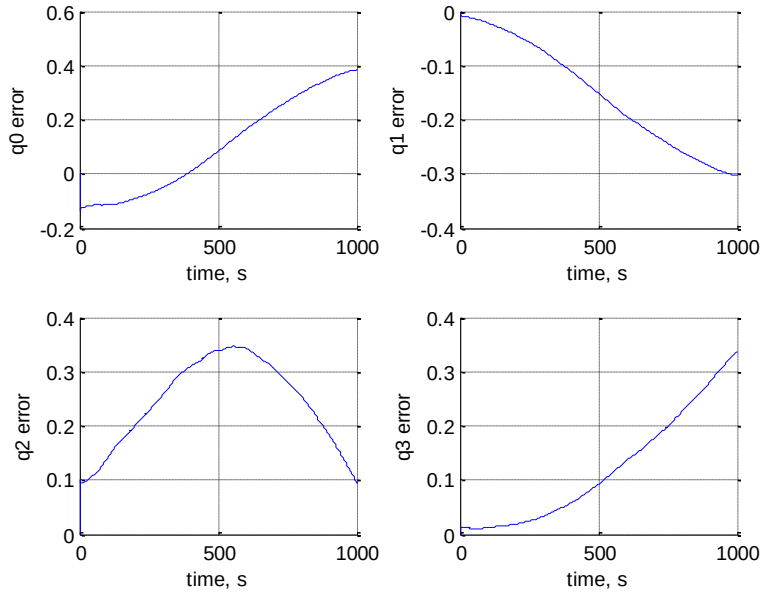

Figure 5.40. Attitude Quaternion Error

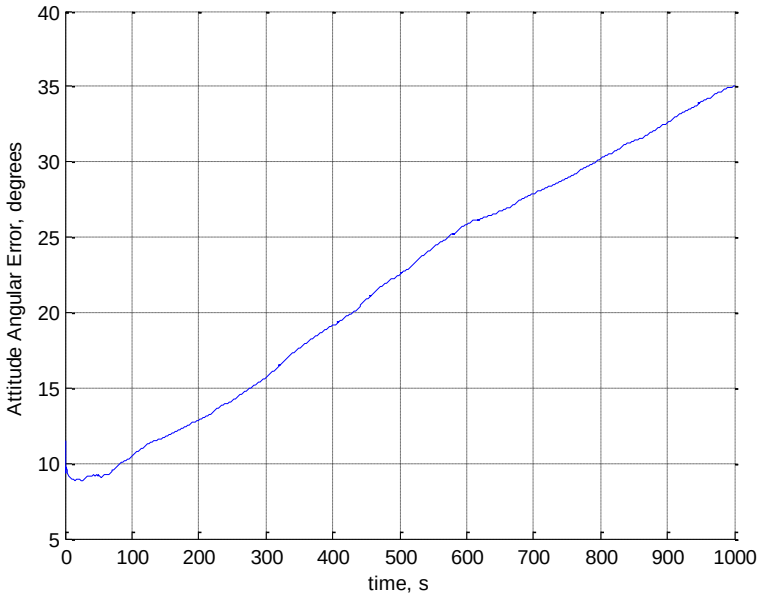

Figure 5.41. Attitude Angular Error

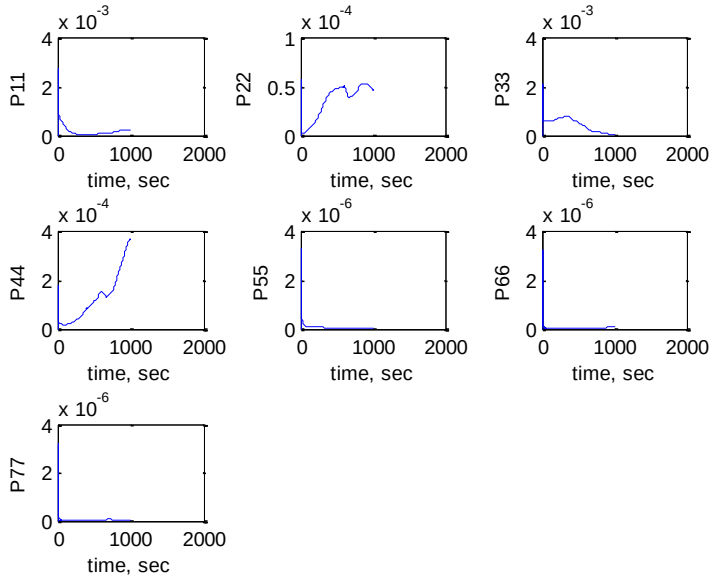

Figure 5.42. Stage-Two Filter Error Covariance Diagonals

Even when the angular velocity pseudomeasurement is used, the attitude determination code is unable to converge. When there is zero angular velocity, even though the angular velocity estimator is almost as accurate as the simulated IMU measurement, there is a bias leading to a small offset in angular velocity. This offset causes the filter to react as if there is a small angular velocity, slowly rotating the spacecraft. The result is a gradually building attitude error. Adding this measurement, therefore, does not lead to the correction of the ambiguity.

5.6. MODIFIED TUNING PARAMETERS

After searching for a method to resolve the ambiguity when the original formulation failed, the observability of the problem was reexamined. The observability of a nonlinear system is not always definitive, particularly with a system as complex as the one developed in this research. Considering the physical nature of the problem, the magnetometer measurement always immediately provides two axis resolution. Resolution of the third axis rotation can be problematic, as the spacecraft can have any orientation when rotating about the magnetic field vector and still give the same measurement. The ability of a filter to add a dynamic model and utilize the time history of the measurements should theoretically, over time, allow the filter to determine the correct solution even without the added information from the magnetic field derivative. Again, this is only possible if the magnetic field vector is changing.

It has been shown that when the spacecraft attitude is inertially fixed, the estimation of the magnetic field derivative is inaccurate. So this pseudomeasurement, which is very useful at improving accuracy at higher angular velocities, appears as though it is detrimental at lower angular velocities. The first step in improving performance over the entire range of angular velocities through tuning was to increase the measurement noise covariance related to the magnetic field derivative. A sensor model is typically used to determine measurement noise covariance; however, with a pseudomeasurement, there is no such noise model. As discussed in Reference 32, the first attempt was to examine the state error from the first-stage filter and use a comparable Guassian model to choose the noise covariance for the second stage. This

method was unable to converge using those covariance matrices. The filter matrices were instead adjusted to allow convergence.

Increasing the measurement noise covariance corresponding to the magnetic field derivative measurement slowed the divergence of the filter, but did not correct the problem. Next, the estimate of the quaternion was tuned to trust the magnetic field measurement more and rely less on the model. There is no model mismatch; however, if the model is assumed to be perfect, any error in angular rate estimates, either in initial error or filtering error, results in loss of accuracy because the equations depend on angular velocity. It is demonstrated in previous sections that a bias exists in the angular rate estimate from magnetometer data.

Through a trial-and-error process of increasing the process noise covariance led to a set of filter matrices that resulting in the simulation converging as long as the angular velocity initial estimate was very accurate. The filter was able to correct the attitude quaternion, but the restrictions on initial angular velocity estimate were too stringent to be considered a global solution. The filter parameters were further tuned to allow the angular rate corrections to be smaller and that solution allowed the baseline cases with angular rates set to zero to converge even with initial state error present.

The resulting retuned filter matrices were determined to be robust and accurate for the zero angular velocity case when they were set as:

$$P_0 = \begin{bmatrix} 5\times10^{-3} I_{4\times4} & 0_{4\times3} \\ 0_{4\times3} & 5\times10^{-3} \frac{\deg^2}{s^2} I_{3\times3} \end{bmatrix} \tag{109}$$

$$Q = \begin{bmatrix} 1\times10^{-2} I_{4\times4} & 0_{4\times3} \\ 0_{4\times3} & 1\times10^{-9} \frac{\deg^2}{s^2} I_{3\times3} \end{bmatrix} \tag{110}$$

$$R = \begin{bmatrix} 0.64 mG^2 I_{3\times3} & 0_{3\times3} \\ 0_{3\times3} & 2.56\times10^{5} \frac{mG^2}{s^2} I_{3\times3} \end{bmatrix} \tag{111}$$

These tuning parameters lead to the results shown in Figures 5.43-5.50. The simulation took longer to converge so the time was extended to fully evaluate the performance.

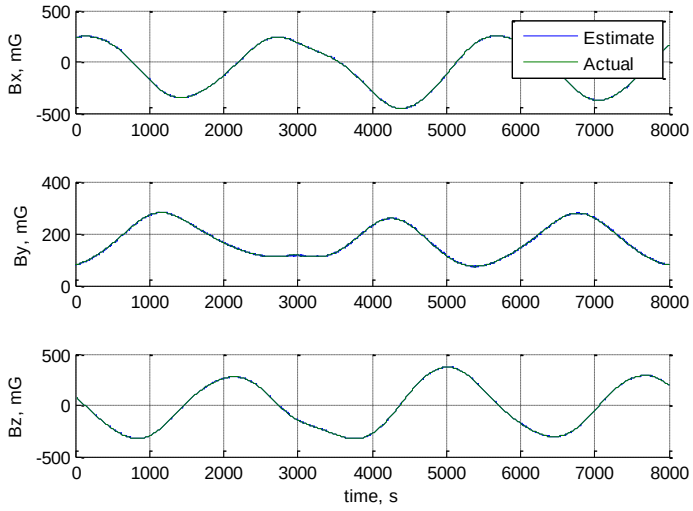

Figure 5.43. Magnetic Field Vector

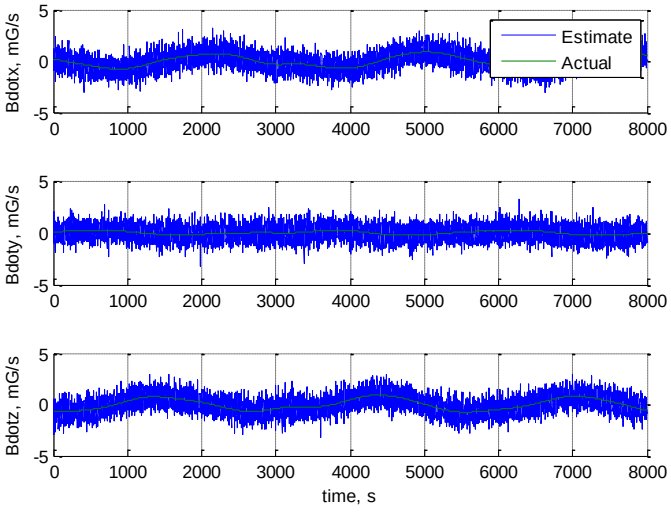

Figure 5.44. Magnetic Field Vector Derivative

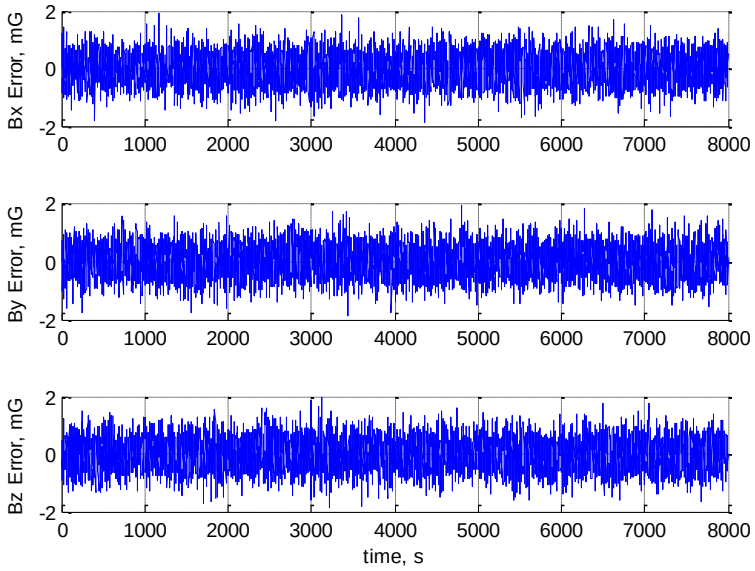

Figure 5.45. Magnetic Field Vector Estimation Error

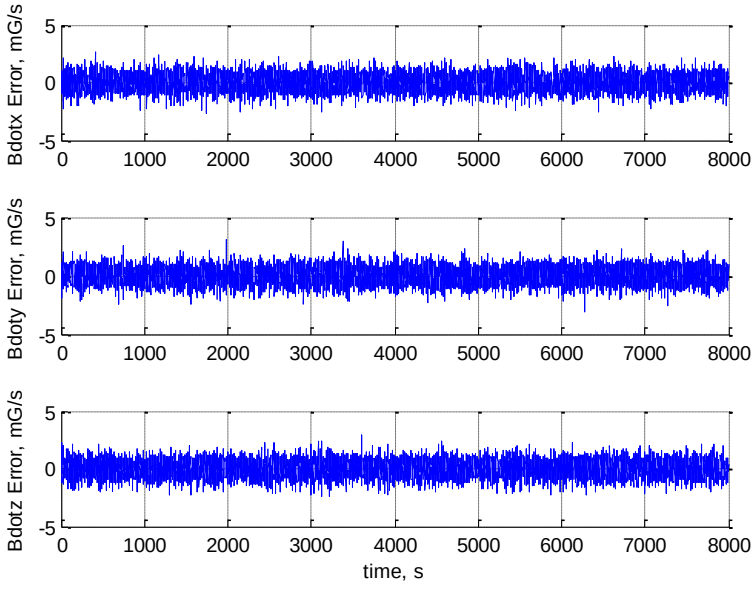

Figure 5.46. Magnetic Field Vector Derivative Estimation Error

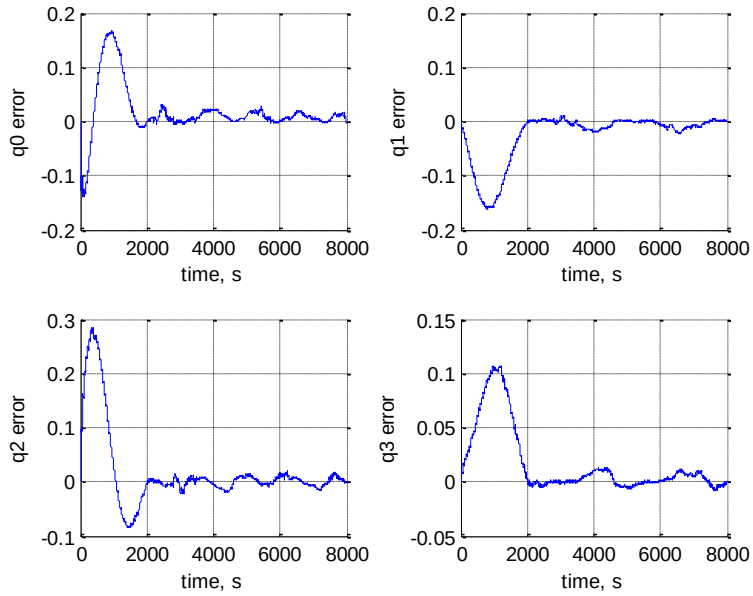

Figure 5.47. Attitude Quaternion Estimation Error

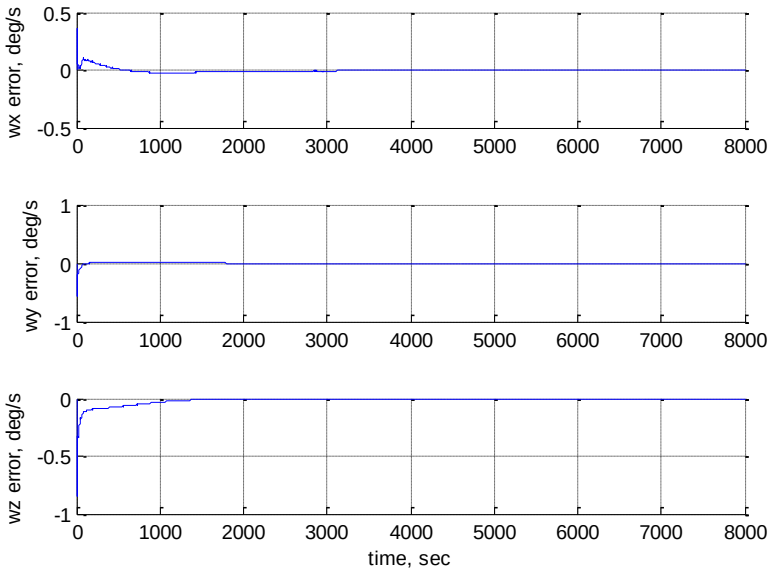

Figure 5.48. Angular Velocity Estimation Error

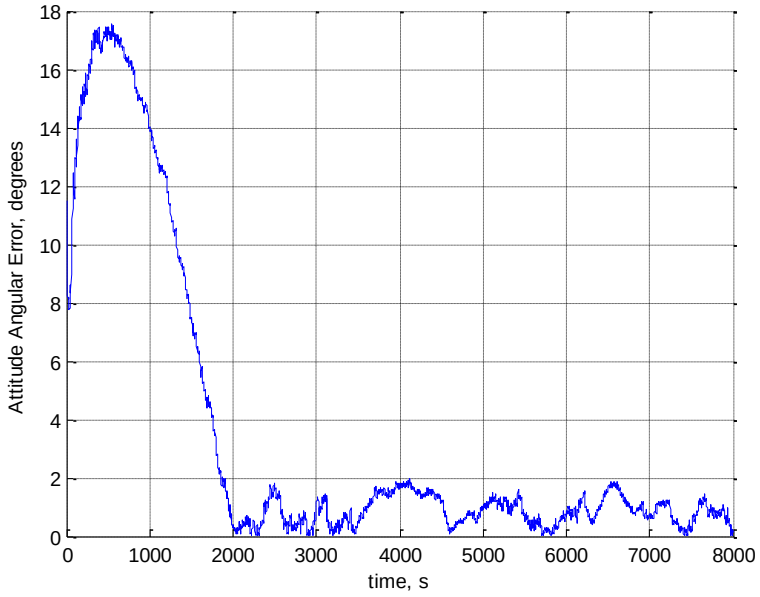

Figure 5.49. Attitude Angular Error

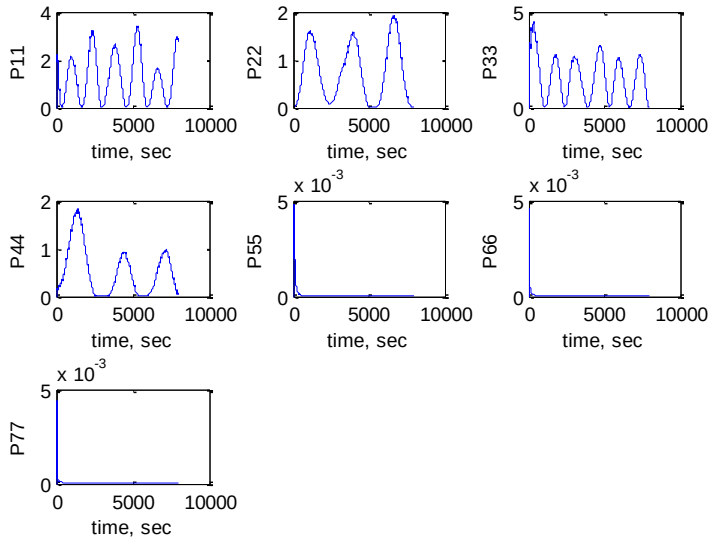

Figure 5.50. Stage-Two Filter Error Covariance Diagonals

The new tuning parameters used for the zero angular velocity case do not quite provide the attitude accuracy exhibited by the filter tuned differently at higher angular rates. However, the estimation of the angular velocity is better, on the order of 10^{-4}. It is important to next check if the newly tuned filter will work, and how well, when angular velocity is present, as shown in Figures 5.51-5.54.

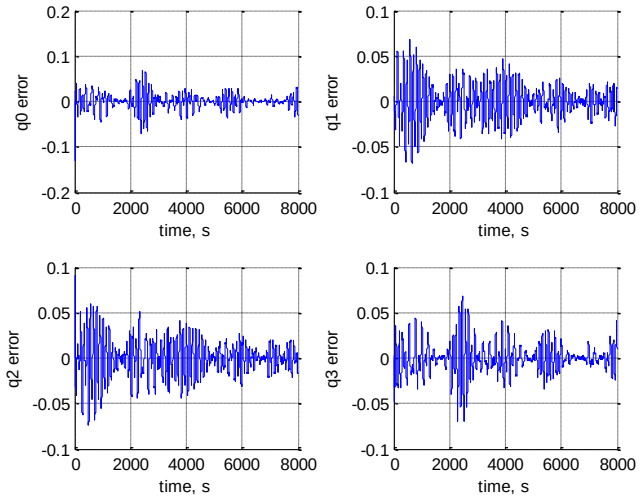

Figure 5.51. Attitude Quaternion Estimation Error

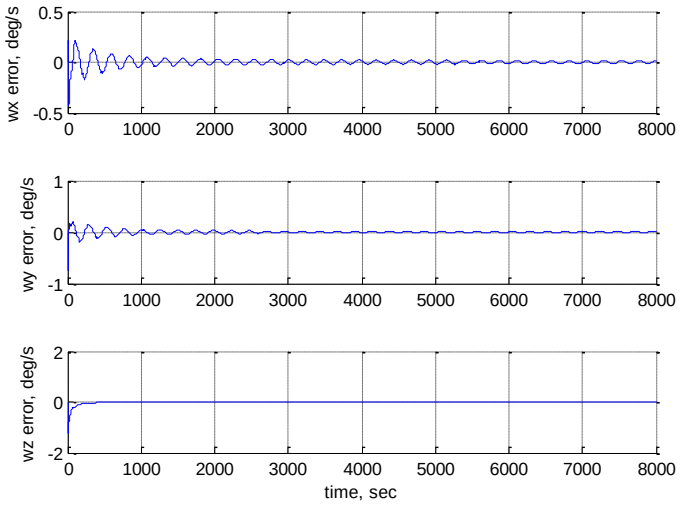

Figure 5.52. Angualar Velocity Estimation Error

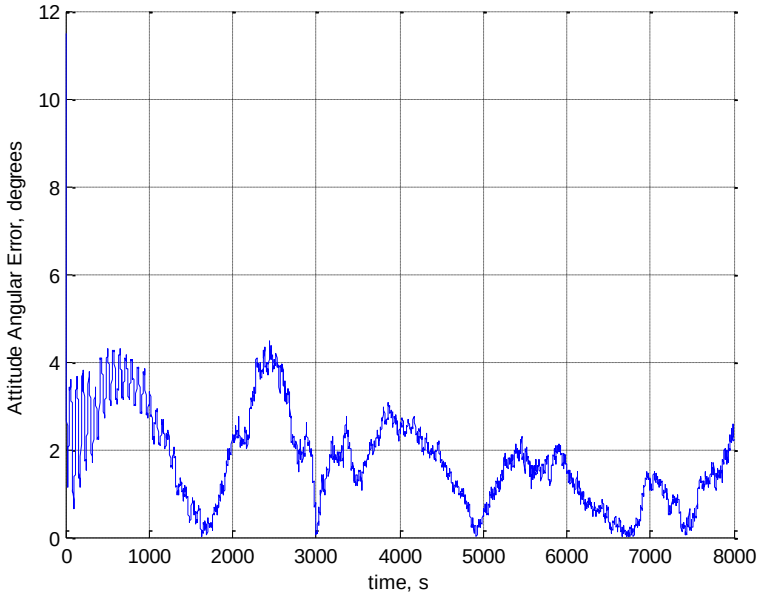

Figure 5.53. Attitude Angular Error

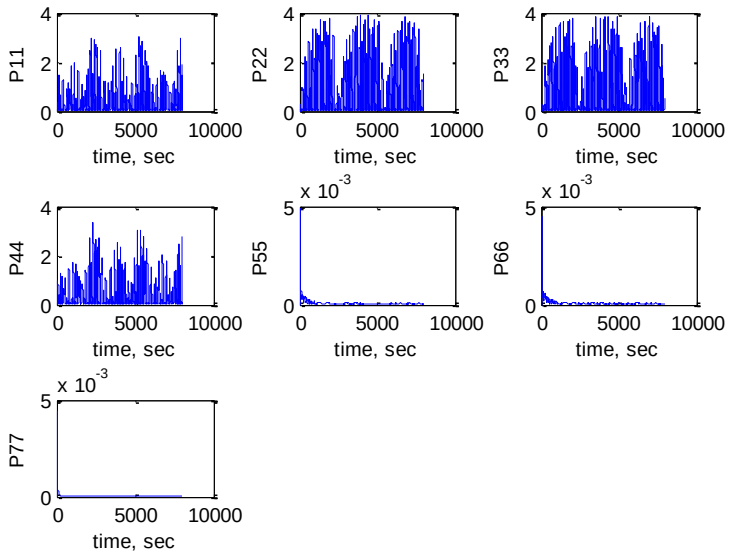

Figure 5.54. Stage-Two Filter Error Covariance Diagonals

It is clearly observed from these results that the new tuning parameters are not optimal for the baseline scenario (because of the rotation). When tuned to give the optimal performance for the baseline scenario, the covariance matrices become:

$$P_0 = \begin{bmatrix} 5\times10^{-3} I_{4\times4} & 0_{4\times3} \\ 0_{4\times3} & 5\times10^{-6} \frac{\text{deg}^2}{s^2} I_{3\times3} \end{bmatrix} \tag{112}$$

$$Q = \begin{bmatrix} 1\times10^{-9} I_{4\times4} & 0_{4\times3} \\ 0_{4\times3} & 1\times10^{-9} \frac{\text{deg}^2}{s^2} I_{3\times3} \end{bmatrix} \tag{113}$$

$$R = \begin{bmatrix} 0.64\ mG^2\ I_{3\times3} & 0_{3\times3} \\ 0_{3\times3} & 2.56\ \frac{mG^2}{s^2} I_{3\times3} \end{bmatrix} \tag{114}$$

The above covariance matrices allow the filter to estimate the spacecraft attitude to within 0.2 degrees for the baseline case and with even higher accuracy as the angular velocity is increased, as shown in Figures 5.55-5.58.

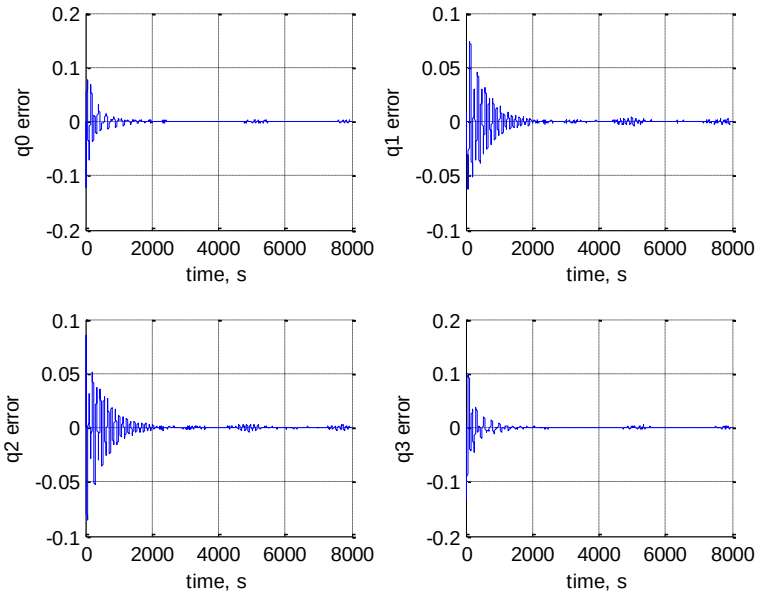

Figure 5.55. Attitude Quaternion Estimation Error

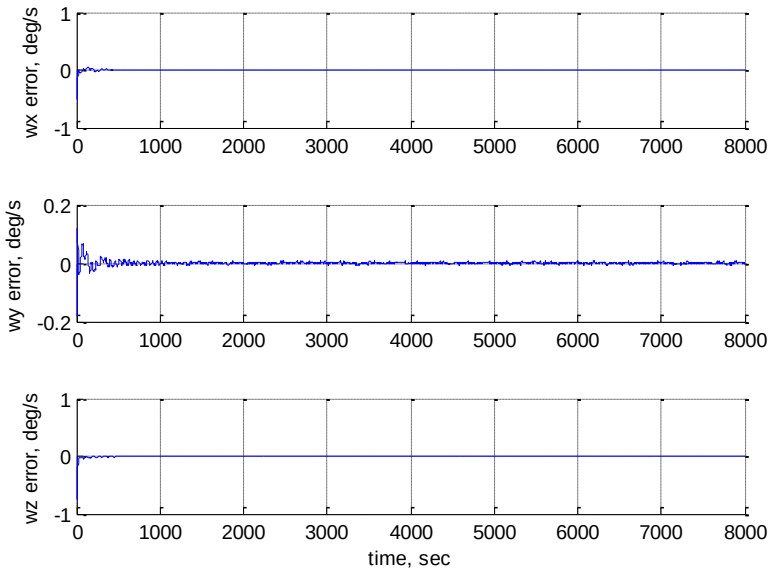

Figure 5.56. Angualar Velocity Estimation Error

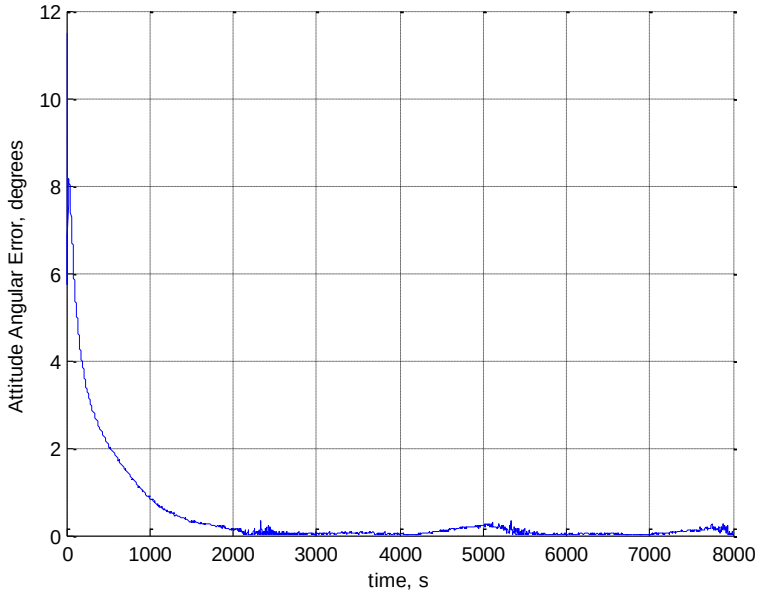

Figure 5.57. Attitude Angular Error

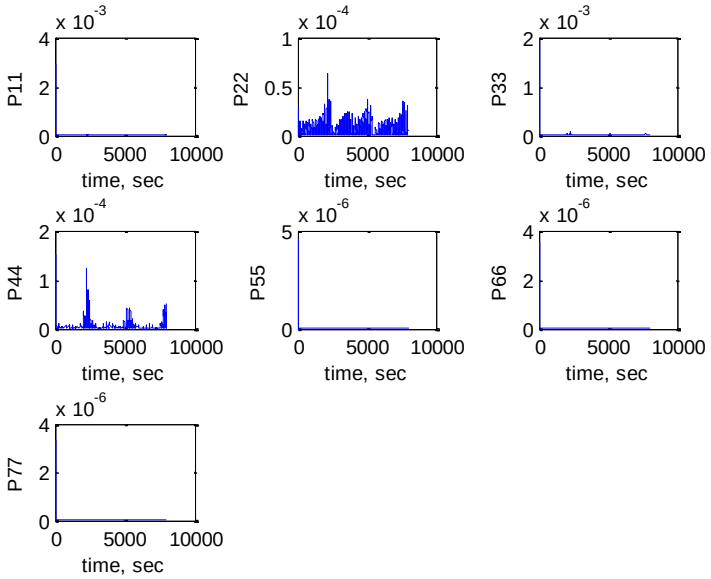

Figure 5.58. Stage-Two Filter Error Covariance Diagonals

The filter is now sufficiently versatile, with variable covariance matrices, to estimate the spacecraft attitude regardless of angular velocity. The accuracy of the finely tuned method with a spinning spacecraft provides accuracies that meet or exceed those presented in the literature. The scenario where the spacecraft is inertially fixed (with no rotation) has not previously been shown in the literature to be observable. The method allows for attitude determination at zero angular velocity on the order of 1.5 degrees accuracy and angular rate estimation with accuracies on the order of 10^{-3} degrees per second.

6. DUAL-STAGE FILTER VARIABLE COVARIANCE SOLUTION

This section forms the culmination of the research described in Sections 4 and 5. The solution presented here combines the most accurate and robust filter solution found during this dissertation study.

6.1. METHOD DESCRIPTION

The first attempt at defining the first stage used a Kalman filter with the magnetic field vector modeled using a Markov Model. This produced an accurate estimate of the magnetic field derivative, which was proven to be sufficiently accurate for attitude calculation if the spacecraft was spinning. The goals defined in this study included developing different methods to use for the first stage that produce more accurate results or produce more "information" that would allow the second-stage filter to estimate the attitude even at low to zero values of the spacecraft angular velocity.

After experimenting with the addition of angular rate measurements from an IMU, it was determined that the best likely solution to the robustness difficulty is to estimate the angular velocity in the first stage and use this estimate in the second stage. A significant portion of Section 3 is devoted to exploring the system dynamics, searching for possible methods to estimate or calculate the angular velocity of the spacecraft.

One tested method updates the Markov model used in Reference 32 to include a dynamic model that relates the magnetic field to the angular velocity. This allows for the addition of angular velocity as a state. The filter estimates the angular velocity accurately; however, there is a bias in the estimate. Section 4.3 shows that the there is a linear dependence in the equations relating angular velocity to the magnetic field vector derivative. This problem can be averted by adding another equation that approximates the angular velocity magnitude from consecutive magnetic field measurements. This approach is used to produce an additional pseudomeasurement for use by the first stage filter. Unfortunately, the addition of this pseudomeasurement was unable to improve the estimation bias in the angular velocity estimates. The accuracy of both of these first-

stage filters exceed that presented in Reference 34. However, the bias in the estimate made this method insufficient as a pseudomeasurement for the second-stage filter.

The development of a deterministic method was also completed. The deterministic method showed that the attitude and angular rates could be estimated accurately when there was no measurement noise considered. When noise was added to the simulation, coarse attitude determination was possible to within about four degrees; however, the initial guess needed to be sufficiently accurate for the method to converge. The performance of the deterministic method was deemed insufficient for the goals of the attitude determination algorithm sought in this study.

With the convergence of the numerical deterministic solution approach established, even in the zero angular velocity case, it was postulated that a sufficient amount of data needed for successful attitude estimation is embedded within the magnetic field vector and its derivative. This notion is further supported when considering using past measurement history is a key attribute of a filter. The original idea was reinvestigated to consider if manipulating the tuning parameters or covariance matrices of the Kalman filter, even if the solution needed to be piecewise, would yield acceptable results for the zero angular velocity case. The investigation led to a solution that at first was susceptible to errors in the initial angular velocity estimate. By gradually tuning the covariance parameters, a more robust solution was found for the case with zero and low angular velocity that was able to estimate the attitude to within about 1.5 degrees. This accuracy is not as good as the method can achieve with alternate noise covariance matrices at higher angular rates, however, a piecewise covariance matrix set can be implemented so that if the angular rates are found to be low, one set can be utilized and if the rates are high, a different set can be used to obtain better results.

6.2. PARAMETRIC STUDY AND RESULTS

The table below, Table 6.1, displays the covariance matrices sets that were used to produce the most accurate attitude determination results depending on orbit inclination and spacecraft angular rate. If the spacecraft is in an equatorial orbit with an inertially fixed attitude, this provides the lowest observability of any scenario, which specifies that

the tuning needs to be very carefully done to allow the filter more time to resolve the attitude by relying more on the magnetic field measurement and allowing the filter to run for an extended time. If the magnetic field measurement were fixed within the spacecraft, the problem would be completely unobservable. However, even in this worst-case orbit scenario there is still a small amount of change in the magnetic field vector over time.

Table 6.1. Applicable Regions for Covariance Sets

Inclination (deg)	0-45 degrees	45+ degrees
Angular Rate (deg/s)		
0-0.1	Set 1	Set 2
0.1-0.5	Set 2	Set 3
0.5-1	Set 3	Set 4
1+	Set 4	Set 5
2+	Set 5	Set 5

The following sets of filter matrices were used for the simulations described in the table above. The list was prepared for the baseline case, but an equatorial orbit was also considered that required more modifications to allow the filter to accurately estimate the attitude and rates in a sufficient amount of time.

Set 1:

$$P_0 = \begin{bmatrix} 5\times10^{-3} I_{4\times4} & 0_{4\times3} \\ 0_{4\times3} & 5\times10^{-3} \frac{\text{deg}^2}{s^2} I_{3\times3} \end{bmatrix} \tag{115}$$

$$Q = \begin{bmatrix} 1\times10^{-2} I_{4\times4} & 0_{4\times3} \\ 0_{4\times3} & 1\times10^{-9} \frac{\text{deg}^2}{s^2} I_{3\times3} \end{bmatrix} \tag{116}$$

$$R = \begin{bmatrix} 0.64\ mG^2\ I_{3\times3} & 0_{3\times3} \\ 0_{3\times3} & 2.56\times10^{3} \frac{mG^2}{s^2} I_{3\times3} \end{bmatrix} \tag{117}$$

Set 2:

$$P_0 = \begin{bmatrix} 5\times10^{-3} I_{4\times4} & 0_{4\times3} \\ 0_{4\times3} & 5\times10^{-3} \frac{\text{deg}^2}{s^2} I_{3\times3} \end{bmatrix} \tag{118}$$

$$Q = \begin{bmatrix} 1\times10^{-2} I_{4\times4} & 0_{4\times3} \\ 0_{4\times3} & 1\times10^{-9} \frac{\text{deg}^2}{s^2} I_{3\times3} \end{bmatrix} \tag{119}$$

$$R = \begin{bmatrix} 0.64\ mG^2\ I_{3\times3} & 0_{3\times3} \\ 0_{3\times3} & 2.56\times10^{5} \frac{mG^2}{s^2} I_{3\times3} \end{bmatrix} \tag{120}$$

Set 3:

$$P_0 = \begin{bmatrix} 5\times10^{-3} I_{4\times4} & 0_{4\times3} \\ 0_{4\times3} & 5\times10^{-3} \frac{\text{deg}^2}{s^2} I_{3\times3} \end{bmatrix} \quad (121)$$

$$Q = \begin{bmatrix} 1\times10^{-4} I_{4\times4} & 0_{4\times3} \\ 0_{4\times3} & 1\times10^{-9} \frac{\text{deg}^2}{s^2} I_{3\times3} \end{bmatrix} \quad (122)$$

$$R = \begin{bmatrix} 0.64\ mG^2\ I_{3\times3} & 0_{3\times3} \\ 0_{3\times3} & 10.24 \frac{mG^2}{s^2} I_{3\times3} \end{bmatrix} \quad (123)$$

Set 4:

$$P_0 = \begin{bmatrix} 5\times10^{-3} I_{4\times4} & 0_{4\times3} \\ 0_{4\times3} & 5\times10^{-3} \frac{\text{deg}^2}{s^2} I_{3\times3} \end{bmatrix} \quad (124)$$

$$Q = \begin{bmatrix} 1\times10^{-4} I_{4\times4} & 0_{4\times3} \\ 0_{4\times3} & 1\times10^{-9} \frac{\text{deg}^2}{s^2} I_{3\times3} \end{bmatrix} \quad (125)$$

$$R = \begin{bmatrix} 0.64\ mG^2\ I_{3\times3} & 0_{3\times3} \\ 0_{3\times3} & 4 \frac{mG^2}{s^2} I_{3\times3} \end{bmatrix} \quad (126)$$

Set 5:

$$P_0 = \begin{bmatrix} 5\times10^{-3} I_{4\times4} & 0_{4\times3} \\ 0_{4\times3} & 5\times10^{-6} \frac{\text{deg}^2}{s^2} I_{3\times3} \end{bmatrix} \tag{127}$$

$$Q = \begin{bmatrix} 1\times10^{-9} I_{4\times4} & 0_{4\times3} \\ 0_{4\times3} & 1\times10^{-9} \frac{\text{deg}^2}{s^2} I_{3\times3} \end{bmatrix} \tag{128}$$

$$R = \begin{bmatrix} 0.64\ mG^2\ I_{3\times3} & 0_{3\times3} \\ 0_{3\times3} & 2.56 \frac{mG^2}{s^2} I_{3\times3} \end{bmatrix} \tag{129}$$

When these sets of covariance matrices were applied to the scenarios listed in Table 6.1, successful convergence and accurate estimation resulted. The covariance matrices that were tuned for the spinning case provides a high level of accuracy, comparable to or surpassing other approaches documented in the literature, while modifying these covariance matrices lead to the dual filter method successfully converging to a solution when the spacecraft's attitude was inertially fixed. It is noted that this a problem for which the literature search revealed no known solution in this case. The covariance set can be chosen by starting at the lowest set, which works in all cases, but is very slow to converge and is not as accurate in the spinning case. Once the filter converges, the angular rate is known and the best possible set can be substituted. The orbit inclination will be known in advance, so selecting the set based on inclination does not need to be determined online.

The following simulation results demonstrate the accuracy of the second-stage filter in each of the applicable regions. The simulation time was extended to show the performance over a longer time span. Figures 6.1-6.8 show the results of the simulation using an equatorial orbit and a non-rotating spacecraft. This scenario provides the

smallest amount of magnetic field vector change and is therefore the most difficult scenario to estimate accurately.

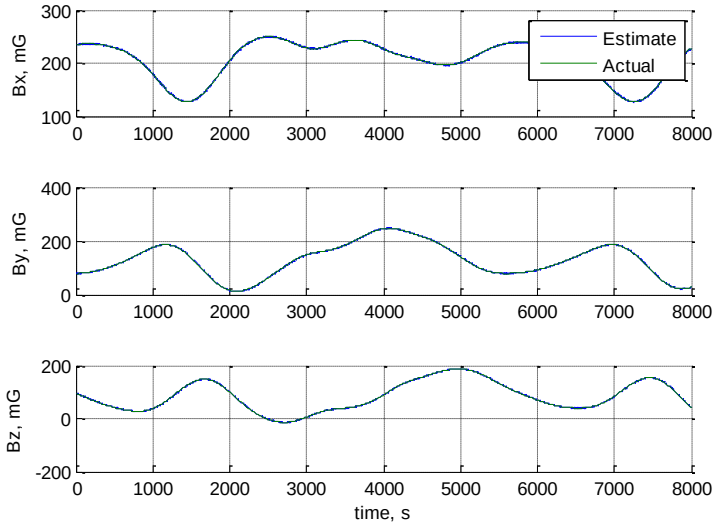

Figure 6.1. Magnetic Field Vector

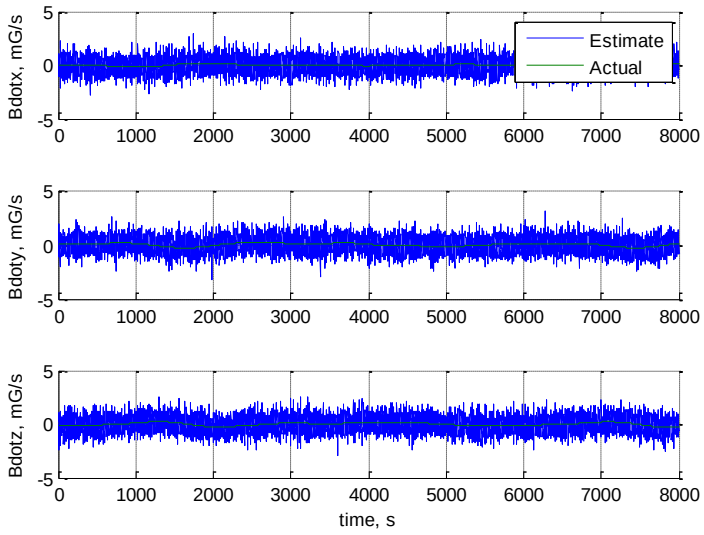

Figure 6.2. Magnetic Field Vector Derivative

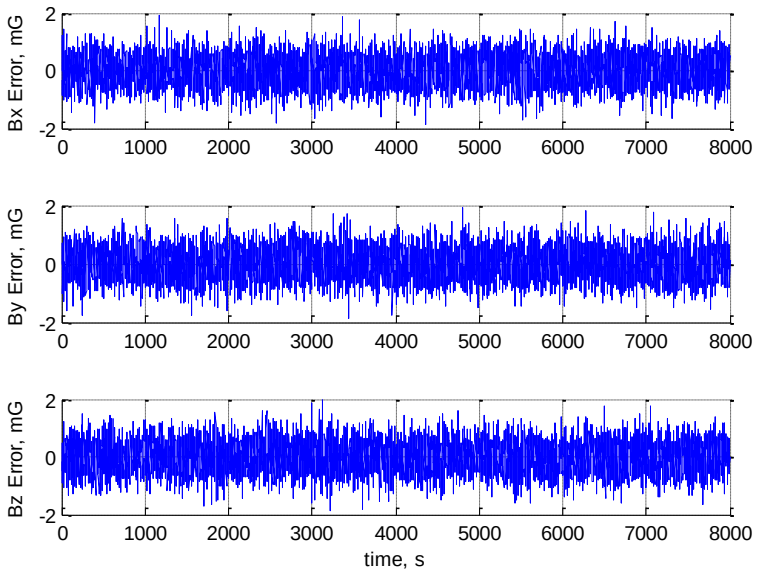

Figure 6.3. Magnetic Field Vector Estimation Error

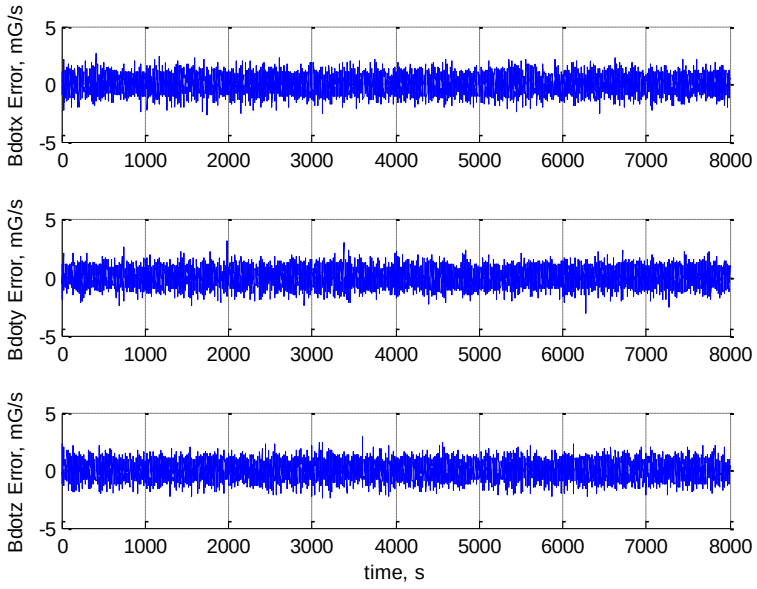

Figure 6.4. Magnetic Field Vector Derivative Estimation Error

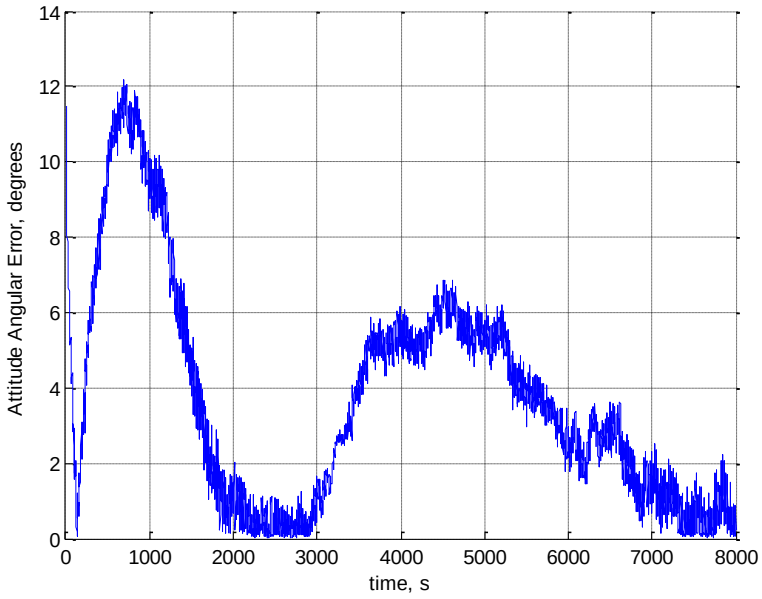

Figure 6.5. Attitude Angular Error

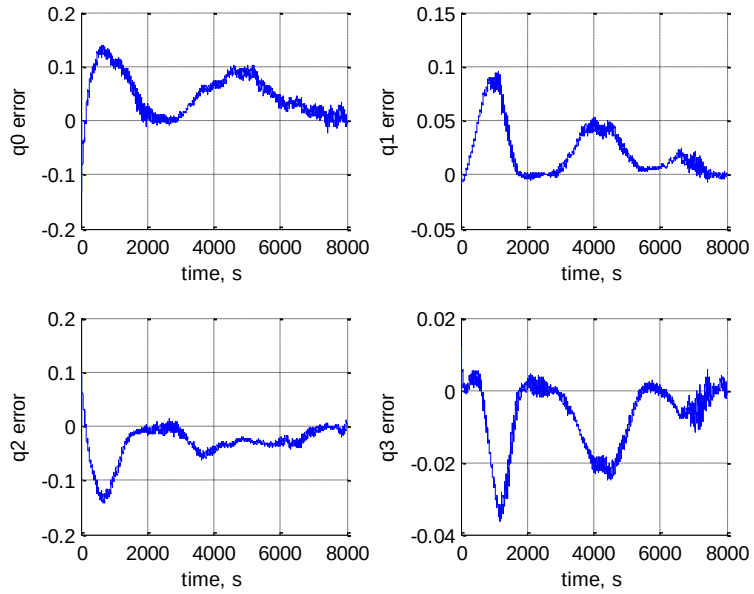

Figure 6.6. Attitude Quaternion Estimation Error

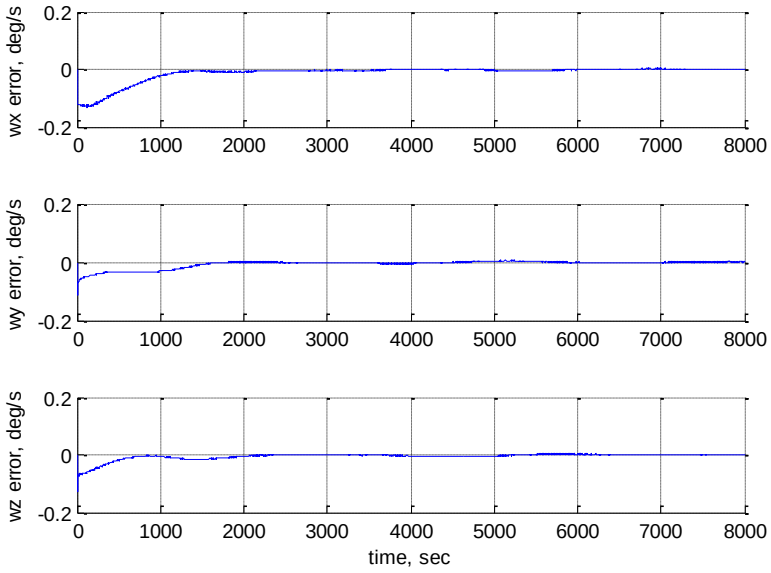

Figure 6.7. Angular Velocty Esimation Error

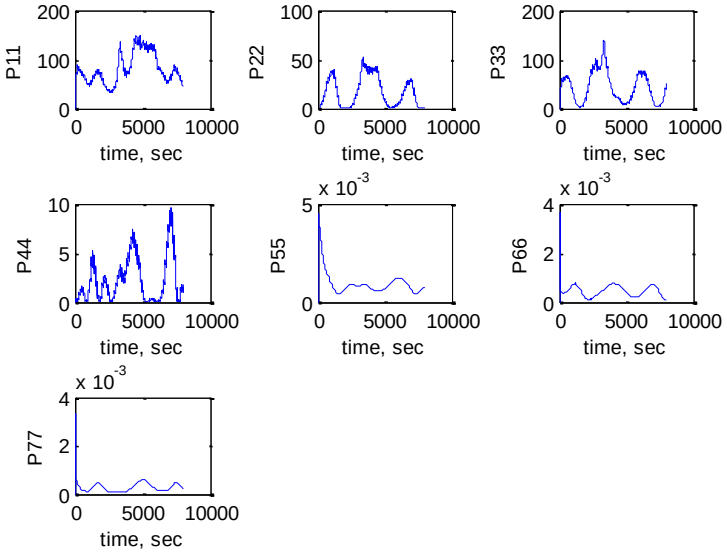

Figure 6.8. Stage-Two Filter Error Covariance Diagonals

The tuning parameters used in this scenario can be used in any of the scenarios with moderate accuracy. However, with slight alterations, the filter can provide more accurate estimations for higher spacecraft angular velocities. The second case was set at 45 degrees inclination when the spacecraft was not rotating. The results of this simulation can be observed in Figures 6.9-6.16. The results again show that the attitude can be estimated within two degrees and angular rate errors are on the order of 10^{-3} degrees per second.

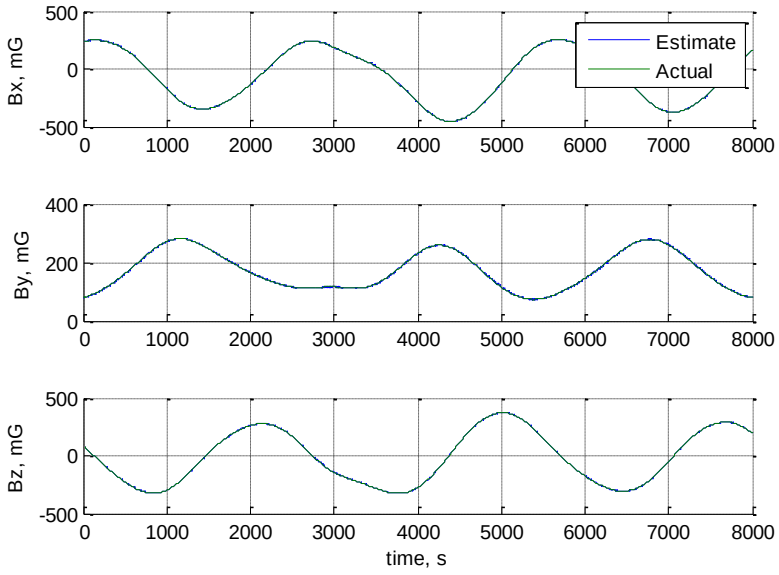

Figure 6.9. Magnetic Field Vector

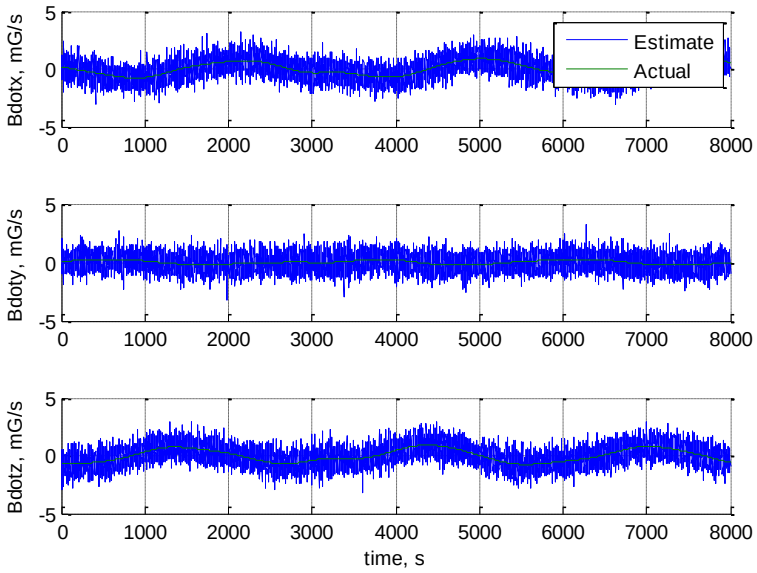

Figure 6.10. Magnetic Field Vector Derivative

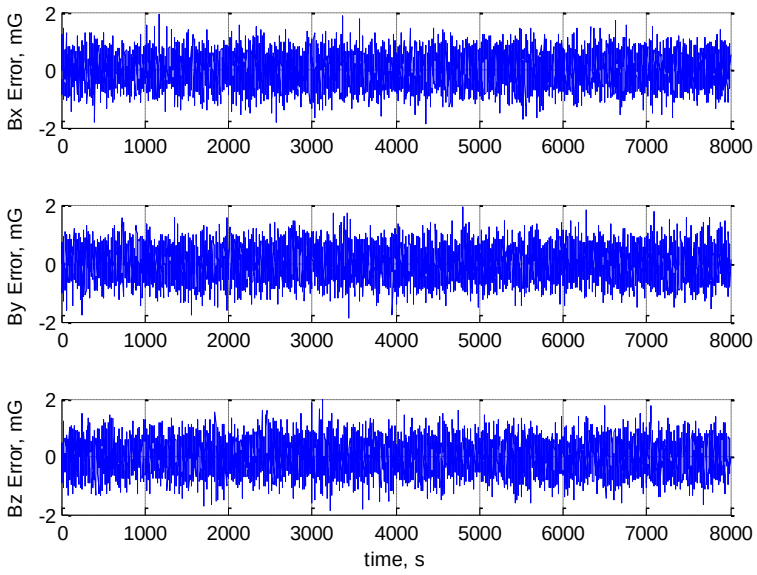

Figure 6.11. Magnetic Field Vector Estimation Error

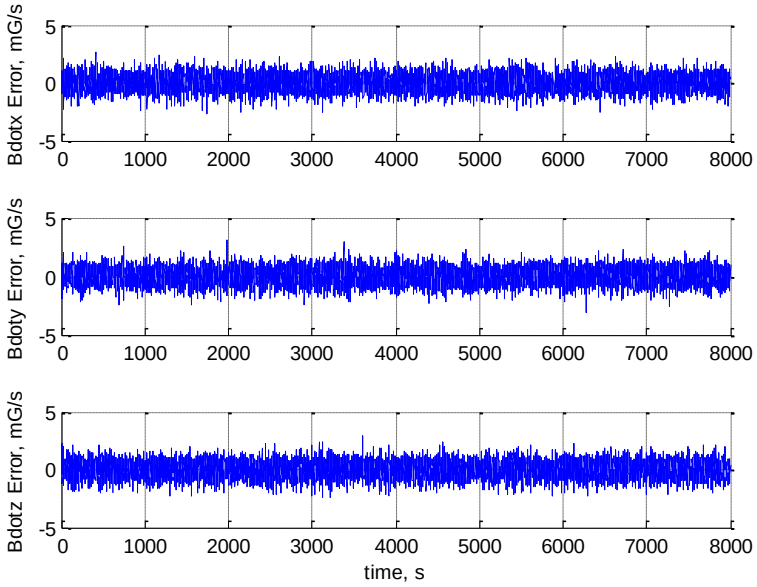

Figure 6.12. Magnetic Field Vector Derivative Estimation Error

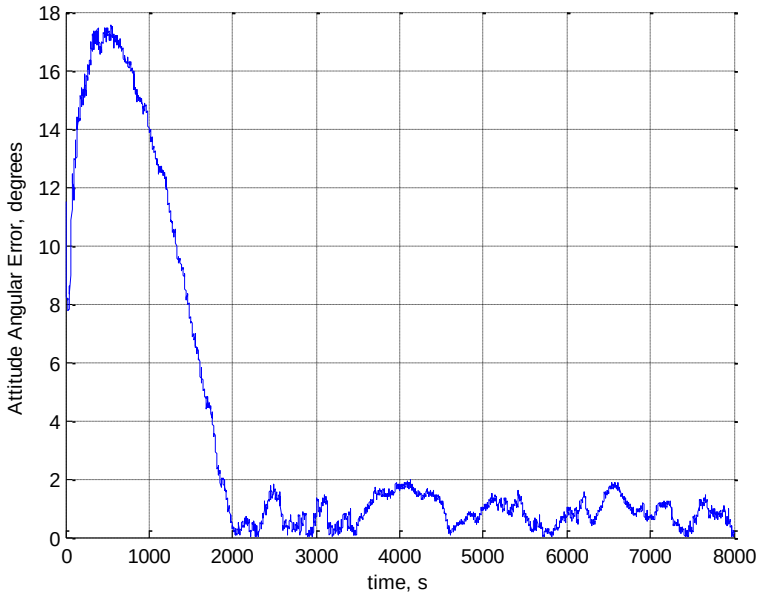

Figure 6.13. Attitude Angular Error

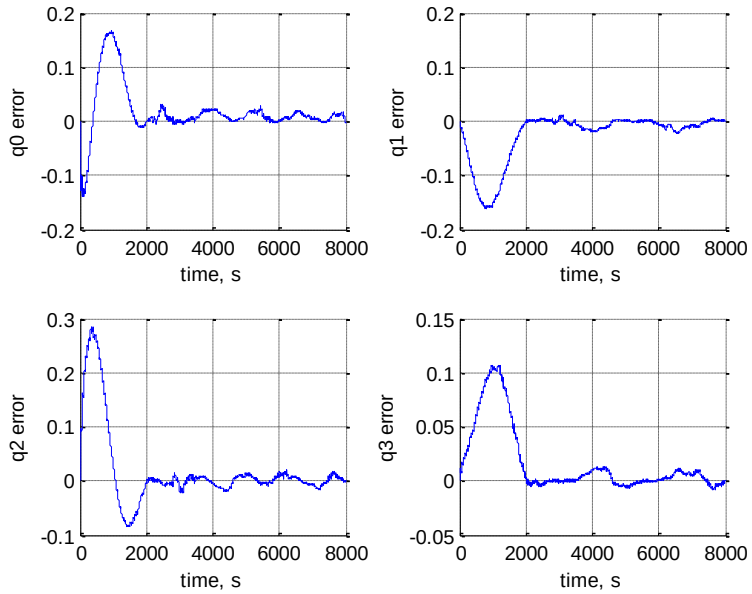

Figure 6.14. Attitude Quaternion Error

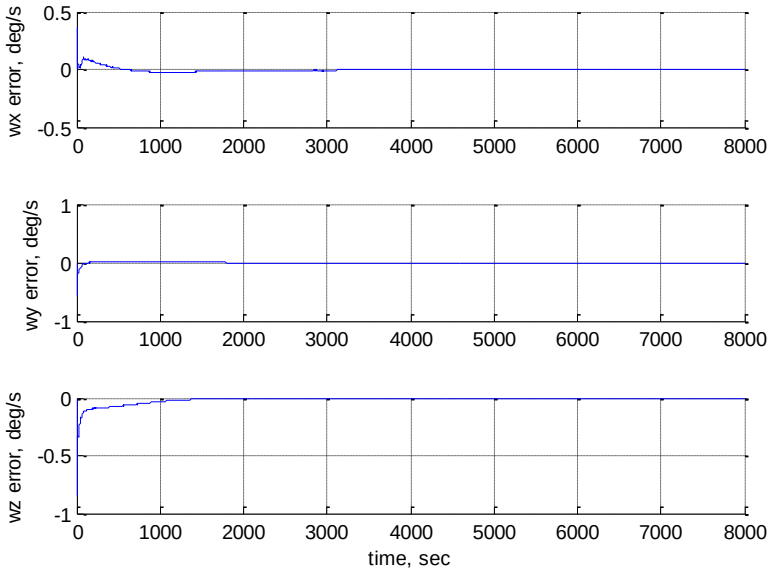

Figure 6.15. Angular Velocity Error

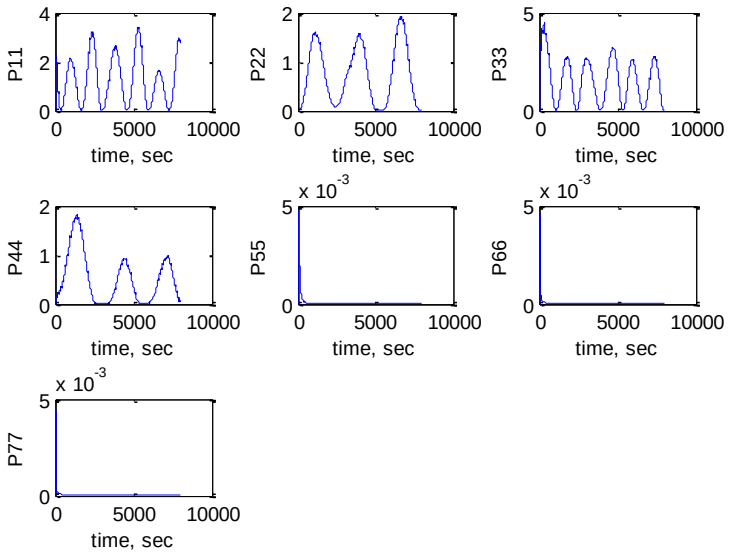

Figure 6.16. Stage-Two Filter Error Covariance Diagonals

Next, the angular velocity was increased to 0.1 degrees per second along each direction and the filter was tuned to provide convergence as fast as possible with acceptable accuracies. Figures 6.17-6.24 demonstrate that with the increased rotation rate of 0.1 degrees per second, the filter is now able to estimate the attitude to within about a degree and the rates to within 10^{-3} degrees per second.

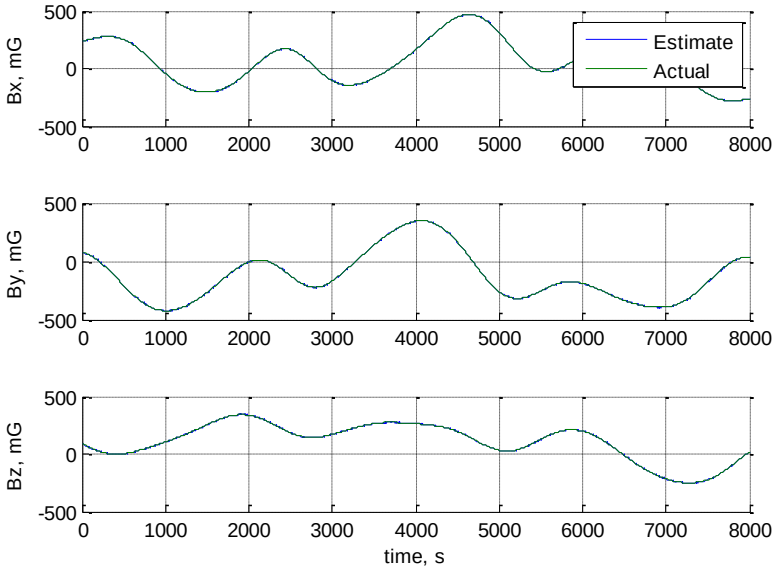

Figure 6.17. Magnetic Field Vector

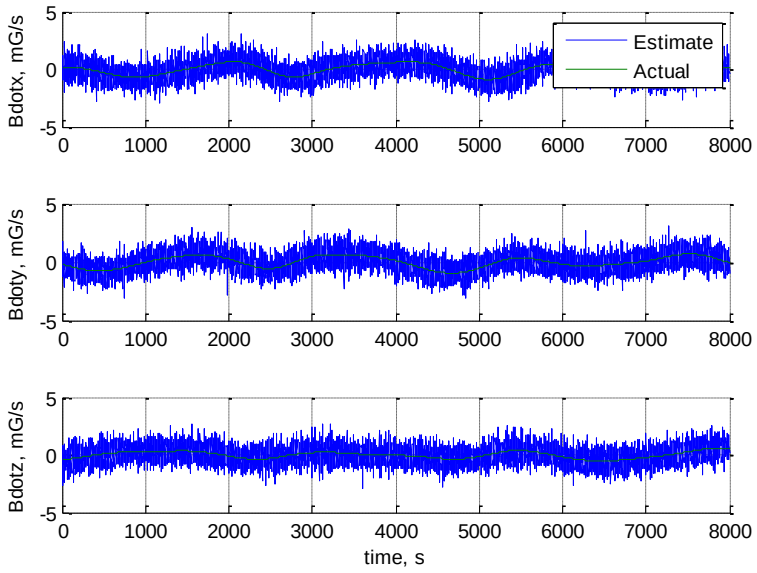

Figure 6.18. Magnetic Field Vector Derivative

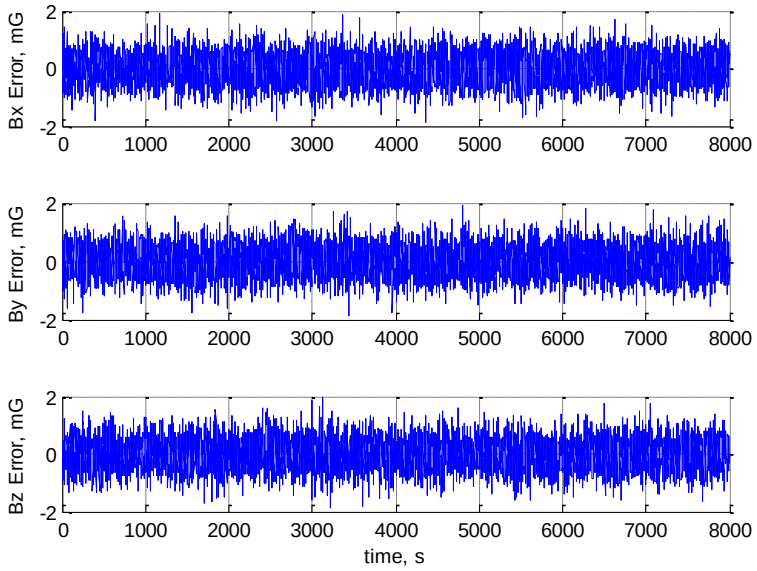

Figure 6.19. Magnetic Field Vector Estimation Error

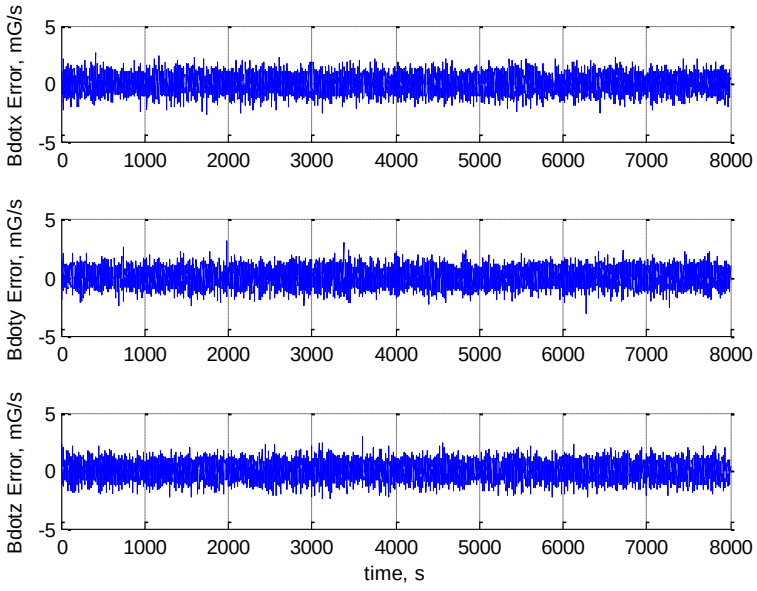

Figure 6.20. Magnetic Field Vector Derivative Estimation Error

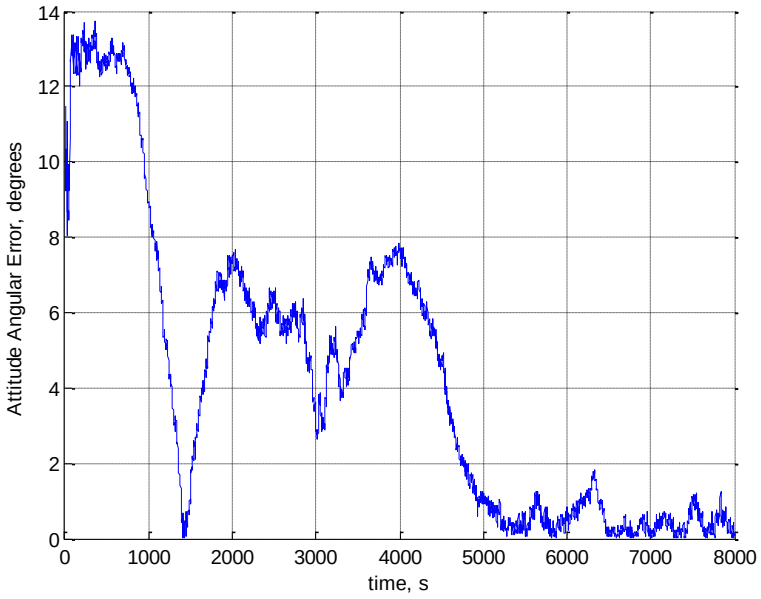

Figure 6.21. Attitude Angular Error

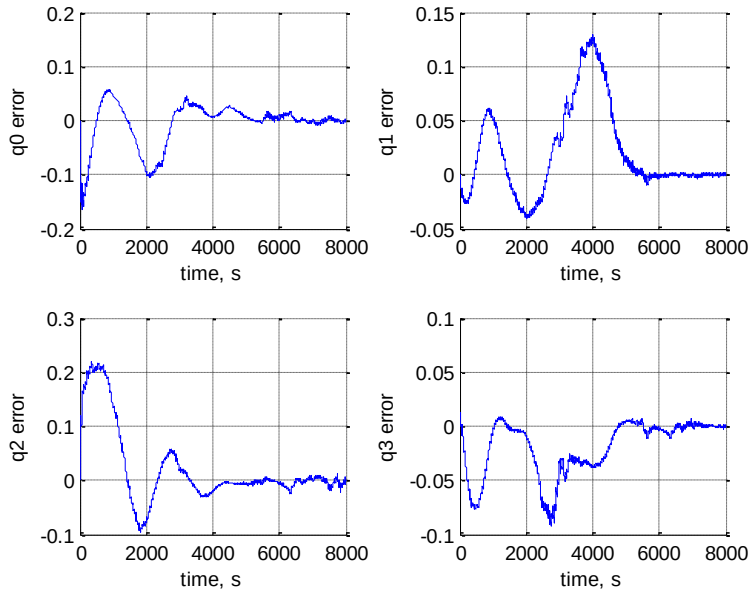

Figure 6.22. Attitude Quaternion Error

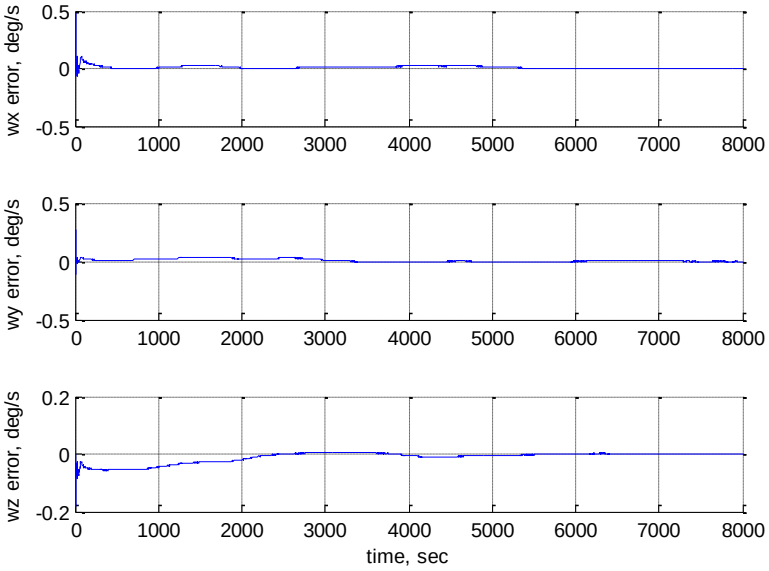

Figure 6.23. Angular Velocity Error

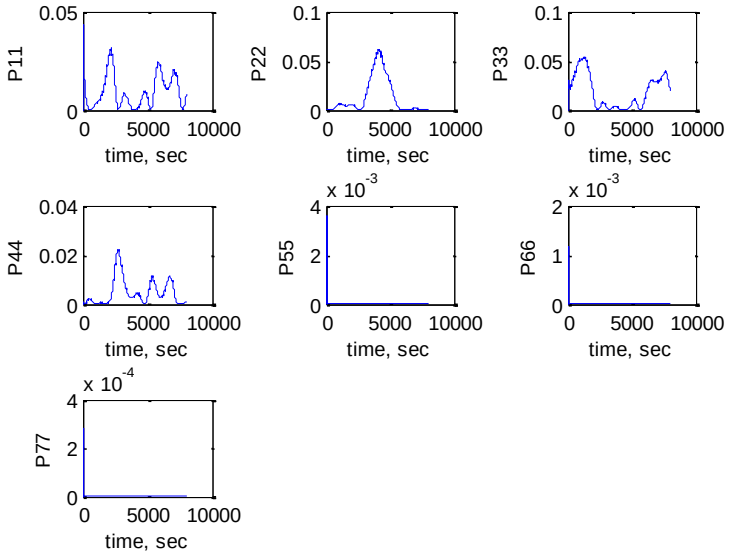

Figure 6.24. Stage-Two Filter Error Covariance Diagonals

The simulation angular velocity was now further increased to 0.5 degrees per second with the covariance matrices tuned again to produce the best estimation results, presented in Figures 6.25-6.32. It is clear from these results that as the rotation of the spacecraft in the simulations increase and the filter is properly tuned the accuracy of the attitude estimation improves.

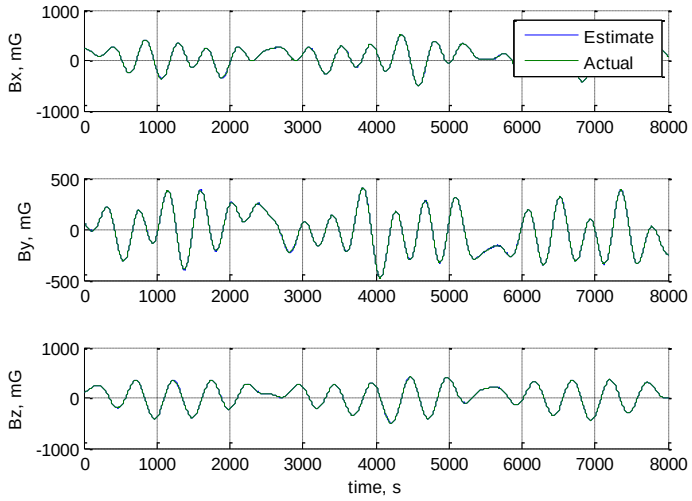

Figure 6.25. Magnetic Field Vector

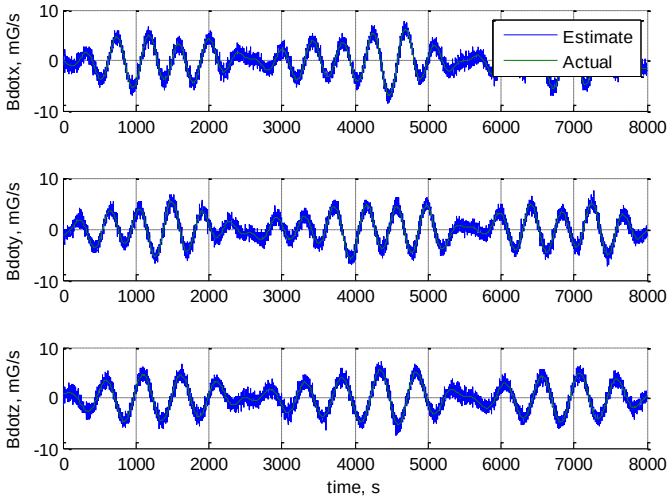

Figure 6.26. Magnetic Field Vector Derivative

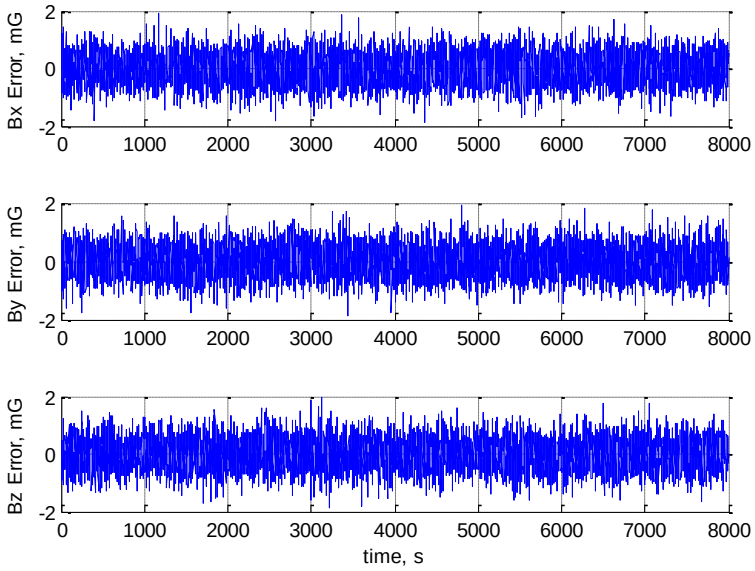

Figure 6.27. Magnetic Field Vector Estimation Error

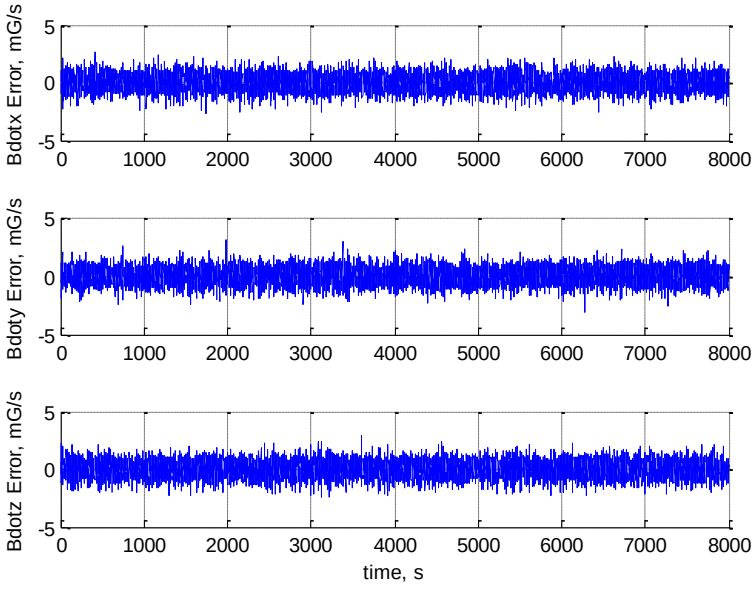

Figure 6.28. Magnetic Field Vector Derivative Estimation Error

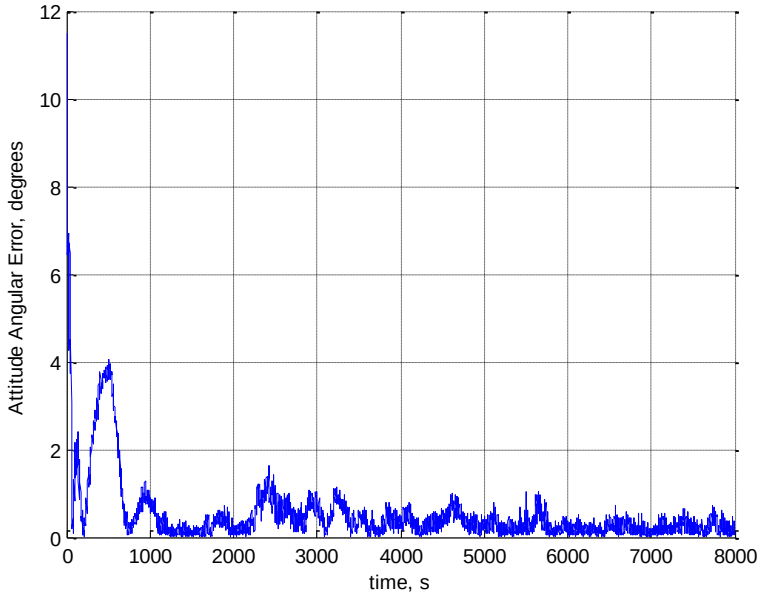

Figure 6.29. Attitude Angular Error

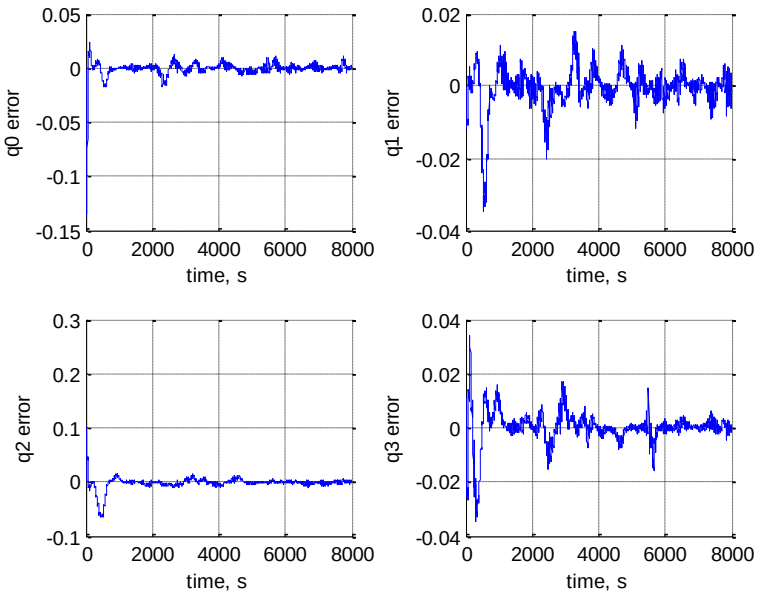

Figure 6.30. Attitude Quaternion Estimation Error

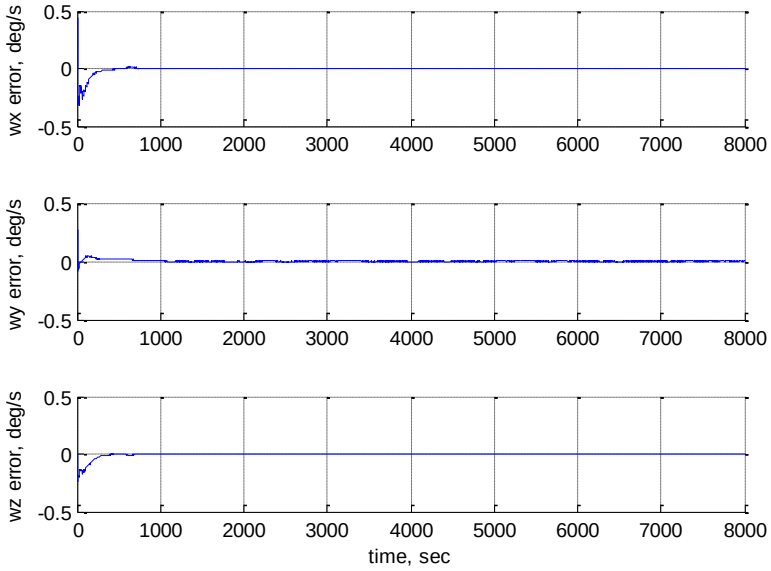

Figure 6.31. Angular Rate Estimation Error

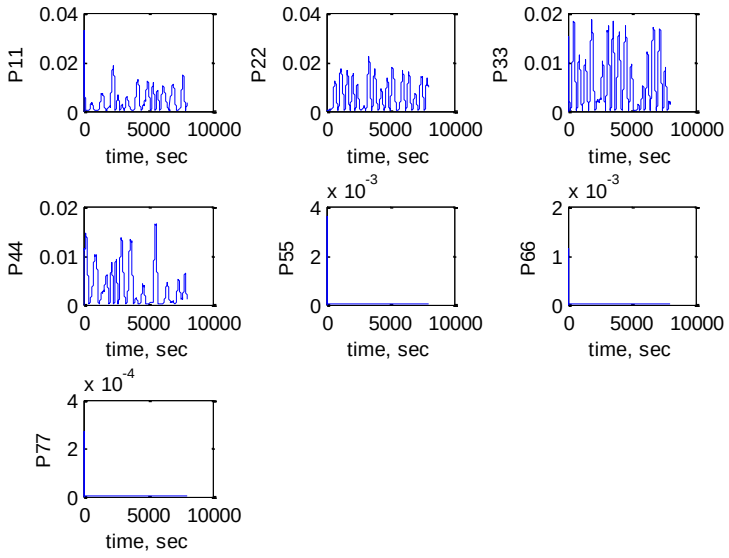

Figure 6.32. Stage-Two Filter Error Covariance Diagonals

The last change to the filter covariance matrices was for a case with the attitude rate greater than one degree per second. Above this limit, the same filter matrices work very well for any angular velocity up to at least 30 degrees per second. The next set of simulation results, as demonstrated by Figures 6.33-6.40, show the performance of the filter when angular velocity is one degree per second along each axis.

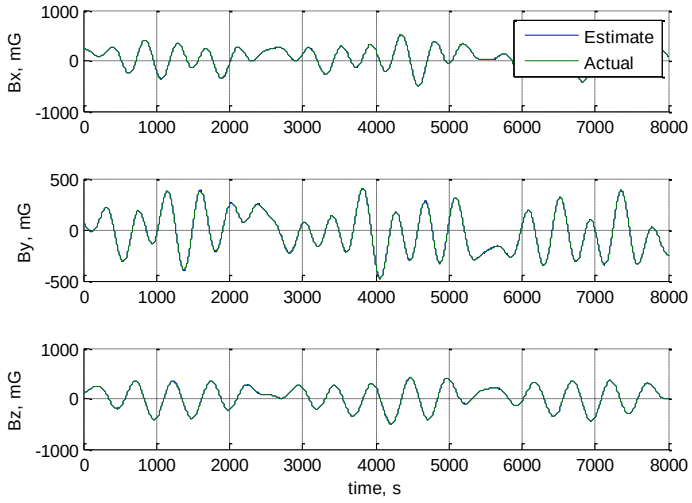

Figure 6.33. Magnetic Field Vector

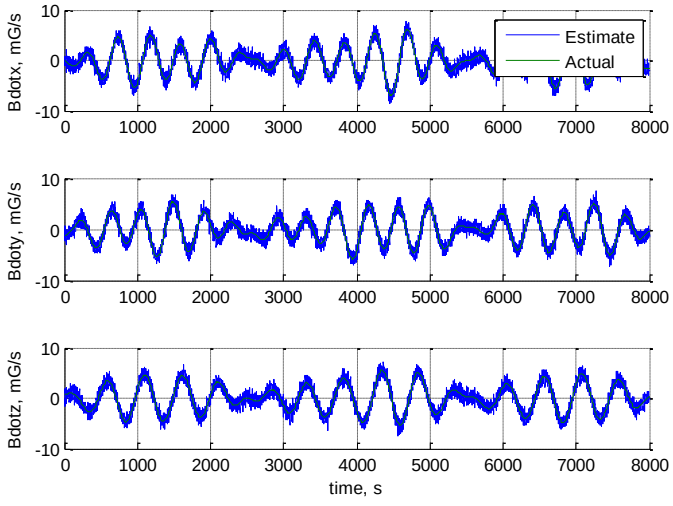

Figure 6.34. Magnetic Field Vector Derivative

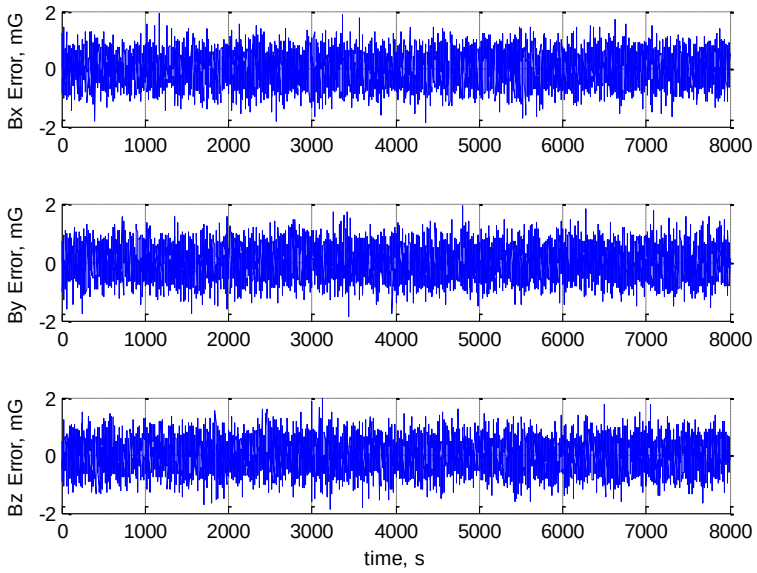

Figure 6.35. Magnetic Field Vector Estimation Error

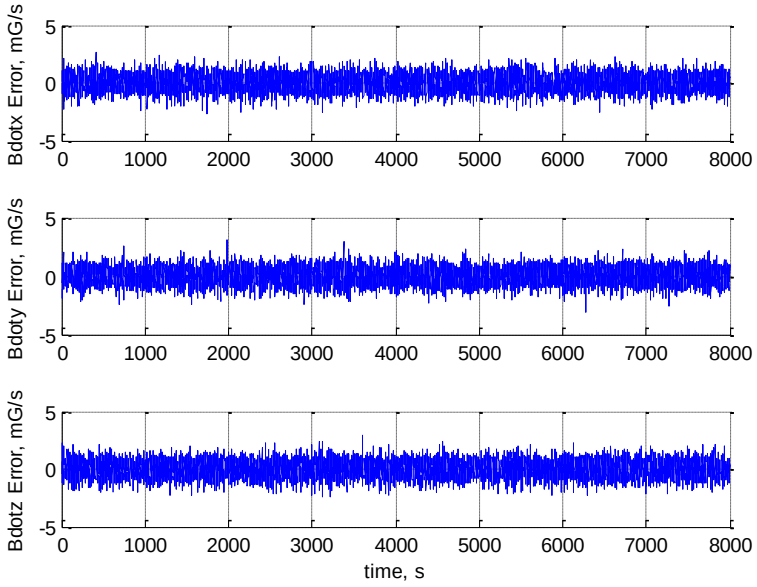

Figure 6.36. Magnetic Field Vector Derivative Estimation Error

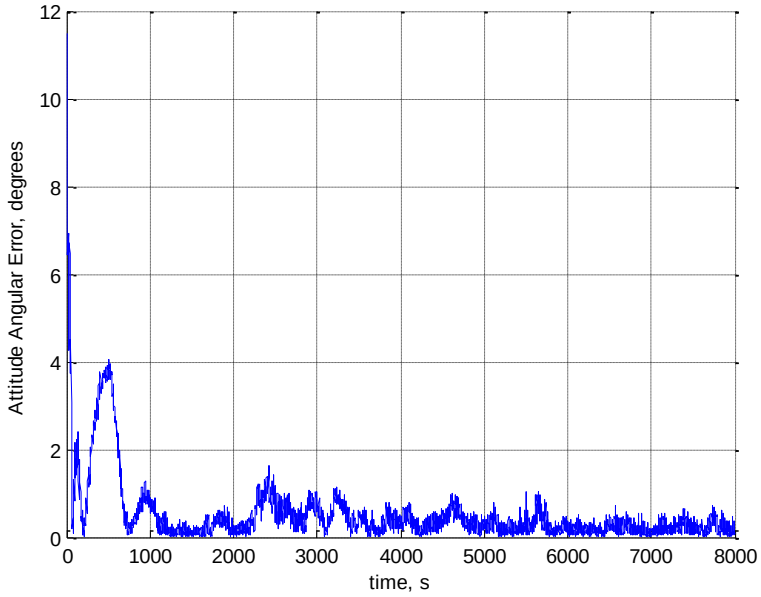

Figure 6.37. Attitude Angular Error

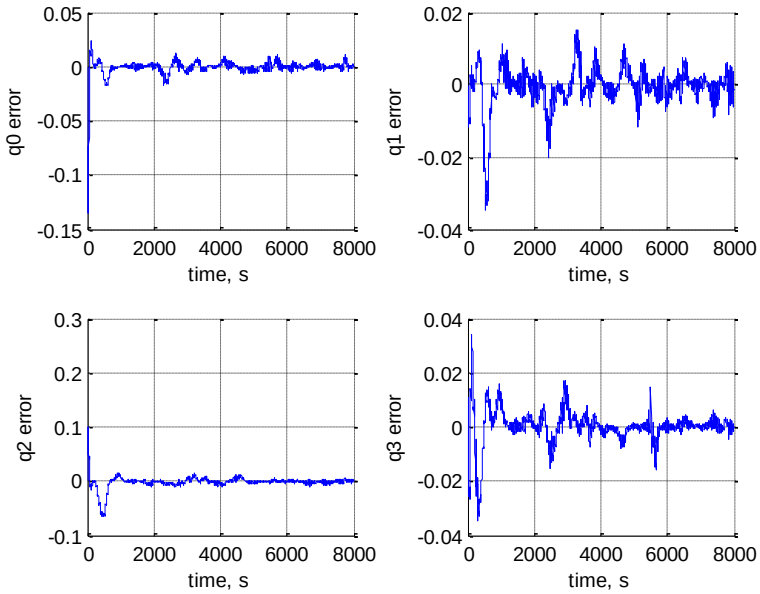

Figure 6.38. Attitude Quaternion Error

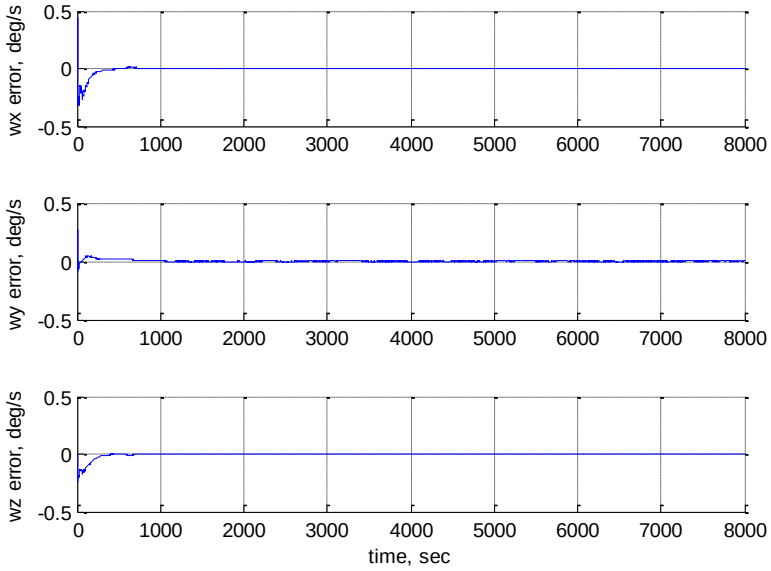

Figure 6.39. Angular Velocity Error

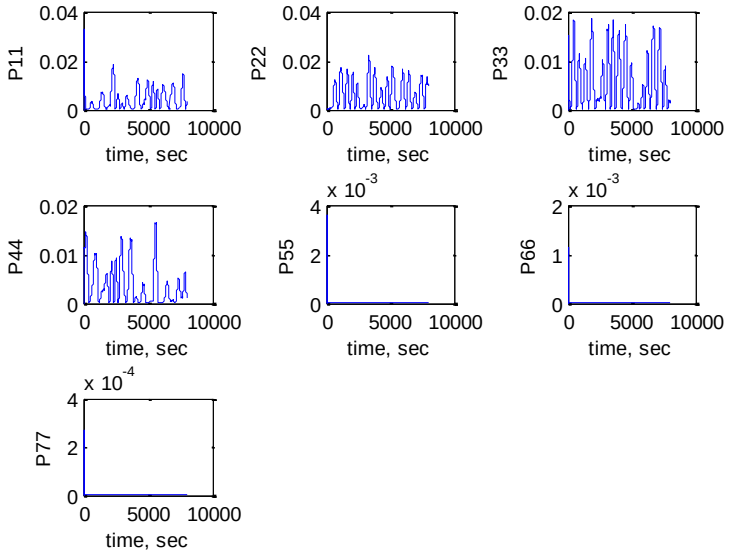

Figure 6.40. Stage-Two Filter Error Covariance Diagonals

7. CONCLUSIONS

7.1. CONCLUSION OF DISSERTATION RESEARCH

The process of extending the research of Reference 32 was extensive, involving creating several new methods to address the observability problems of the low angular velocity case. Algorithms were developed in an attempt to improve the accuracy and computational efficiency of the first stage. An attempt was also made to estimate more information in the first stage to increase the second stage filter's ability to estimate the correct solution. The problem scenario was examined closely to determine if more information could be extracted from the measurements.

First, in an effort to determine the required amount of information to fully determine the attitude, the magnetometer algorithm was modified to accept angular rate measurements from an IMU. These measurements were simulated with typical accuracy for a commercial off-the-shelf unit that would be common on a small satellite. The addition of the angular velocity measurement resulted in convergence in every case tested without modification to the magnetometer-only algorithm. This led to the conclusion that the lack of observability of the angular velocity was the root cause of the difficulties encountered when the IMU measurements were not available. The outcome is a magnetometer and IMU combined filter that is different from those found in the literature. Attitude accuracies of less than one degree and angular rate errors of less than 0.1 degrees per second were achieved using an IMU with 0.1 degrees per second three-sigma measurement accuracy.

With the filter working for cases in which the angular velocity is measured, the next step was to determine if the angular rates could be calculated directly from the magnetometer measurement. The basic kinematic equation was used to relate the magnetic field derivative to the angular rate. The angular rate cannot be directly calculated due to the lack of a unique "inverse" cross product. However, a filter can be used to estimate the angular velocity. An angular rate estimator was created to increase the accuracy of an estimator found in literature.[34] The new estimator is able to estimate the spacecraft angular velocity, without the need of estimating the attitude quaternion, to within about 0.1 degrees per second, similar to the IMU measurement accuracy.

The angular velocity filter was used to produce an angular velocity pseudomeasurement that was then provided to the second-stage filter. The estimation bias from the first filter caused error in the second filter. Even though the rates were known almost as accurately as the IMU measurement, the mean of the pseudomeasurement was not equal to the actual angular rate. Adding bias terms to the second-stage filter in an attempt to account for the bias failed to resolve the problem. The outcome was an angular rate estimator that is more accurate than those found in literature; however, the results were not helpful in achieving the main goal of this dissertation study.

Next, an attempt at developing a deterministic solution was made using the same equations used by the measurements in the second stage filter. The first attempt was to use Newton's method to numerically find the solution to the system of equations. When the Jacobian was found, it was not full rank, eliminating the possibility of using Newton's method and showing that the system was underdetermined. After adding an approximation of the angular velocity magnitude found by analyzing the angle between two measurements, the system of equations was treated as an optimization problem. The problem has many solutions, but if the initial guess is sufficiently close, it was thought that the correct solution may be found. The implementation was successful and the attitude quaternion was able to be estimated to within four degrees in the zero angular velocity case. However, the results were not sufficiently accurate to satisfy the attitude requirements that this study was striving to achieve.

The last solution attempt was to inspect the observability of the problem to determine if alterations to the formulation could be made to improve the robustness and applicability of the method. When the spacecraft is aligned with the magnetic field and not changing in any way other than possibly rotating about the magnetic field vector, the problem is unobservable. This scenario is highly unlikely to happen in practice; however, there is one test scenario that closely resembles this case. When the spacecraft is not rotating and is in an equatorial orbit, the magnetic field vector measured by the spacecraft will only change slightly. If the Earth was a perfect sphere and the magnetic field vector was "perfectly behaved," this scenario would be unobservable. However, there is a slight change in the observed vector in this case.

It was determined that a successful approach may involve the tuning of the second-stage Kalman filter. The filter must rely less on the derivative pseudomeasurement because it is less accurate when the field changes so slowly. The filter must also be able to process a sufficient number of observations to make the corrections. It would make sense that a longer time history would be needed in order for the filter solution to converge. It was noticed during testing that when the angular rates were lowered to zero, the filter would detect a steady state error in the angular rate estimate and that error would cause the spacecraft solution to slowly rotate at a constant rate, not correcting to the true solution. To remedy this situation, the process noise matrix elements corresponding to the attitude quaternion were raised so that the filter would trust the measurement more and the model less. In addition to this, the measurement noise covariance for the magnetic field derivative pseudomeasurement was raised so that it would provide less input to the filter. Lastly, the correction time of the angular rate needed to be decreased for faster convergence, so the initial error covariance was altered.

The result was a filter that is able to estimate the attitude and rates of a spacecraft when the angular rates were zero using only magnetometer data. However, the performance of the cases when the rates were higher was negatively impacted. To circumvent this, a group of Kalman filter matrices were selected that allowed for the best attitude and angular rate estimation for different regimes of magnetic field variation. The two parameters that most directly affect the variation of the magnetic field with respect to the spacecraft are the spacecraft angular rate and the orbital inclination.

The variable tuning parameter dual-filter is capable of estimating the spacecraft attitude to within 2 degrees and the angular rates to within 10^{-3} degrees per second, converging within a maximum of 8000 seconds for all regimes of angular velocity and orbital inclination considered. In each of the lower angular velocity cases, the error was still decreasing at 8000 seconds. In the higher angular velocity cases, the attitude was estimated to within 0.1 degrees and the angular rates to within 10^{-4} degrees per second. The solution methodology developed here was not found in the literature survey. The published magnetometer-only methods found were unsuccessful in estimating the spacecraft angular velocity when the spacecraft was in an inertially fixed orientation.

This research has produced three contributions that could be useful in estimating the attitude of a small spacecraft. The first is a new angular velocity estimator that is able to estimate the spacecraft angular rates to within 0.1 degrees per second, without the need to estimate the spacecraft attitude. The estimator has been shown to work when the spacecraft is both rotating and not rotating. The second contribution involves the numerical solution of a system of equations that estimates the spacecraft attitude to within about four degrees in the presence of noise. The method is less computationally efficient and less accurate than the filter version, so its application is primarily as a proof-of-concept to show that the attitude can be calculated in certain circumstances such as the zero angular velocity case. The final contribution offered as a consequence of this research is a robust and highly accurate dual-filter magnetometer-only attitude determination algorithm. This technique was shown to be reliable and applicable across a broad spectrum of scenarios. Originally thought of as a backup or contingency method, the magnetometer-only algorithm presented here achieves accuracies that rival or surpass systems that are augmented with additional measurements. The developed algorithm would not be sufficiently accurate enough for missions requiring precise pointing, but its application to a number of small satellite missions is likely beneficial.

Small satellites have modest computing budgets. The method presented uses a Kalman filter, which is better suited for small satellites compared to nonlinear techniques such as the particle filter or Unscented Kalman Filter. The design only needs a magnetometer, decreasing cost, mass, and volume required for attitude determination. These savings are important for small satellites. MATLAB is not a compiled language and therefore runs slower than a compiled language that would be used onboard the spacecraft. Simulations in MATLAB that were performed with simulation times above two hours took less than three minutes to run on an average laptop computer.

The method could be improved by generating a function based covariance matrix calculation that would adapt in real time to the correct tuning parameters. This would remove the need for a table of matrix elements and provide a more autonomous correction. All of the simulations performed used MATLAB, creating the need to convert the code into flight ready C code. Some simplifications to propagating the filter covariance would add computational efficiency, but was not done for ground testing due

the abundance of processing power on the ground. Lastly, the deterministic approach may be able to reduce the possible solution set by examining the angular momentum of the spacecraft. The reduction of possible solutions could improve the numerical solving routine creating a faster estimate that is more likely to converge to the correct solution.

REFERENCES

[1] Lu, G. "Development of a GPS Multi-Antenna System for Attitude Determination," *UCGE Reports*, No. 20073, Ph.D. Dissertation, 1995.

[2] Gebre-Egziabher, D. D. Gebre-Egziabher, Elkaim, G.H., Powell, J. D., and Parkinson, B. W. "A Gyro-Free Quaternion Based Attitude Determination System for Implementation Using Low Cost Sensors," *Proceedings of the IEEE Position Location and Navigation Symposium*, San Diego, CA, 2000.

[3] Crassidis, J. L. and Markley, F. L. "A Minimum Model Error Approach for Attitude Estimation," *Journal of Guidance, Control and Dynamics*, Vol. 20, No. 6, November-December 1997.

[4] Santoni, F. and Bolotti, F. "Attitude Determination of Small Spinning Spacecraft Using Three Axis Magnetometer and Solar Panels Data," *Proceedings of the IEEE Aerospace Conference*, 2002.

[5] Ma, G. and Jiang, X. "Unscented Kalman Filter for Spacecraft Attitude Estimation and Calibration using Magnetometer Measurements," *Proceedings of the Fourth International Conference on Machine Learning and Cybernetics*, Guangzhou, China, August 2005.

[6] Bar-Itzhack, I. Y. and Oshman, Y. "Attitude Determination from Vector Observations," *IEEE Transactions on Aerospace and Electric Systems*, Vol. AES-21, No. 1, January 1985.

[7] Lizarralde, F. and Wen, J. "Attitude Control without Angular Velocity Measurements: A Passivity Approach," *Proceedings of the Conference on Robotics and Automation*, Osaka, Japan, 1995.

[8] Wang, P. K. C. "Synchronized Formation Rotation and Attitude Control of Multiple Free-Flying Spacecraft," *AIAA Journal of Guidance and Control*, August, 1998.

[9] Markley, F. L. "Attitude Determination using Vector Observations and the Singular Value Decomposition," *The Journal of the Astronautical Sciences*, Vol. 38, No. 3, July-September 1988, pp. 245-258.

[10] Crassidis, J. L. and Lai, K. "Real-Time Attitude-Independent Three-Axis Magnetometer Calibration," *AIAA Journal of Guidance, Control and Dynamics*, Vol. 28, No. 1, 2005, pp. 115-120.

[11] Crassidis, J. L. and Lightsey, E. G. "Attitude Determination Using Combined GPS and Three-Axis Magnetometer Data," *Space Technology,* Vol. 22, No. 4, 2001, pp. 147 – 156.

[12] Shuster, M. D. and Oh, S. D. "Three-Axis Attitude Determination from Vector Observations," *AIAA Journal of Guidance and Control,* Vol. 4, No. 1, 1980, pp. 70 – 77.

[13] Liebe, C. C. "Star Trackers for Attitude Determination," *IEEE Aerospace and Electronic Systems Magazine,* June 1995.

[14] M. S., Natanson, J. Challa, Deutschmann, D., and Baker, F. "Magnetometer-Only Attitude and Rate Estimation for Gyroless Spacecraft," *Proceedings of the Third International Symposium on Space Mission Operations and Ground Data Systems,* NASA Conference Publication 3281, NASA-GSFC, Greenbelt, MD, November 1994.

[15] Challa, M. and Wheeler, C. "Accuracy Studies of a Magnetometer-Only Attitude and Rate Determination System," *Flight Mechanics/Estimation Theory Symposium,* NASA Goddard Space Flight Center, Greenbelt, MD, 20771, May 1996.

[16] Humphreys, T. "Attitude Determination for Small Satellites with Modest Pointing Constraints," *Proceedings of the Sixteenth Annual AIAA/USU Conference on Small Satellites,* Logan, Utah, 2002.

[17] Shuster, M. D. "Kalman Filtering of Spacecraft Attitude and the QUEST Model," *The Journal of the Astronautical Sciences,* Vol. 38, No. 3, 1990, pp. 377-393.

[18] Shuster, M. D. "A Survey of Attitude Representations," *The Journal of the Astronautical Sciences,* Vol. 41, No. 4, 1993, pp. 439-517.

[19] Van Dyke, M. C., Schwartz, J. L., and Hall, C. D. "Unscented Kalman Filtering for Spacecraft Attitude State and Parameter Estimation," *The Journal of the Astronautical Sciences,* Vol. 41, No. 4, 1993, pp. 439-517.

[20] Psiaki, M. and Martel, F. "Three-Axis Attitude Determination Via Kalman Filtering of Magnetometer Data," *Journal of Guidance, Control and Dynamics,* Vol. 13, No. 3, 1990, pp. 506 – 514.

[21] Wahba, G. "A Least Squares Estimate of Satellite Attitude," *SIAM Review,* Vol. 7, No. 3, 1965, pp. 409-409.

[22] Wertz, J. R. *Spacecraft Attitude Determination and Control,* Reidel Publishing Company, 1980.

[23] Shuster, M. "The Quest for Better Attitudes," *The Journal of the Astronautical Sciences,* Vol. 54, Nos. 3 & 4, December 2006, pp. 657 – 683.

[24] Keat, J. "Analysis of Least Squares Attitude Determination Routine DOAOP," Computer Sciences Corporation, CSC/TM-77/6034, February, 1977.

[25] Davenport, P. B. "Attitude Determination and Sensor Alignment via Weighted Least Squares Affine Transformations," *NASA X-514-71-312,* August 1971.

[26] Simon, D., *Optimal State Estimation,* Wiley-Interscience, Hoboken, New Jersey, 2006.

[27] Kuipers, J. B., *Quaternions and Rotation Sequences*, Princeton University Press, Princeton, New Jersey, 1999.

[28] Sidi, M., *Spacecraft Dynamics & Control*, Cambridge University Press, New York, New York, 1997.

[29] Hughes, P. C., *Spacecraft Attitude Dynamics,* Dover Publications, Mineola New York, 2004.

[30] Levant, Arie, "Robust Exact Differentiation via Sliding Mode Technique," Automatica, Vol. 34, Issue 3, March 1998, pp. 379-384.

[31] "World Magnetic Model," National Geospatial-Intelligence Agency, <http://www.ngdc.noaa.gov/geomag/WMM/DoDWMM.shtml>.

[32] Searcy, Jason D., "Magnetometer-Only Attitude Determination with Application to the M-SAT Mission," *Missouri University of Science and Technology Master's Thesis,* May 2011.

[33] Searcy, Jason D., Pernicka, Henry J., "Magnetometer-Only Attitude Determination Using Novel Two-Step Kalman Filter Approach," *Journal of Guidance, Control, and Dynamics,* Vol. 35, No. 6, November 2012, pp. 1693 – 1701.

[34] Tortora, Paolo, and Oshman, Yaakov, "Spacecraft Angular Rate Estimation from Magnetometer Data Only Using an Analytic Predictor," *Journal of Guidance, Control, and Dynamics*, Vol. 27, No. 3, May-June 2004, pp. 365 – 373.

VITA

Jason David Searcy was born in Louisville, KY. He graduated from Shelby County High School in May of 2002. From August 2002 through May 2006, he attended the Missouri University of Science and Technology, formerly known as the University of Missouri-Rolla, to obtain a Bachelor's of Science degree in Aerospace Engineering.

Jason started graduate school in August of 2006 and began work toward a Master's Degree in Aerospace Engineering. In August of 2007 he was awarded first place in the Frank J. Redd Scholarship Competition for co-authoring a paper on the attitude determination and control system for the MR SAT spacecraft. The same year, he was awarded a Student Excellence award from the Academy of Aerospace and Mechanical Engineers at Missouri University of Science and Technology. Jason received his Master of Science degree in Aerospace Engineering in May 2011 and will receive his Ph.D. in Aerospace Engineering in December 2013 both from the Missouri University of Science and Technology.